

NASA Contractor Report 189555

NASA-CR-189555
19920011134

Application of Analysis Techniques for Low Frequency Interior Noise and Vibration of Commercial Aircraft

A. E. Landmann, H. F. Tillema, and G. R. MacGregor

Boeing Commercial Airplanes
P. O. Box 3707
Seattle, Washington 98124-2207

FOR REFERENCE

NOT TO BE TAKEN FROM THIS ROOM

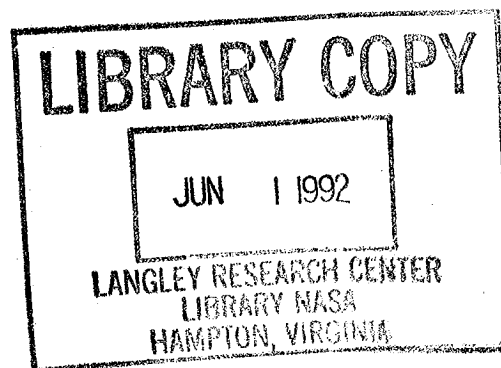
Contract NAS1-18027

January 1992



National Aeronautics and
Space Administration

Langley Research Center
Hampton, Virginia 23665-5225



CONTENTS

	<u>Page</u>
1.0 SUMMARY	1
2.0 INTRODUCTION	3
3.0 FINITE ELEMENT ANALYSIS	9
3.1 1989 Finite Element Analysis	9
3.1.1 Interior Trim Modeling Investigation	10
3.1.2 Modified Acoustic Space Model	11
3.1.3 Comparisons to GVT Data	13
3.1.4 Sensitivity Studies	18
3.2 1990 Finite Element Analysis	19
3.2.1 767-300 Airplane Structure-Acoustic Finite Element Model	19
3.2.2 Comparisons to GVT Data	27
3.2.3 Sensitivity Studies	29
4.0 STATISTICAL ENERGY ANALYSIS	35
4.1 Aft-Mounted Configuration	37
4.2 Addition of Trim Panels	37
4.3 Parametric Studies (Aft-Mounted Engine)	38
4.3.1 Heavy Limp Mass Barrier in Front of Bulkhead	39
4.3.2 Engine Strut Disconnected From the Bulkhead	40
4.3.3 Straight-Through Strut	41
4.3.4 Straight-Through Strut Isolated From the Empennage	42
4.3.5 Addition of Frames to Support the Straight-Through Strut	43
4.3 Wing-mounted Configuration (Airborne Excitation)	44
4.3.1 Results From the Extended Mid-Frequency Model	44
4.4 Noise Suppression Concepts for the Wing-Mounted Engine	46
4.4.1 Modification of the Fuselage Wall	48
4.4.2 Damping Application Results	49
4.4.3 Results for Adding Deep Frames and Lavatories	50
4.4.4 Assessment of the Impact of Wing-Mounted Versus Aft-Mounted Engines for Airborne Excitation	51
4.5 Wing-Mounted Configuration (Structureborne Excitation)	51
4.5.1 Validation of 767-300 Sea Model	51
4.6 Noise and Vibration Reduction Concepts for Wing-Mounted Engine	54
4.6.1 The Effects of Fuel Mass Loading on Airplane Response	54
4.6.2 The Effect of a Stiffer Wing on Reduction of Cabin Noise	59
4.6.3 The Effect of Increased Fuselage Mass on Reduction of Cabin Noise	60
4.6.4 Redirection of Energy as a Means of Reducing Cabin Noise	61
4.7 Comparison of Wing-Mounted vs. Aft-Mounted Configurations for Structure-Borne Noise	64
5.0 PAIN ANALYSIS	65
5.1 FY 1989 PAIN Model Upgrades	65
5.1.1 Predictions of Cabin Sound Level Gradients	65
5.1.2 Pressure Bulkhead Transmission and Radiation	67
5.2 FY 1990 Predictions for Wing-Mounted and Aft-Mounted Propeller Airplanes	70
5.2.1 727 PAIN Model	71
5.2.2 Baseline Predictions	74
5.2.3 Performance of the Baseline Trim System	75
5.2.4 Contribution of the Floor for Wing-Mounted Configuration	76

	<u>Page</u>
5.2.5 Contribution of the Pressure Bulkhead for Aft-Mounted Configuration .	76
5.2.6 Cabin Trim Variations	76
5.2.7 Fuselage Variations	79
5.2.8 Variation of the Pressure Bulkhead	81
5.2.9 Nonconventional Sidewall Treatments	81
5.2.10 Resonator Application to the Pressure Bulkhead	82
6.0 CONCLUSIONS AND RECOMMENDATIONS	85
6.1 Finite Element Analysis	86
6.2 Statistical Energy Analysis	87
6.3 PAIN Analysis	89
7.0 REFERENCES	91

1.0 SUMMARY

This document summarizes the last two years of a four year contract to evaluate the application of selected analysis techniques to low frequency interior noise associated with advanced propeller installations. The first two years of the contract are documented in reference 1. This work was funded by a NASA contract, NAS1-18027.

Three analysis techniques were chosen for evaluation, specifically finite element analysis (FEA), statistical energy analysis (SEA), and a power flow method using elements of SEA, computer program Propeller Aircraft Interior Noise (PAIN)). FEA and SEA models were used to predict cabin noise and vibration and evaluate suppression concepts for structureborne noise associated with the shaft rotational frequency and harmonics (< 100 Hz). SEA and PAIN models were used to predict cabin noise and vibration and evaluate suppression concepts for airborne noise associated with engine radiated propeller tones. Both aft-mounted and wing-mounted propeller configurations were evaluated. Ground vibration test (GVT) data from a 727 airplane modified to accept a propeller engine were used to compare with predictions for the aft-mounted propeller. Similar data from a 767 airplane was used for the wing-mounted model comparisons.

Finite element models generally show good correlation with GVT data under 60 Hz. Discrepancies with data are believed to be primarily related to modeling deficiencies in the connections of the strut-to-empennage for the aft-mounted configuration and the strut-to-wing for the wing-mounted configuration. Studies showed that detailed interior trim models are generally not required below 100 Hz. For the suppression concepts investigated, no one concept leads to a general reduction of noise for all shake conditions and frequencies. Reducing the existing size of the model, while maintaining accuracy in the structure-acoustic response predictions would be beneficial.

SEA did an excellent job of predicting cabin noise when measured accelerations were used as inputs to the model. Measured values were needed as inputs to the SEA model due to difficulties in the SEA modeling of the complex motion of the strut. For the wing-mounted configuration, the only passive concept inboard of the strut that showed potential for reducing structureborne noise was fuel management. Studies showed that a straight-through-strut with body isolators would be the most effective structureborne noise suppression concept for the aft-mounted case.

For airborne excitation, the SEA prediction for the baseline 727 airplane cabin noise level for the wing-mounted configuration was 36 dB higher at the blade passage frequency than the aft-mounted

configuration. A combination of structural changes and barriers gave up to 10 dB reduction for the wing-mounted configuration.

PAIN predictions for cabin sound levels at the blade passage frequency for the wing-mounted and aft-mounted propeller configurations of a 727 airplane are 109 dB and 93 dB, respectively. In order for there to be a significant decrease in cabin levels for the wing-mounted configuration, the floor must be well isolated. For the aft-mounted configuration, the bulkhead is predicted to be the major radiator. A trim panel incorporating Helmholtz resonators has the potential to lower the cabin levels at the blade passage frequency an additional 8 dB. Changes to the primary structure had little effect on the predicted levels. Predictions for the aft-mounted configuration have been adjusted by a calibration run to account for uncertainties in the predicted propeller phase field.

2.0 INTRODUCTION

This document describes the third and fourth years of a four year contract to evaluate the application of selected analysis techniques to low- to mid-frequency cabin noise associated with advanced propeller installations. Work was funded by a NASA contract, NAS1-18027.

The primary sources of cabin noise on advanced propeller-powered aircraft are low- to mid-frequency (< 500 Hz) structureborne noise caused by engine unbalances and airborne noise from engine radiated propeller tones. Conventional sound proofing treatments, such as damping tapes or fiberglass blankets, are not very effective in this frequency range. Also, most low- to mid-frequency design tools tend to be based on idealized cylindrical models of the airplane fuselage which ignore effects of tapered empennage sections, pressure bulkheads, floors, etc. Effective reduction of low- to mid-frequency noise requires the development of improved design analysis tools. These tools will lead to a better understanding of the mechanisms involved and provide guidance for developing new suppression concepts.

Three design analysis techniques were chosen for evaluation including finite element analysis, statistical energy analysis (SEA), and a power flow method using elements of SEA (computer program Propeller Aircraft Interior Noise (PAIN)). Finite element and SEA models were used to assess structureborne noise caused by engine unbalances at the shaft rotational frequency and harmonics (< 100 Hz). SEA and PAIN models were used to assess airborne noise associated with engine radiated propeller tones at the blade passage frequency (169 Hz) and its harmonics.

In finite element analysis, a continuous system is idealized as a discrete system. The discrete system consists of a collection of elements that are connected at selected nodes located on the element boundaries. The elements exhibit a simplified elastic response within their domain when their nodes are displaced, and provide a simplified representation of the elastic properties of the actual system. Material and geometric properties are input for elements typically consisting of rods, beams, plates, and solids. Mass and stiffness matrices are obtained from the relationship between the nodes as defined by the element connectivity. Having obtained the mass and stiffness matrices, the modes of the system can be calculated. The response of the system due to an external excitation can also be calculated.

SEA is a method of analyzing the flow of energy between dynamical systems based on a statistical coupling between the modes of response of the systems. Basic material and geometric parameters are

required along with some knowledge of the types of motion that are possible. The SEA model provides a statistical estimate of the modes involved in energy transfer rather than the discrete definition of frequencies and modes provided by finite element techniques. In SEA the input information describing the model is used to define average properties of variables such as modal density (the average number of resonance frequencies per unit frequency), characteristic wavenumber (a quantity directly related to the average wavelength of a mode), characteristic impedance (the ratio of the maximum force to the maximum velocity for a mode of vibration), and coupling loss factor (a parameter controlling the average flow of energy between two groups of modes). The power expressions are then solved for the modal energies within the substructures. From the modal energies, the response variables of interest for the specified substructures are determined. The input excitation for a SEA model is applied as the power input to a subsystem of modes.

Computer program PAIN was specifically developed for propeller interior noise predictions by L.D. Pope, et al., under the auspices of NASA (refs. 3,4). The PAIN model estimates the space average sound level in an airplane cabin resulting from an excitation field incident on the exterior fuselage. The excitation field consists of the pressure time history for a wing-mounted rotating propeller as defined by a grid of points on the fuselage surface. The fuselage structural model is a cylinder with an integral floor. The effects of sidewall and floor stiffeners (ring frames, stringers, floor beams) are averaged over the fuselage surface. The cabin interior is lined with a multi-element trim to account for increased sidewall transmission loss and cabin absorption. For application to the 727 Demonstrator airplane, PAIN was modified to handle the aft-mounted propeller configuration.

Noise and vibration testing on a 727 airplane, modified for installation of a GE36 counter-rotating propeller engine, provided the data base with which to compare predictions during the first three years of the contract. During ground vibration tests, before the engine was installed, the strut was excited by a shaker to determine airframe and cabin response to engine mount vibration. Response to shaker inputs at each engine mount location was recorded. In addition, side-of-body shake testing was performed on the fin, empennage, and aft passenger cabin to simulate high level acoustic loading from the propellers. Also, flight testing was completed for different cruise and low power flight conditions. The 727 was configured with an acoustic test arena aft of body station 890. Standard 727 interior trim and four passenger seat rows were installed in this area. General arrangement of the airplane is shown in figure 1.

The objective of the FY 1987 task was to evaluate the ability of the three analysis techniques to predict cabin noise and vibration. Predicted levels were compared with measured levels of the 727 Demonstrator airplane. In FY 1988, recommended improvements were incorporated into the models, and

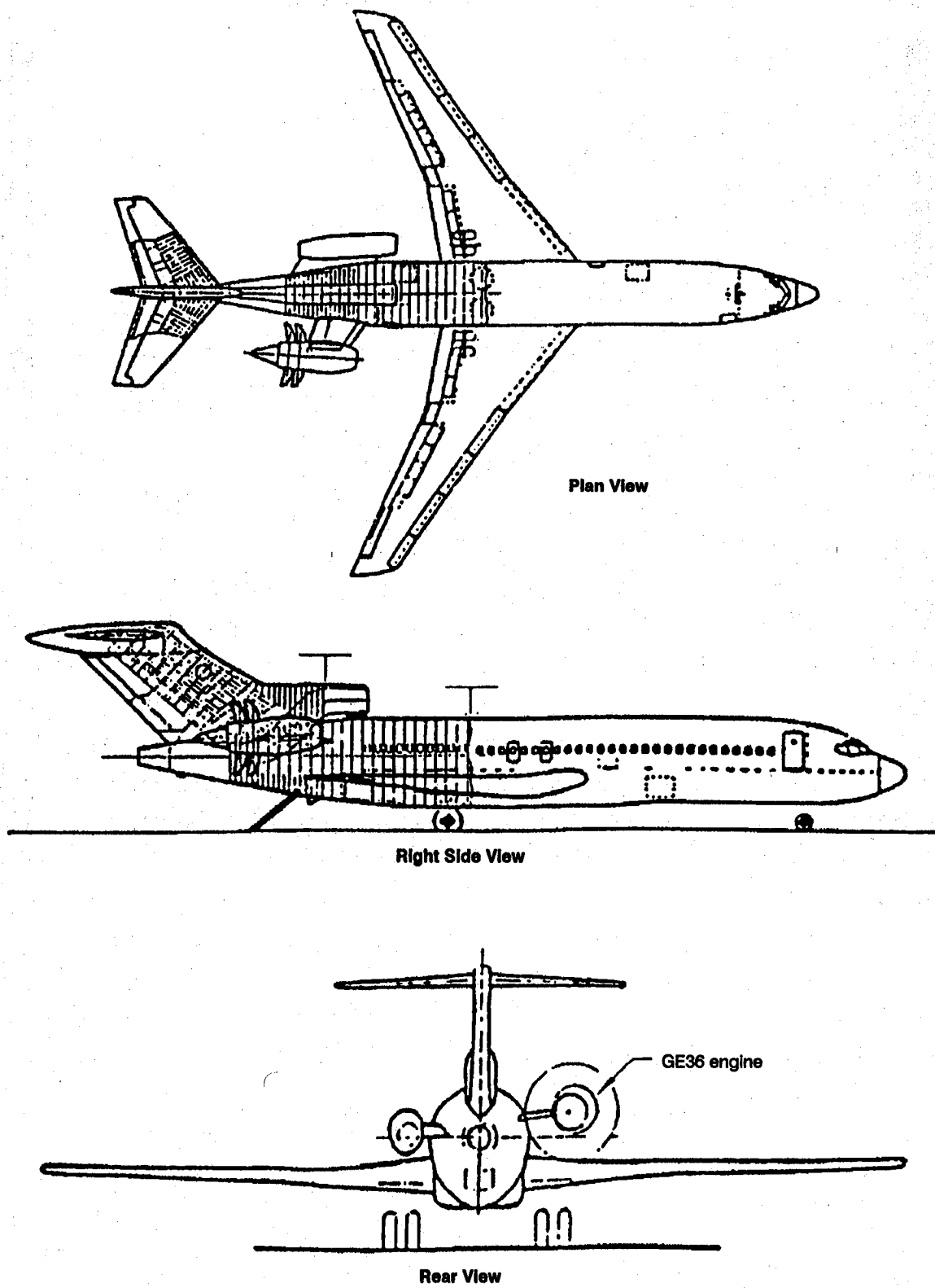


Figure 1. 727 Demonstrator Airplane – General Arrangement

predictions were again compared with the measured levels. Results from these first two years of the contract are documented in reference 1.

Although some discrepancies still existed in the models, the comparisons with data were favorable enough to go ahead and assess noise transmission paths and evaluate suppression concepts on the 727 Demonstrator airplane as part of the FY 1989 and FY 1990 tasks. In addition, implications of a wing-mounted propeller airplane were also investigated in 1990. The FY 1989 and FY 1990 tasks are the subject of this report.

The 767-300 airplane was chosen as the baseline airplane for the finite element and SEA evaluation of the wing-mounted structureborne noise associated with the shaft rotational frequency and harmonics (< 100 Hz). The 767-300 was chosen largely because of the availability of a limited amount of ground vibration test data with which models could be compared. During the ground vibration tests, the engine was removed from the left hand side of the airplane and the strut was excited by a shaker at the different engine mounts. The primary purpose of the test was to generate engine mount compliances and cabin acoustic response to engine mount vibration. As such, the data gathered was not as extensive as that gathered during the 727 Demonstrator airplane ground vibration test, for which the objective was to determine both airframe and cabin response to engine mount vibration. Data for the 767-300 shake test exists primarily on the engine mounts, strut-to-wing attachments, and at microphones within the passenger cabin. Fuselage accelerometer data was gathered for only one shake condition. It was assumed that the wing and fuselage structures for a conventional airplane would be representative of an advanced propeller installation. General arrangement of the airplane is shown in figure 2.

A hypothetical wing-mounted propeller 727 airplane was chosen as the baseline airplane for the SEA and PAIN evaluation of the wing-mounted engine radiated propeller tones. It was assumed, for the purposes of this study, that the propeller acoustic near field used for the 727 Demonstrator airplane configuration was simply shifted forward for the wing-mounted configuration. Since no data exists for the hypothetical wing-mounted airplane, SEA and PAIN models of engine radiated propeller tones were not compared to data.

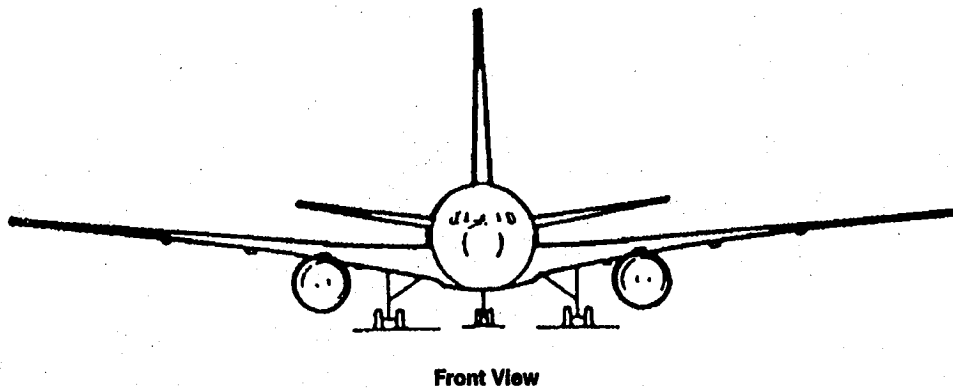
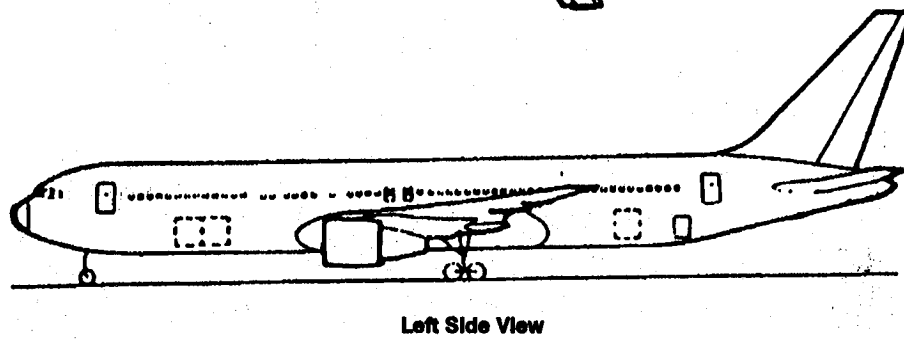
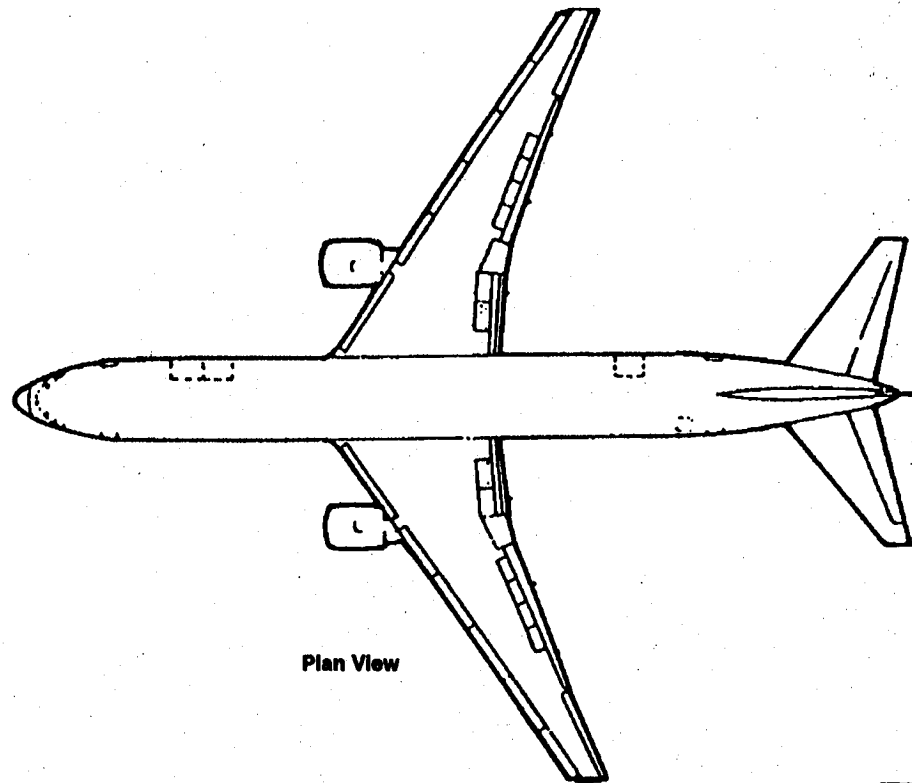
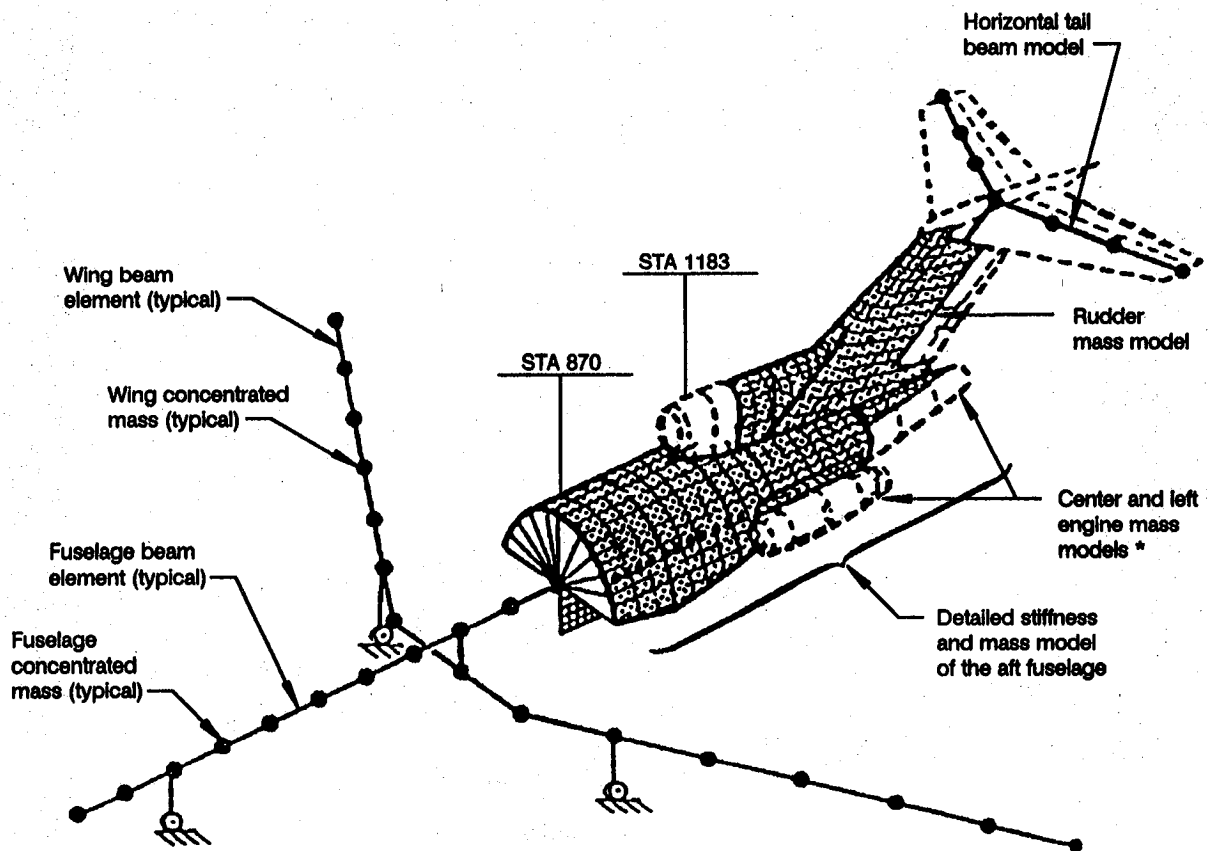


Figure 2. 767-300 Airplane—General Arrangement

3.0 FINITE ELEMENT ANALYSIS

3.1 1989 FINITE ELEMENT ANALYSIS

During the first two years of the contract, finite element analysis of the 727 Demonstrator airplane was limited to under 40 Hz. In 1989, the existing 727 Demonstrator structure-acoustic models were upgraded for predictions at the shaft rotational frequency and harmonics up to 100 Hz. Predictions of the upgraded model were compared to ground vibration test shake conditions. The upgraded model was then used to predict cabin noise reduction associated with various suppression concepts. The 727 Demonstrator airplane finite element model is shown in figure 3.



* Right engine was not included in the GVT configuration.

Figure 3. 727 Demonstrator Airplane – Finite Element Model

3.1.1 INTERIOR TRIM MODELING INVESTIGATION

In previous analyses of the 727 Demonstrator airplane, the interior trim was represented as lumped mass at its attach points to the primary structure. This was considered a valid assumption for the frequency range of interest, 10-40 Hz. In 1989, the importance of modeling the stiffness of the interior trim, as well as its mass, was investigated up to 100 Hz.

Rather than adding a detailed trim model to an already large full airplane model, a simplified one frame bay model was developed to perform basic parameter studies and evaluate the impact of the trim on the acoustic response predictions, below 100 Hz. The one bay model consists of primary structure, sidewall and ceiling panels, airgaps, and cabin acoustic space (fig. 4). Mass and stiffness properties of the sidewall and ceiling panels were smeared uniformly over the panels. The model was excited by harmonic point loads in the lateral direction as shown in the figure. Although a typical ceiling panel spans four bays, it was believed that a one bay representation was adequate for assessing the gross impact of the panel on the acoustic prediction. This limited the size of the problem considerably and led to a more efficient evaluation.

Results show that a lumped mass only representation of the interior trim is a reasonable approximation to a more detailed stiffness/mass representation, up to 100 Hz (fig. 5). For the ceiling panel, two sets of boundary conditions were analyzed. The stiffer boundary conditions are believed to be a more accurate representation of the airplane. However, because of the complexity of the ceiling panel connections, more flexible boundary conditions were also analyzed to bracket the response. As seen in figure 5, the boundary condition has significant effect at 70 Hz. In addition, parametric studies of the sidewall trim show the acoustic response to be insensitive to the sidewall parameters (fig. 6). The one exception is panel density. There is a general reduction of noise above 80 Hz for a heavier panel. There is also a 6 dB reduction at 53 Hz associated with a heavier panel. The peak in the response at 53 Hz is related to the fundamental cross cabin acoustic resonance. It should be noted that previous experience with using simplified models for parameter studies indicates that the simpler models are generally more sensitive to changes than a larger full airplane model.

The reasonable comparison of a mass only model to a mass/stiffness model of the interior trim and the relative insensitivity of the cabin acoustic response to the sidewall trim parameters indicates the low frequency cabin response is being controlled by the primary structure. Thus, modification to the interior trim is not a reasonable alternative in controlling low-frequency noise. Based on the above results, stiffness models of the interior trim were not added to the full 727 Demonstrator airplane finite element model for analysis up to 100 Hz.

Primary structure

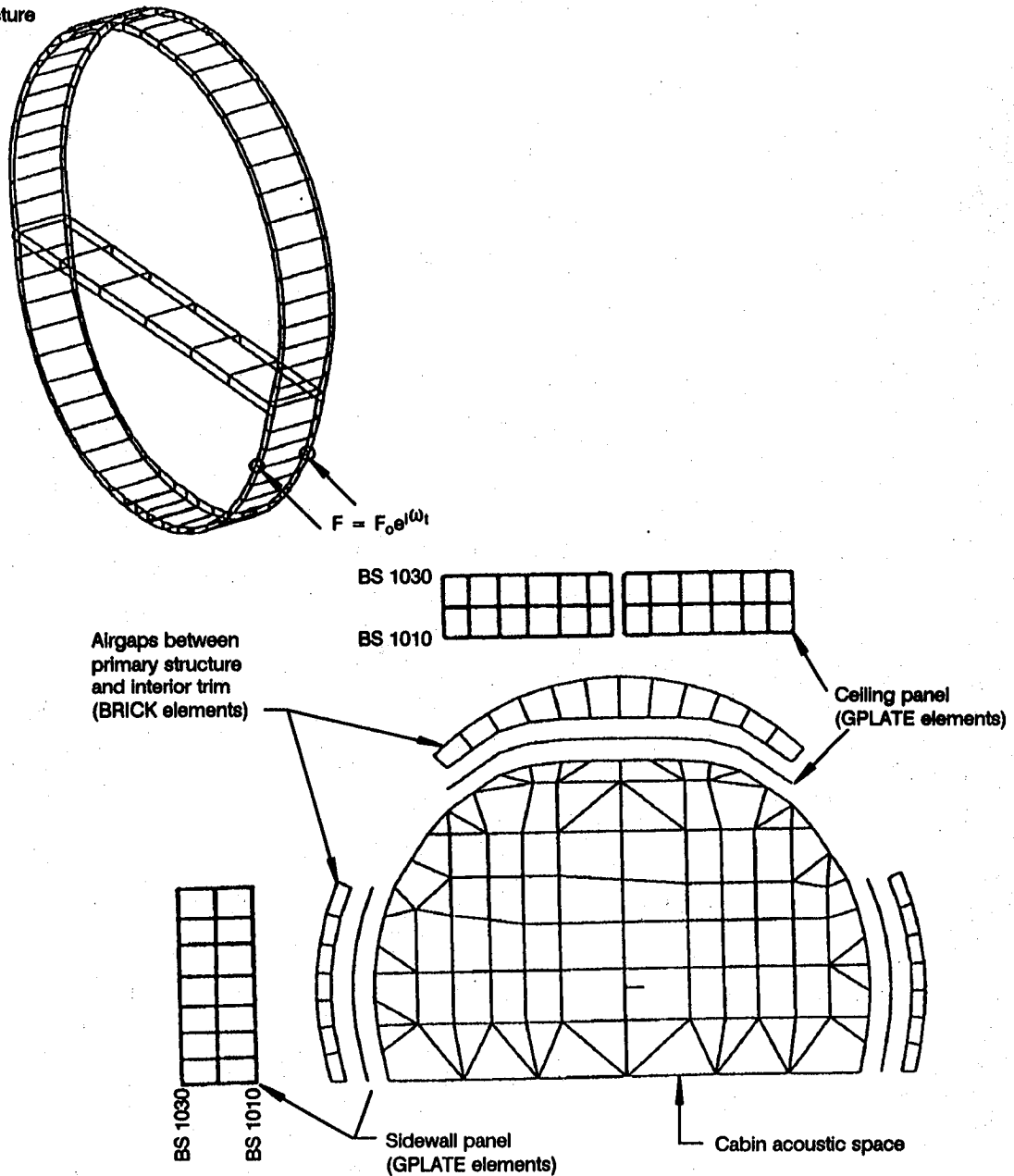


Figure 4. 727 Demonstrator Airplane One Frame Bay Model for Interior Trim Study

3.1.2 MODIFIED ACOUSTIC SPACE MODEL

In the initial finite element analysis of the 727 Demonstrator airplane the frequency range was limited to under 40 Hz. This led to several simplifying assumptions of the original cabin acoustic model. For analysis up to 100 Hz, the simplifications of the original model were no longer seen as being valid. Thus, the original cabin acoustic model was modified to account for the extended analysis frequency range. Essentially, the acoustic model was modified to reflect the surface geometry of the interior trim rather than the primary structure (fig. 7).

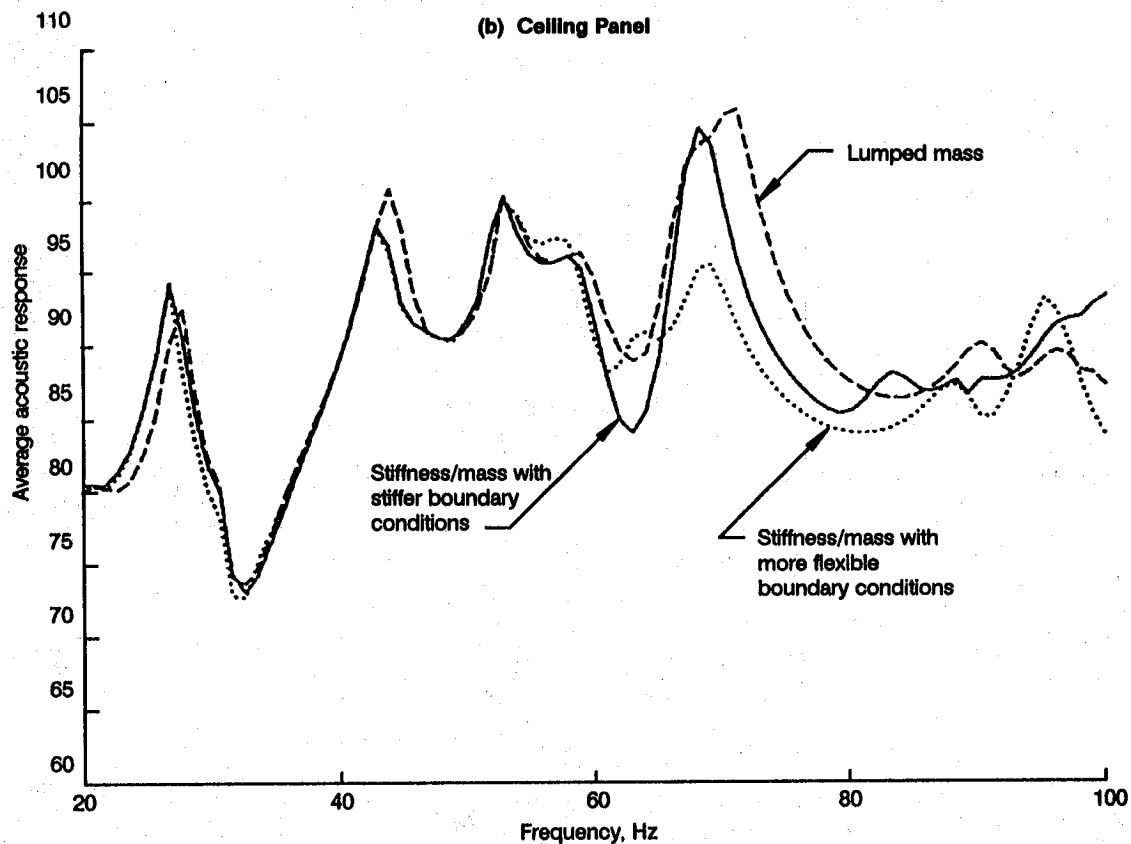
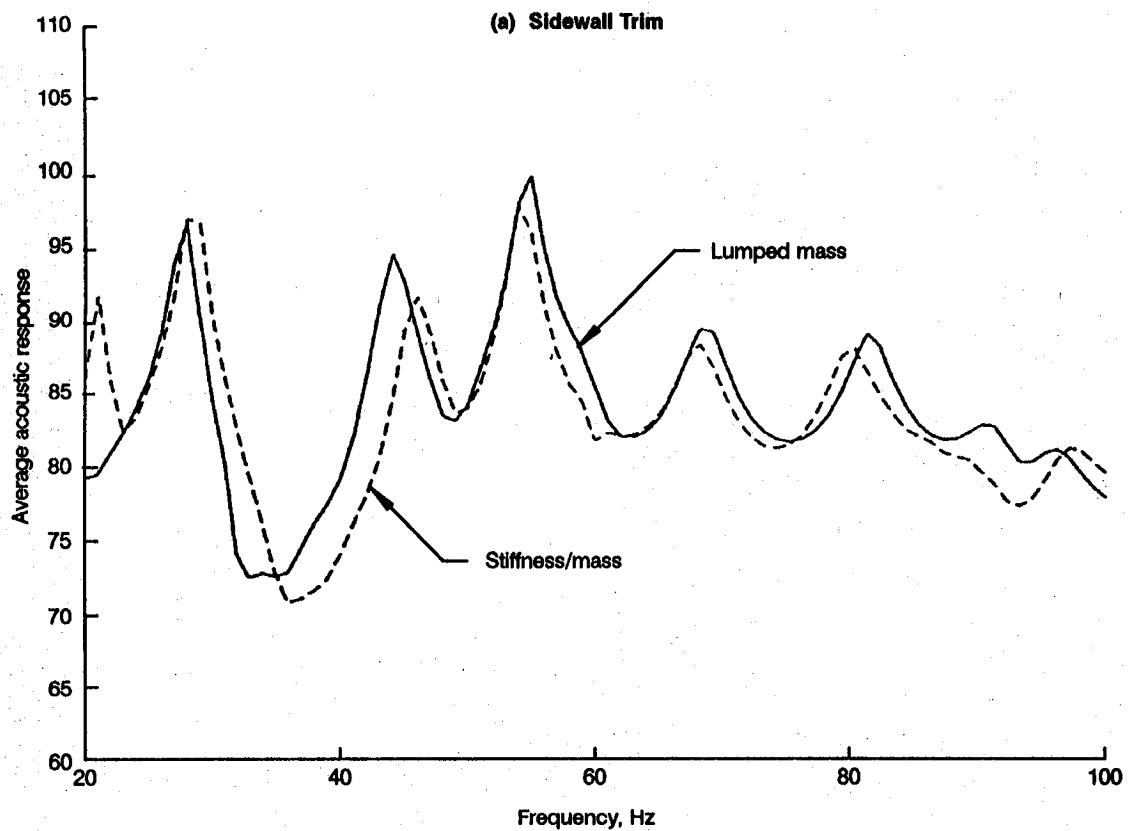


Figure 5. 727 Demonstrator One Frame Bay Interior Trim Modeling Study—Comparison of Mass/Stiffness Models Versus Mass-Only Representations

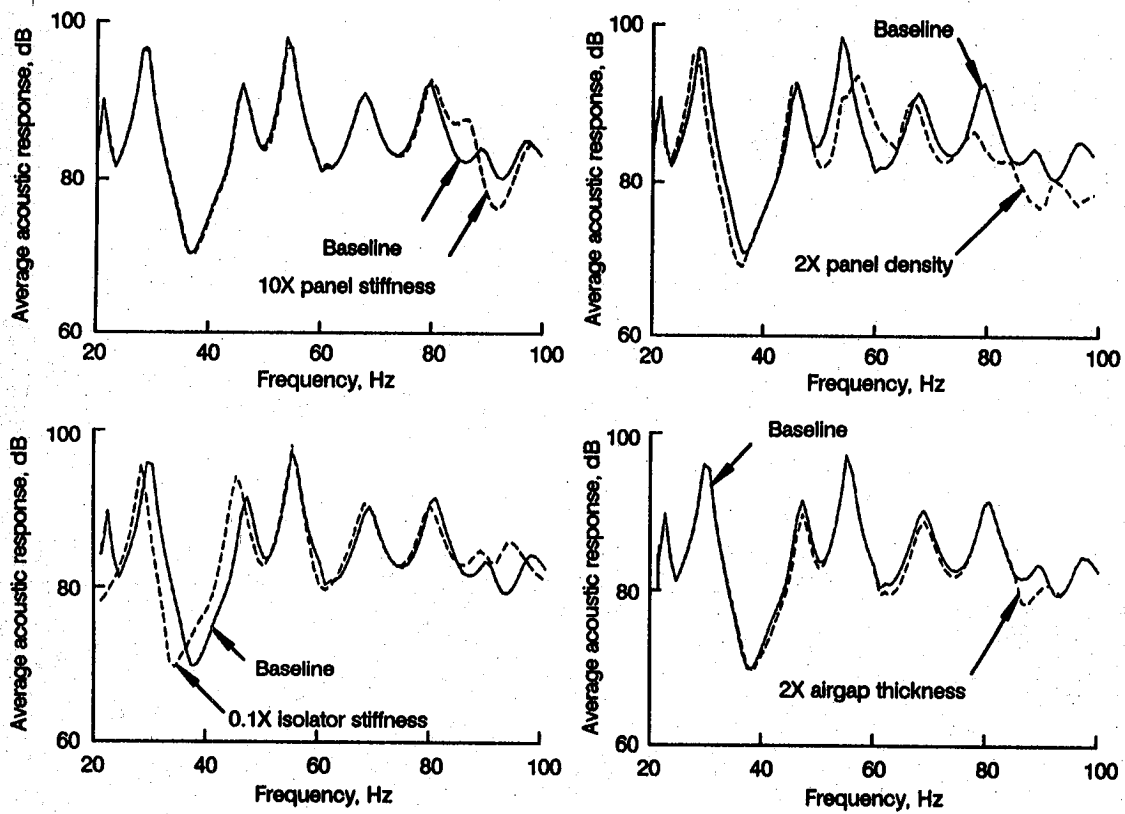


Figure 6. 727 Demonstrator One Frame Bay Sidewall Trim Parameter Study

Figure 8 shows a comparison of predictions using the baseline and upgraded acoustic finite element models. Results show that below the first cross-cabin mode (approximately 50 Hz) the model is fairly insensitive to the geometric changes incorporated. Above the first cross-cabin mode a more accurate description of the geometry has significant impact on the predicted acoustic response. This can be largely seen by the additional predicted response peaks at 60 Hz and 80 Hz from the upgraded model.

3.1.3 COMPARISONS TO GVT DATA

Predictions from the 727 Demonstrator airplane structure-acoustic model were compared to ground vibration test data for three GE36 engine mount shake conditions. These three shake conditions are vertical, lateral, and axial shakes on the aft lower mount of the strut. Comparisons were made in the frequency range 10-100 Hz for the drive point acceleration, bulkhead acceleration, floor acceleration, station 1010 frame acceleration, and cabin seat microphones. Station 1010 lies approximately half way between the aft pressure bulkhead and the acoustic curtain bounding the test arena. 727 Demonstrator

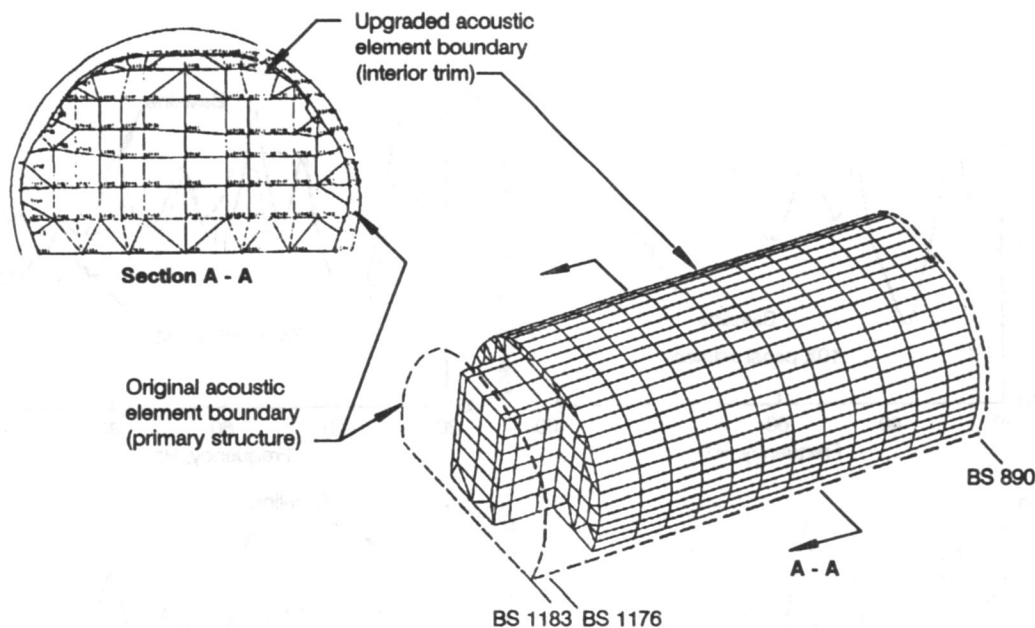


Figure 7. 727 Demonstrator Airplane Finite Element Model Acoustic Mesh

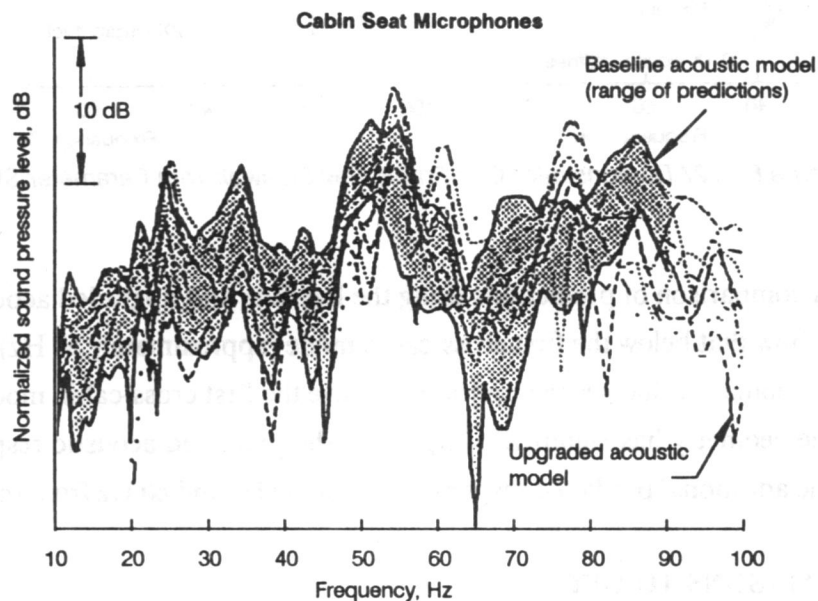


Figure 8. Effects of Modified Acoustic Space on Cabin Microphone Predictions

airplane finite element model predictions are compared to ground vibration test data in figures 9, 10, and 11.

Overall, the upgraded model shows good correlation with GVT data under 60 Hz. Predictions generally fall within the range of test data. Above 60 Hz, the model tends to overpredict the fuselage and floor response. This in turn leads to an overprediction of the cabin acoustic response in the same frequency-range. Also, the model generally underpredicts the bulkhead response over the entire frequency range.

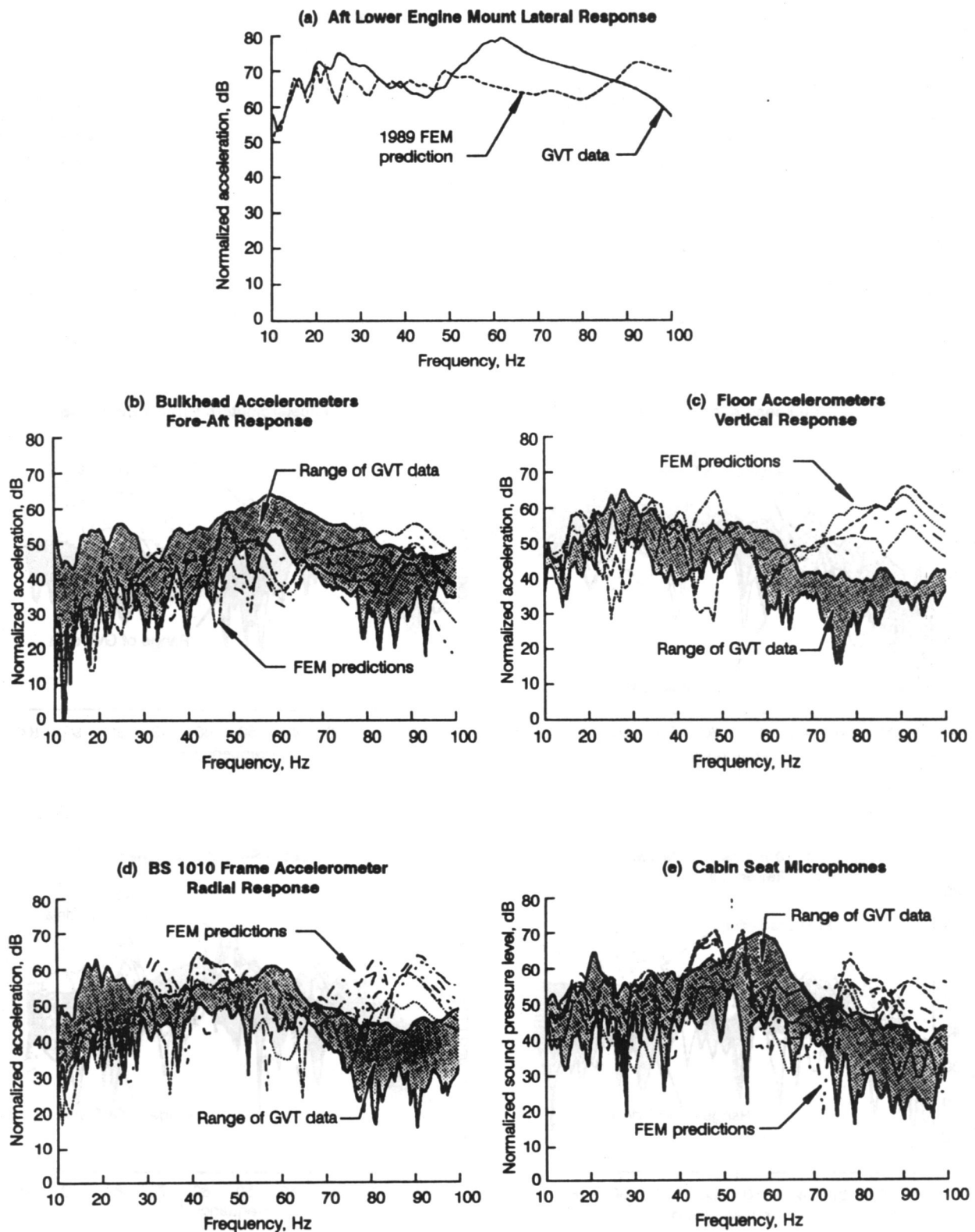


Figure 9. Finite Element Prediction Versus 727/GE36 Demonstrator Test (Ground Vibration Test—Aft Lower Mount Vertical Shake)

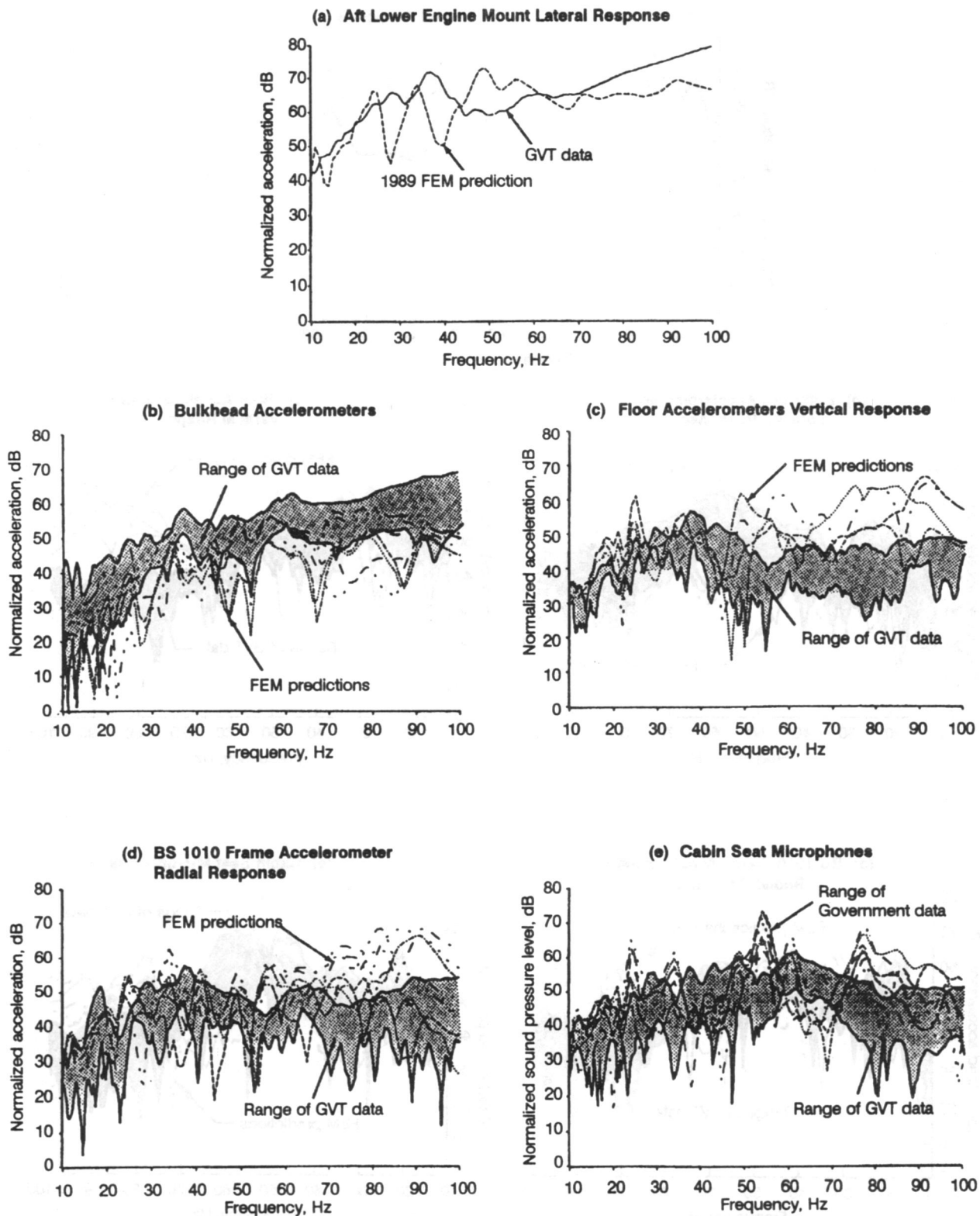


Figure 10. Finite Element Prediction Versus 727/GE36 Demonstrator Test (Ground Vibration Test—Aft Lower Mount Lateral Shake)

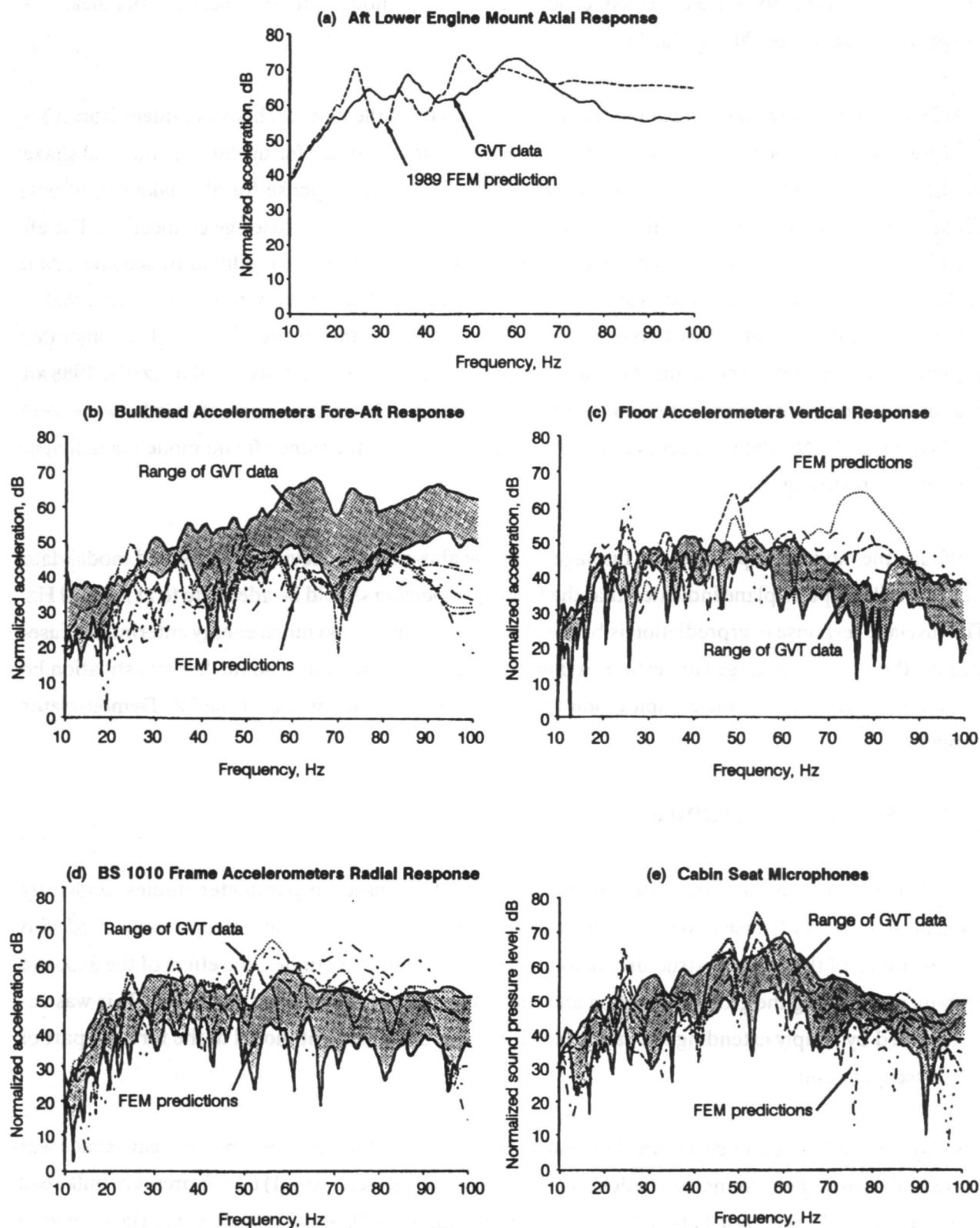


Figure 11. Finite Element Prediction Versus 727/GE36 Demonstrator Test (Ground Vibration Test – Aft Lower Mount Axial Shake)

This is most obvious for the axial shake condition where the model underpredicts the bulkhead response above 60 Hz by 20 dB (fig. 11).

In 1988, it was reported that there appeared to be deficiencies in the model. This was evident from a 3-4 Hz difference in response peaks (< 40 Hz) between prediction and test for the lateral and axial shake conditions as well as a general underprediction of the bulkhead response for all shake conditions. These differences were attributed to modeling difficulties of the strut-to-fuselage connection. The aft end of the 727 Demonstrator airplane is a complex, non-typical structure modified to accommodate the GE36 demonstrator strut and as such is very difficult to model. However, it was recommended at the time that no further investigations be made into understanding the aft end of the 727 Demonstrator airplane. Since there were no changes to the structural model for 1989 analysis (10-100 Hz) the 1988 aft end modeling deficiencies are reflected in 1989 results as well. Differences above 40 Hz between 1989 predictions and GVT data are believed to be primarily related to the same aft end modeling deficiencies noted previously.

Although the model overpredicts the fuselage response above 60 Hz, previously measured modal data from a similar type airplane indicated that the fuselage modeling should be adequate to at least 80 Hz. The fuselage response overprediction is believed to be the result of too much energy entering the fuselage via the strut-to-fuselage connection. Again, it was recommended that no further investigation be made into understanding the complex, non-typical structure of the aft end of the 727 Demonstrator airplane.

3.1.4 SENSITIVITY STUDIES

The 727 Demonstrator airplane structure-acoustic model was used for parameter studies to identify transmission paths of noise into the cabin and investigate noise suppression concepts associated with modifications of the primary structure. Before beginning parameter studies, the effect of the acoustic curtain, used during the ground vibration and flight tests, was removed from the model. This was accomplished by simply extending the cabin acoustic space finite element model to the forward part of the passenger cabin.

A study was performed to determine how much each surface bounding the cabin acoustic space was contributing to the interior noise predictions. The bounding surfaces were 1) the aft pressure bulkhead at station 1183, 2) the floor between station 1183 and station 890, and 3) the fuselage shell between station 1183 and station 890. The contribution of each surface was obtained for a vertical and lateral input at the aft lower mount by assigning the structure-acoustic coupling so that only one surface at a

time was allowed to excite the acoustic space. Figure 12 gives the relative contribution of each surface radiating into the acoustic space. Results indicate that the acoustic response is being controlled by the fuselage shell and floor. The importance of the shell and floor varies with frequency and shake direction. With the exception of a few frequencies, contributions of the bulkhead are predicted to be insignificant.

Various cabin noise suppression concepts were investigated using the upgraded finite element model. Suppression concepts considered were 1) reducing the stiffness of the GE36 strut (fig. 13), 2) increasing the empennage stiffness (fig. 14), 3) decreasing the bulkhead stiffness (fig. 15), and 4) increasing the weight of the floor (fig. 16). For the concepts investigated, no one concept leads to a general reduction of cabin noise for all frequencies and shake directions.

Below 30 Hz, empennage stiffness and floor mass have an influence on acoustic response. By changing the mass of the floor and stiffness of the empennage, dominant modes are shifted to different frequencies, thus lowering the response at the resonant frequencies of the baseline model. This can be used to advantage by designing the airplane so dominant structural modes do not occur in the frequency range of interest.

The acoustic response is very sensitive to strut stiffness above 30 Hz. Around the 55 Hz acoustic response peak, bulkhead stiffness also significantly influences the response. The 55 Hz response peak is suspected to be due to a bulkhead mode. In addition, increased empennage stiffness shows slight benefits above 70 Hz for both shake directions.

3.2 1990 FINITE ELEMENT ANALYSIS

In FY 1990, a 767-300 airplane structure-acoustic finite element model was compared to ground vibration test data (20-75 Hz). This model was then used to investigate the sensitivity of cabin noise and vibration to various parametric changes.

3.2.1 767-300 AIRPLANE STRUCTURE-ACOUSTIC FINITE ELEMENT MODEL

The finite element model of the 767-300 airplane was developed from previously generated finite element models that had been used for static internal loads analysis. Because of airplane symmetry only the left side of the 767-300 airplane was modeled. The full airplane response was then obtained by combining the symmetric and the anti-symmetric solutions. The model consists of (a) beam element models that represent the gross stiffness and mass properties of the fuselage section forward of station

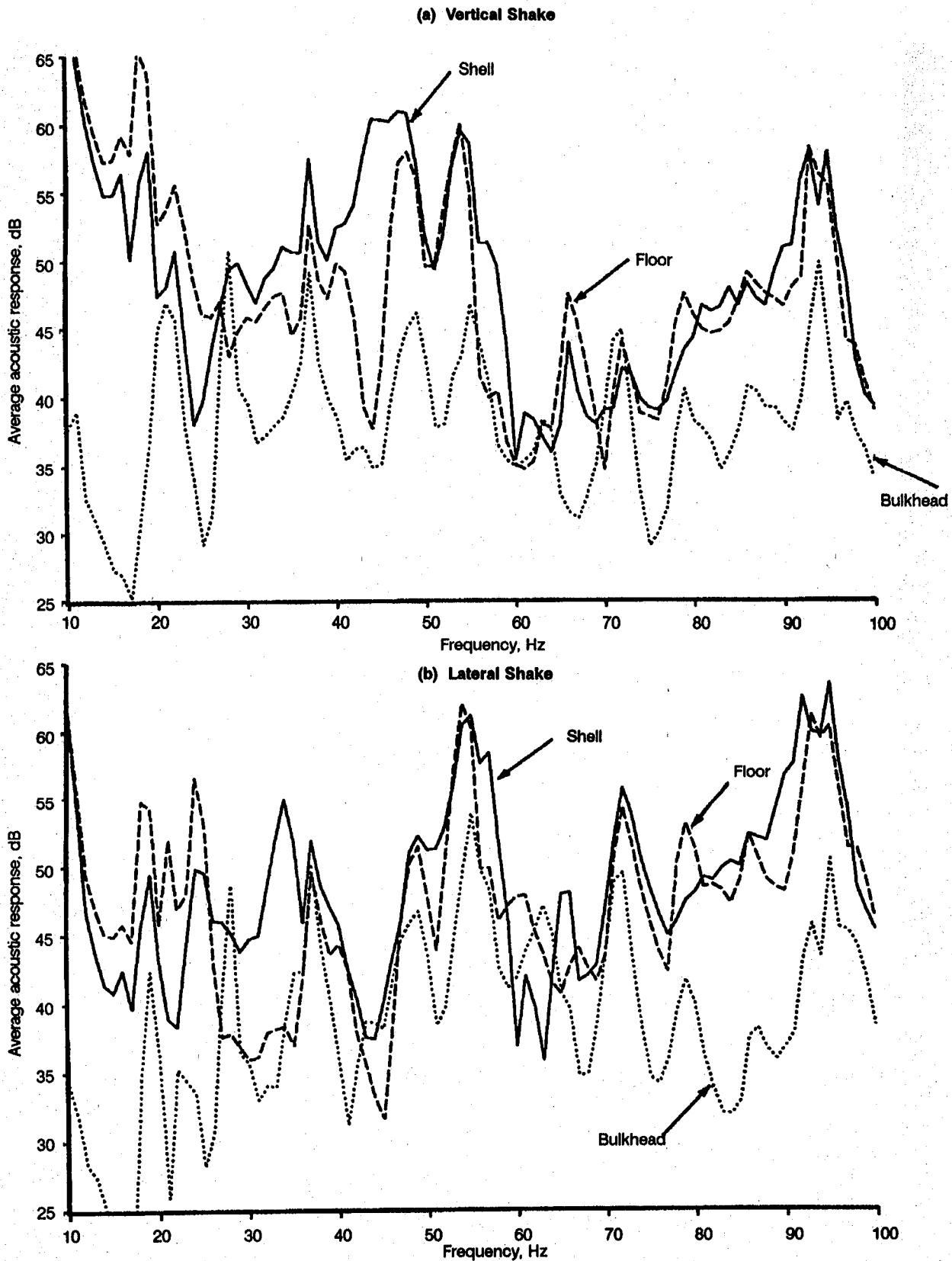


Figure 12. 727 Demonstrator Airplane Finite Element Model—Contribution of Shell, Floor, and Bulkhead to Cabin Noise

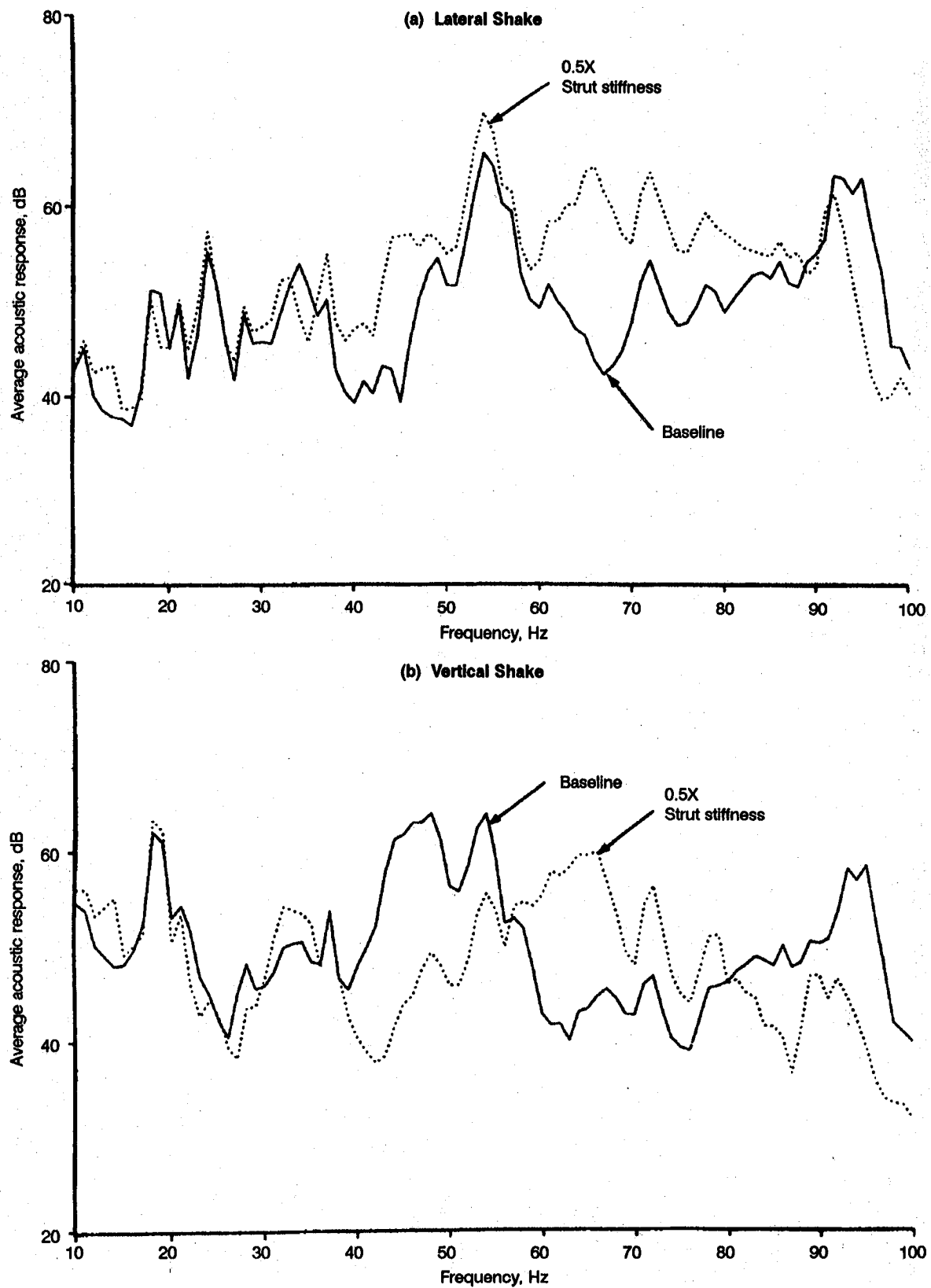


Figure 13. 727 Demonstrator Airplane Finite Element Model Parameter Study – 0.5X Strut Stiffness

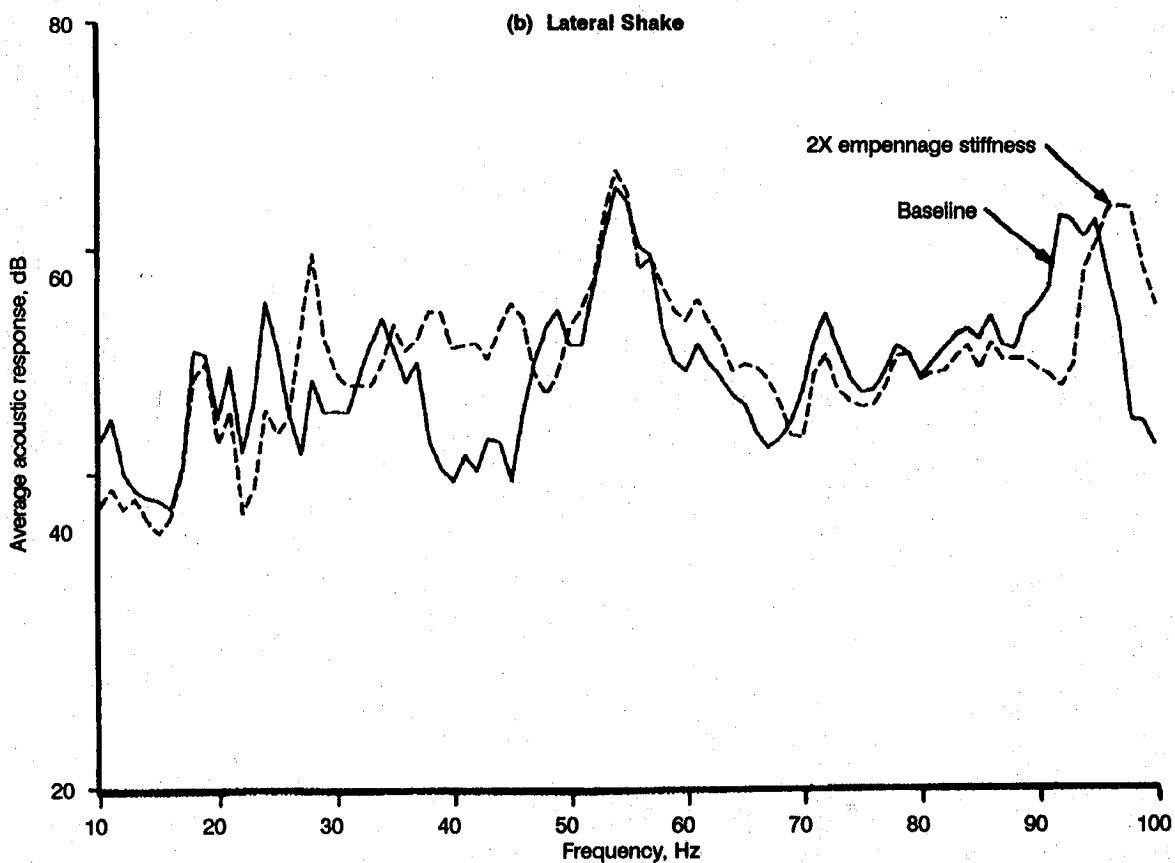
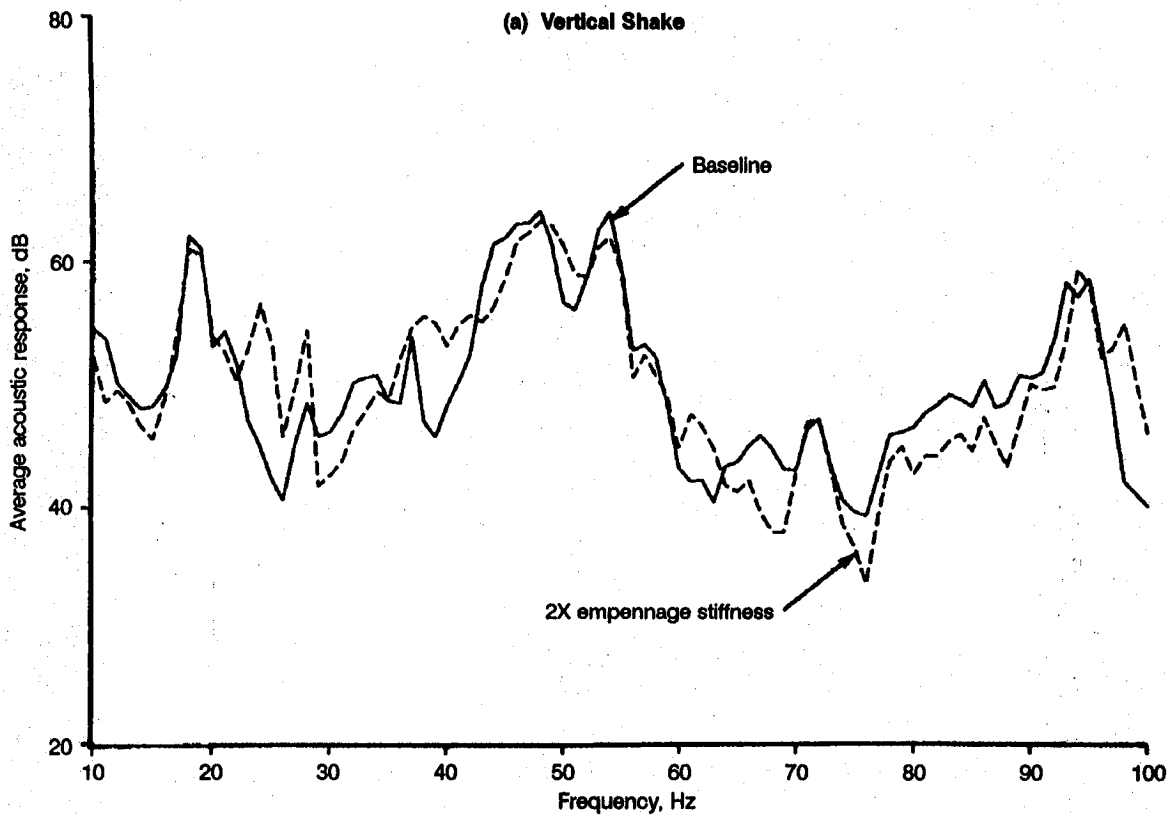


Figure 14. 727 Demonstrator Airplane Finite Element Model Parameter Study—
2X Empennage Stiffness

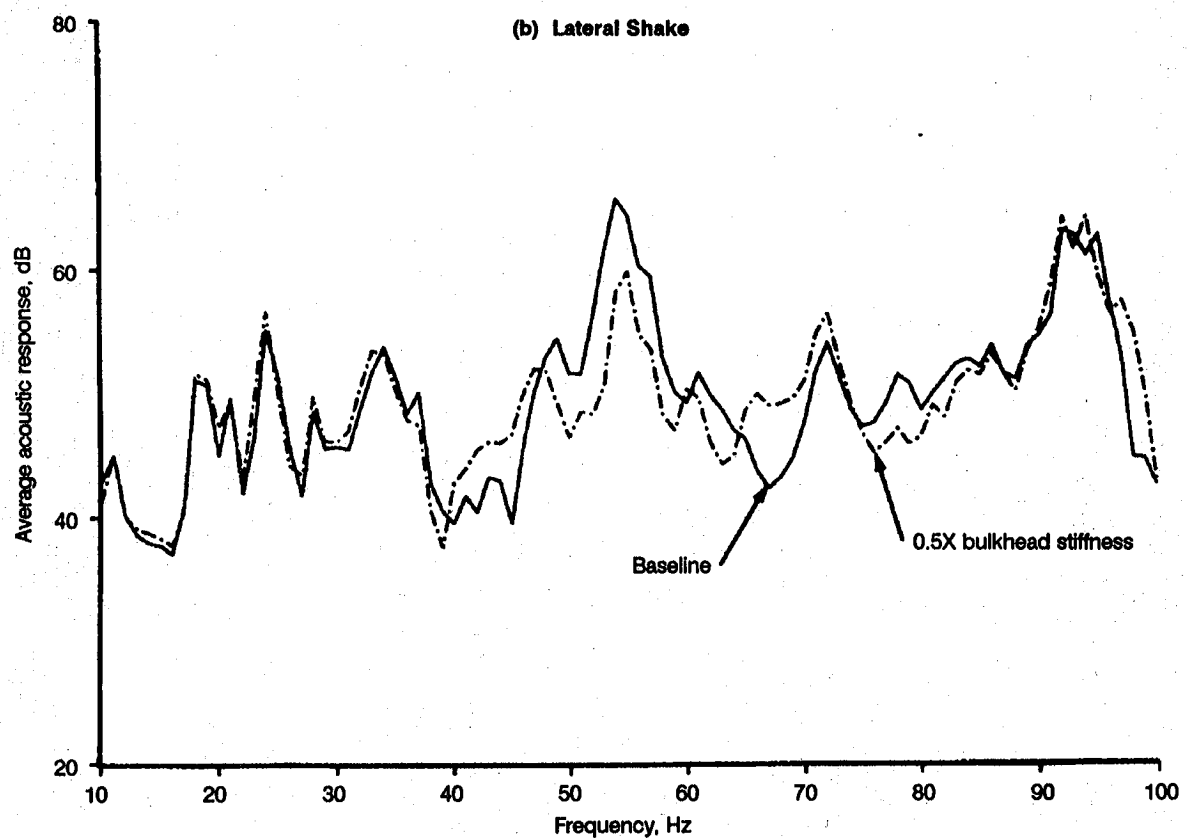
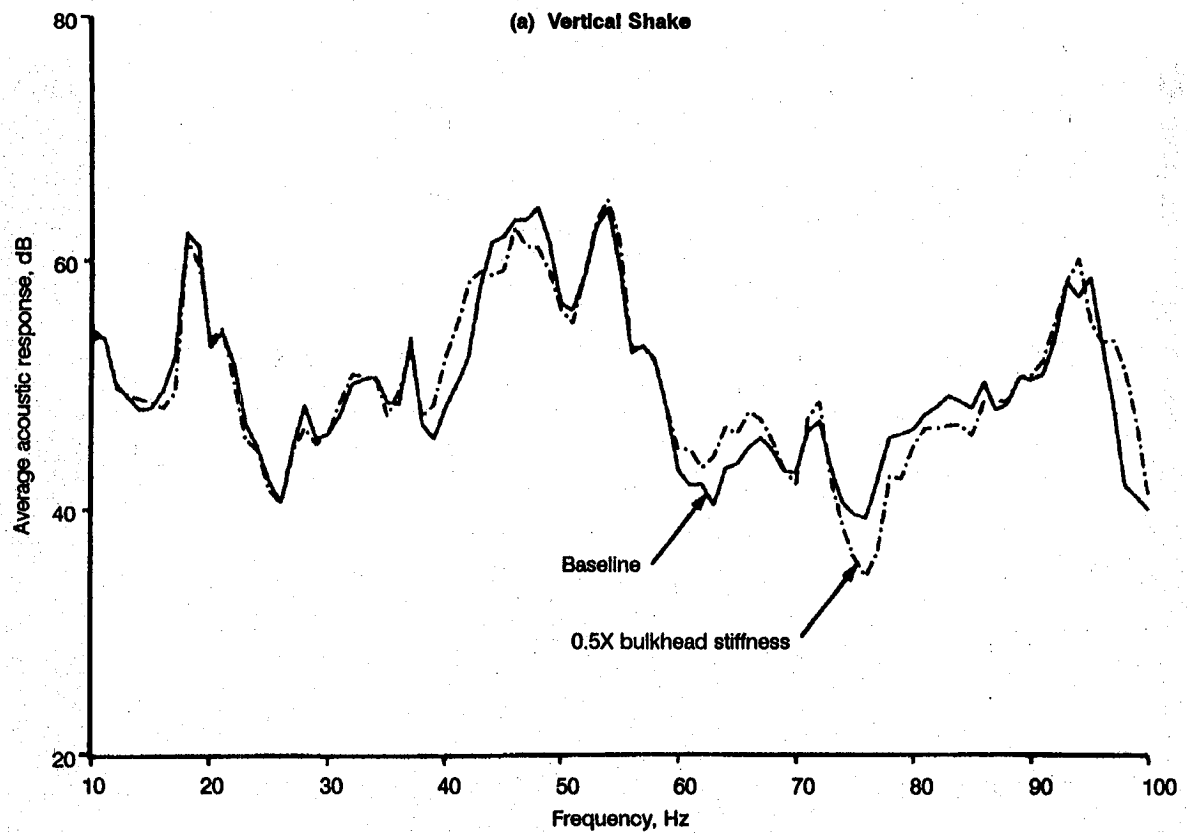


Figure 15. 727 Demonstrator Airplane Finite Element Model Parameter Study—
0.5X Bulkhead Stiffness

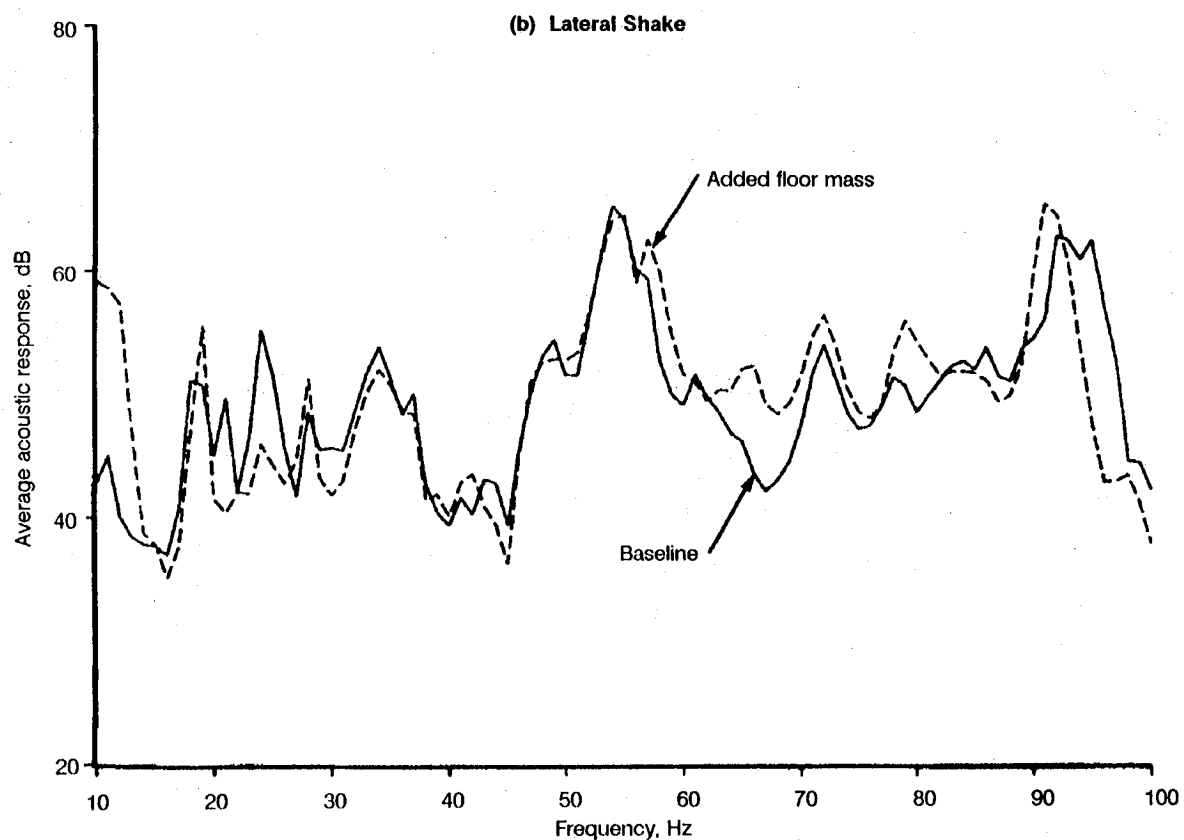
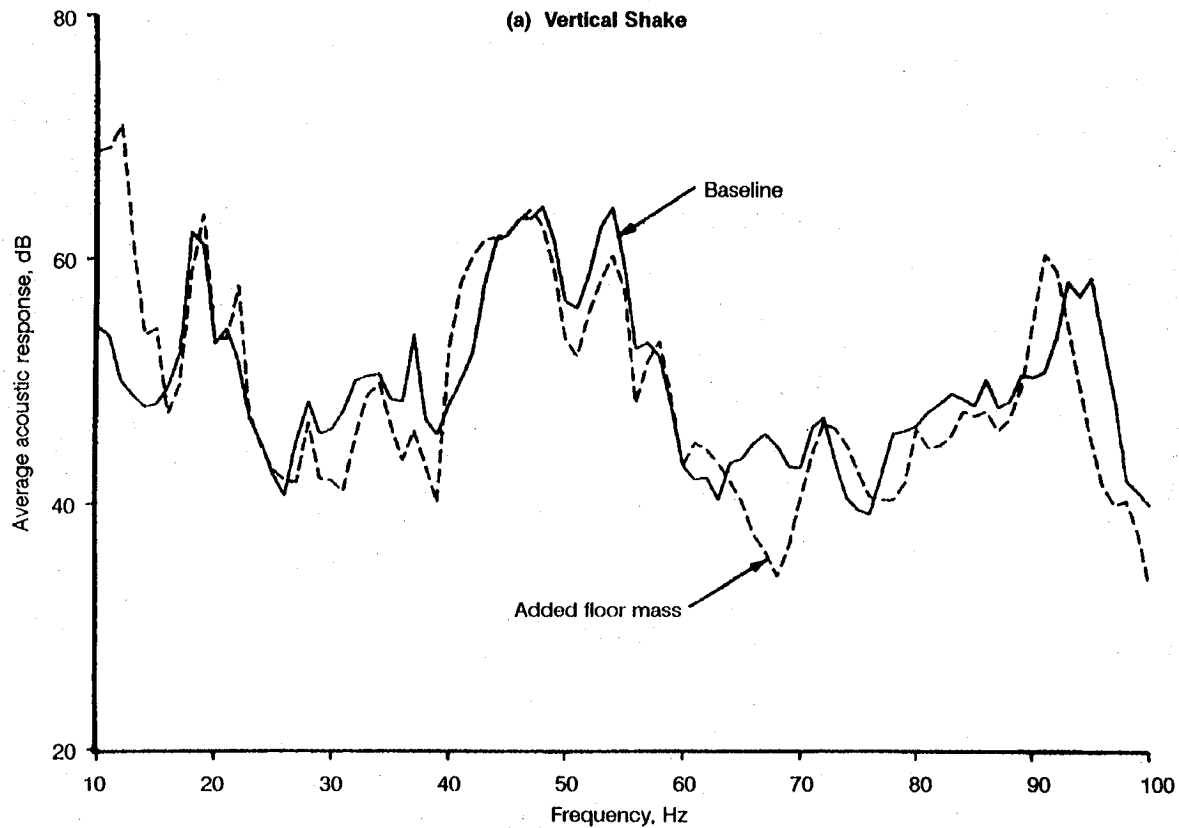


Figure 16. 727 Demonstrator Airplane Finite Element Model Parameter Study—
Added Floor Mass (5,000 lb)

357 and the section aft of station 1329, (b) detailed finite element models of the fuselage structure between station 357 and station 1329, and (c) detailed finite element models of the wing structure. The resulting finite element mesh is shown in figure 17 for the ground vibration test (GVT) configuration. For the sensitivity studies, the landing gear was retracted (flight configuration).

The cabin space acoustic model extends the entire length of the 767-300 cabin. However, the acoustic model is interfaced with the structure model between station 357 and station 1219, only. The structural floor nodes are interfaced directly to the acoustic floor nodes occupying the same location. For the sidewall, the structural nodes representing the frames at the outer mold line are interfaced to the acoustic nodes representing the inboard side of the trim panel. The distance between the outer mold line and the inboard side of the trim panel is approximately five inches. For the ceiling, the models are interfaced by connecting the structural nodes along the crown of the airplane to the acoustic nodes representing the surfaces of the overhead bins and ceiling panels (fig. 18). Previous studies have shown that the interface as depicted in figure 18 is adequate for making acoustic response predictions under 80 Hz.

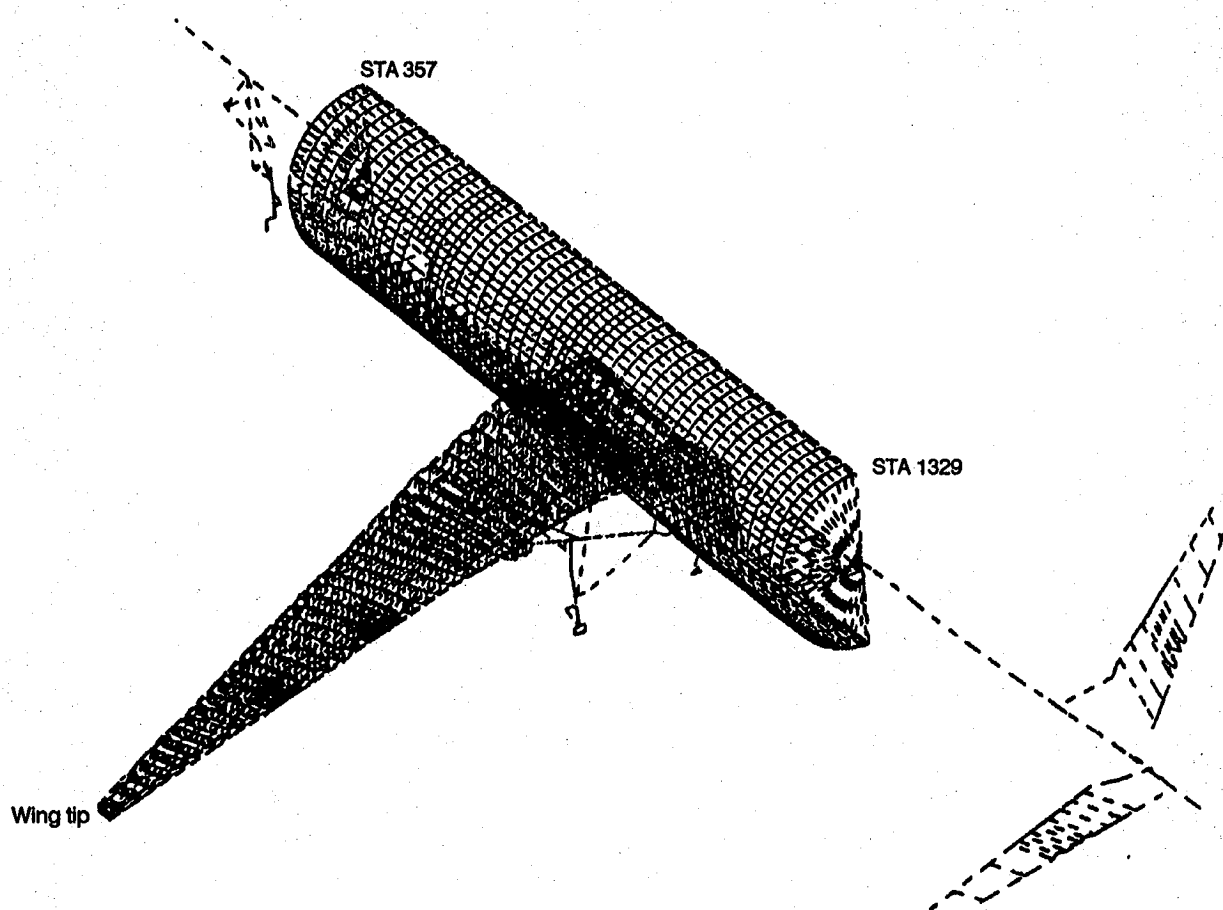


Figure 17. 767-300 EVRN Detailed Finite Element Model

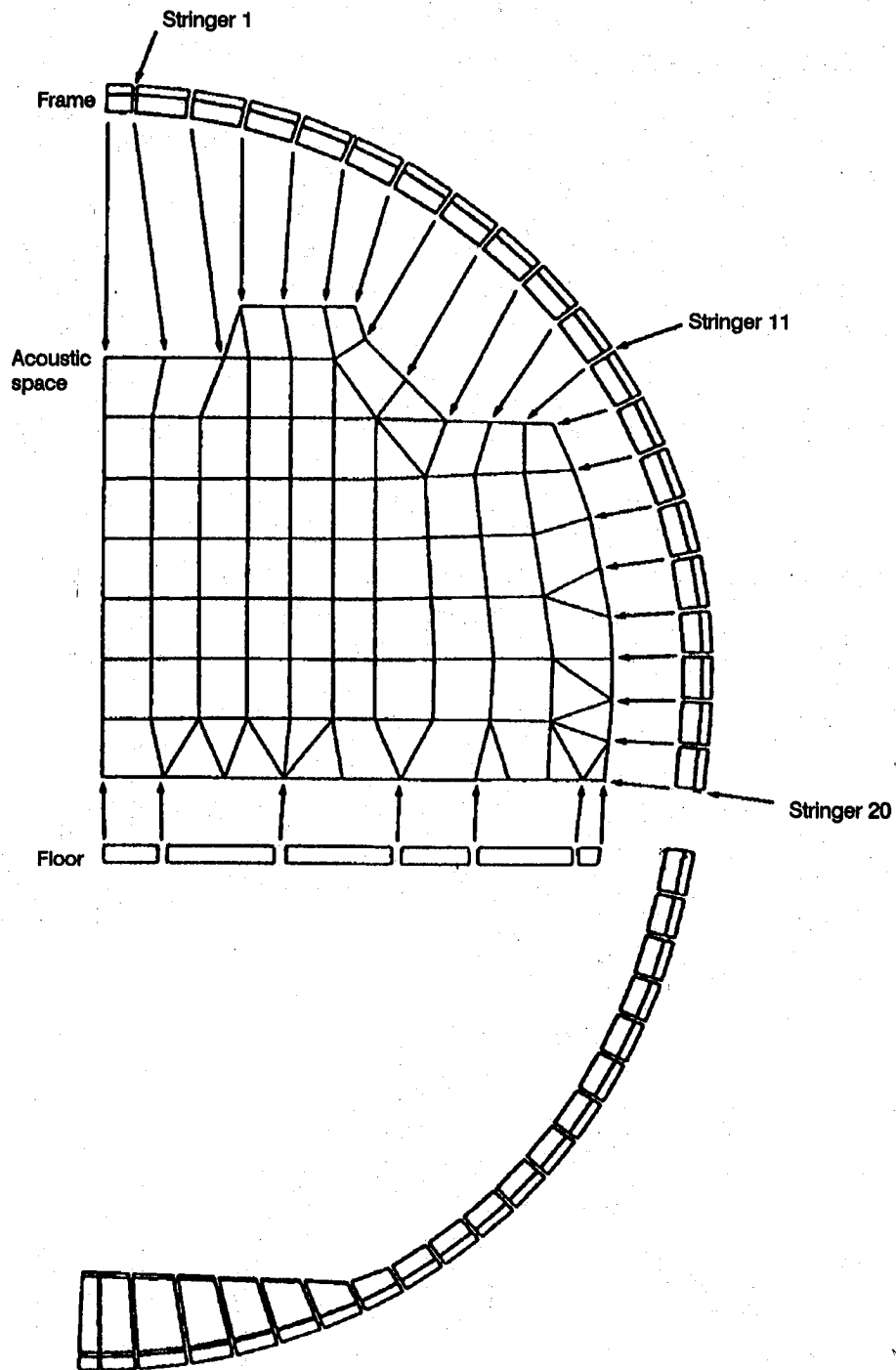


Figure 18. 767-300 Structure/Acoustic Interface—Typical Cross Section

Conclusions from FY 1989 regarding the modeling of interior trim and the sensitivity to geometric changes in the acoustic space model were incorporated in to the construction of the baseline 767-300 airplane finite element model.

3.2.2 COMPARISONS TO GVT DATA

Predictions from the 767-300 airplane structure-acoustic finite element model were compared to data from three ground vibration test engine mount shake conditions. For this report, comparisons were made in the frequency range 20-75 Hz for the mid spar fitting vertical response and the cabin seat microphones. In addition, for the rear mount vertical shake, comparisons were also made to fuselage accelerometers. Fuselage accelerometer data were gathered only for the rear mount vertical shake during ground vibration testing. Layout of the engine mounts and instrumentation used in the comparisons are depicted in figure 19.

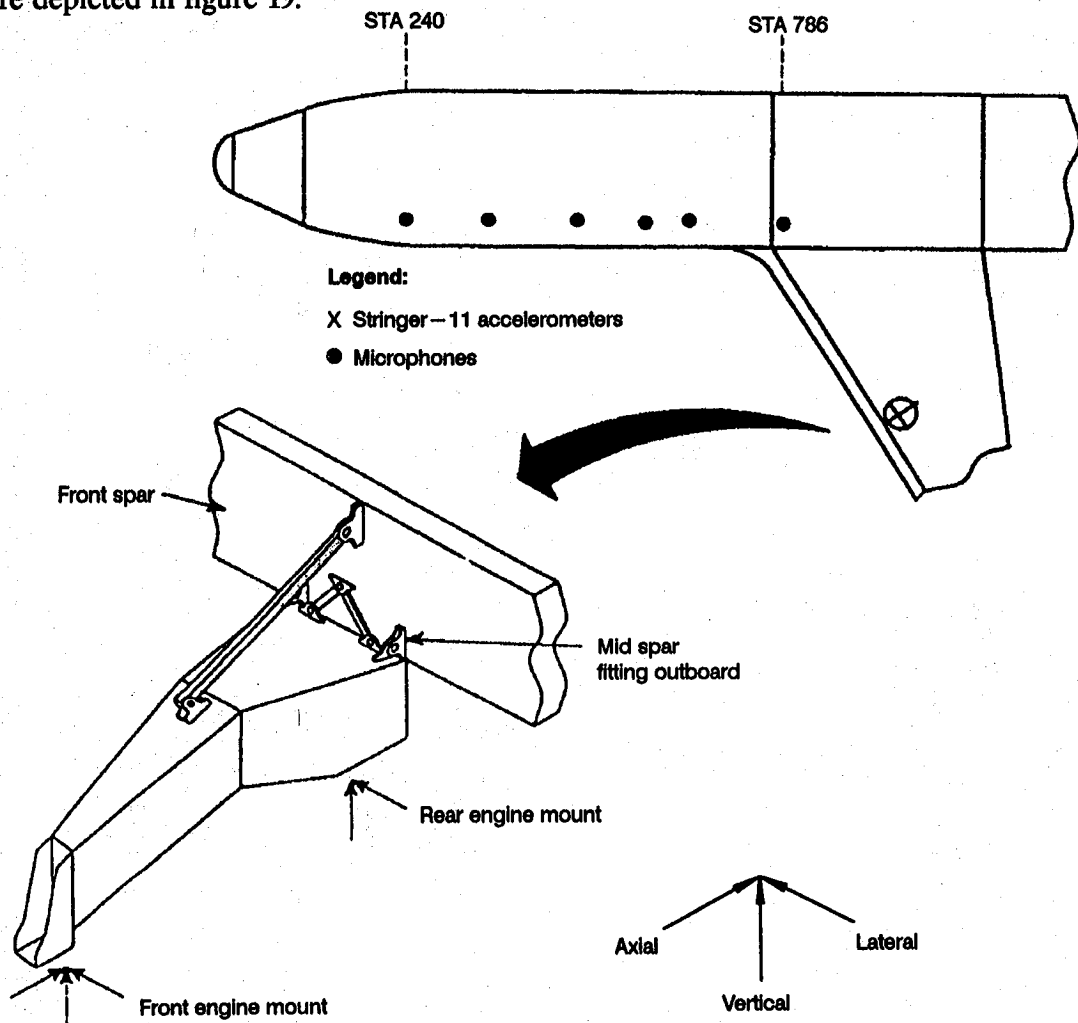


Figure 19. 767-300 FEM Prediction Measurement Comparison Points

The front mount vertical shake condition response predictions are shown in figure 20. For the front mount vertical shake the model fails to predict a sharp drop in the mid spar fitting vertical response between 50-55 Hz. This in turn leads to an overprediction in the cabin acoustic response by as much as 20 dB. These differences are believed to be primarily the result of modeling deficiencies in the strut and/or strut-to-wing connections. Further analysis is required to determine the modeling requirements of the strut and/or strut-to-wing connections for accurate predictions at the mid spar fitting. In defining the modeling requirements, one must keep in mind the ultimate goal of predicting cabin noise due to engine unbalance. Since the mass of the strut is small compared to an engine and the wing and fuse-

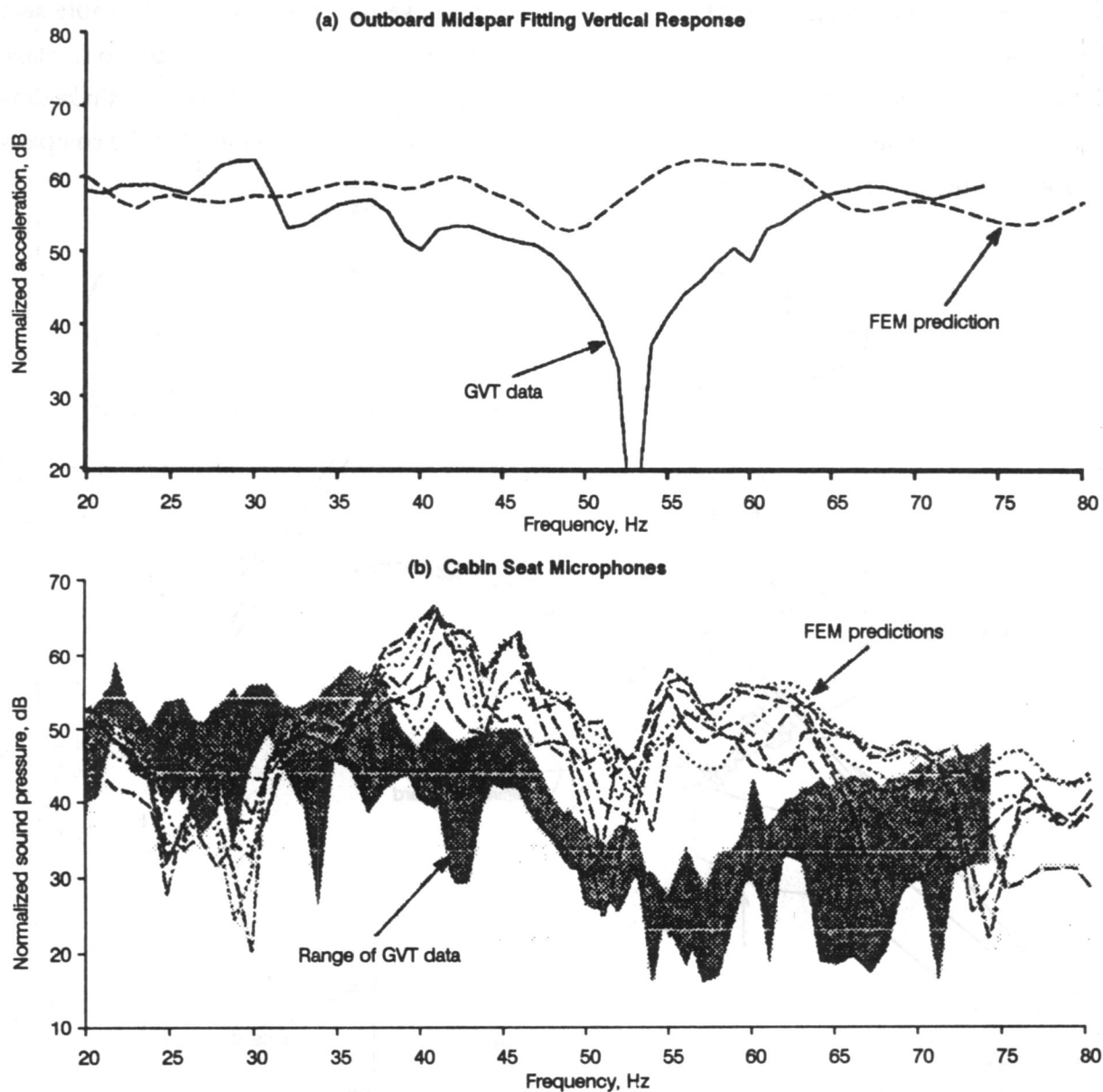


Figure 20. Finite Element Prediction Versus 767-300 Ground Vibration – Front Mount Vertical Shake

large portions of the airplane, the modeling requirements on the strut may be less stringent once an engine is integrated into the system, than for a ground vibration test in which the engine has been removed.

The rear mount vertical shake condition response predictions are shown in figure 21. For the rear mount vertical shake, the model generally shows good correlation with ground vibration test data. The model overpredicts the GVT response peak at 47 Hz for the mid spar fitting vertical response by approximately 4 Hz and 3 dB. This error is amplified in the predictions of the fuselage response, in the 45-55 Hz range, where the model tends to overpredict the response by 10 dB. This in turn leads to an overprediction of the acoustic response by 5-10 dB in the same frequency range. Although the previously discussed modeling deficiencies in the strut and/or strut-to-wing connections could be contributing to the overprediction of the responses for the rear mount vertical shake condition, the amplification of the error between the strut and the fuselage indicates a potential deficiency in the wing-fuselage portion of the model. It is very difficult to separate the effects of the strut from the rest of the model in determining the source of the deficiency. As such, it is recommended that the wing-fuselage model be validated independent of the strut. This would require additional ground vibration testing with the strut removed, and shaker inputs going directly into the wing at the strut attach points.

The front mount lateral shake condition predictions are shown in figure 22. The model generally predicts the GVT data trends for the mid spar fitting vertical response. As with the rear mount vertical shake condition, the model overpredicts the 47 Hz peak in the GVT data by approximately 4 Hz and 3 dB. Acoustic response predictions generally fall within the range of the measured data. Consistent with the rear mount shakes, the model overpredicts the 50 Hz acoustic response for the front mount lateral shake by 7-10 dB. Above 65 Hz the model greatly overpredicts the acoustic response. This overprediction appears to be related to a smaller predicted peak in the mid spar fitting response at 72 Hz.

3.2.3 SENSITIVITY STUDIES

Sensitivity studies were run to evaluate the effect of parametric changes to the finite element structure model on the predicted structure-acoustic response. Parametric changes to the model included the addition of fuel loading (mass) and major stiffness increases to the wing primary structure inboard of the strut attachments (fig. 23). Since for an advanced propeller installation the strut would probably be radically different than the current strut, the strut was removed from the model for the sensitivity studies. Also, removing the strut eliminated the suspected modeling deficiencies in the strut and/or strut-to-wing connections, as seen in the comparison to ground vibration test data for the front mount vertical shake condition. For the parametric studies, the model was excited in the vertical direction at

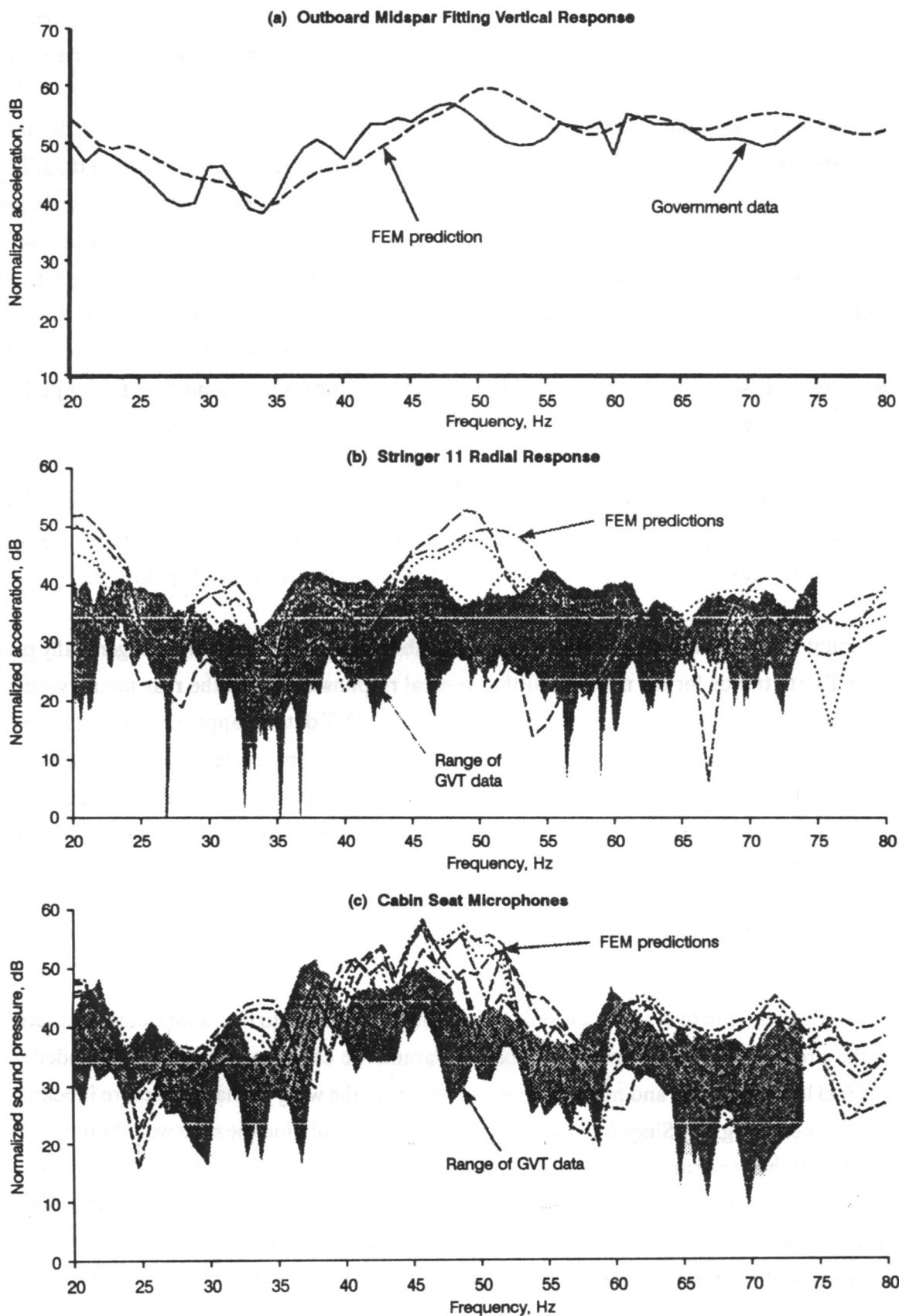


Figure 21. Finite Element Prediction Versus 767-300 Ground Vibration Test—Rear Mount Vertical Stake

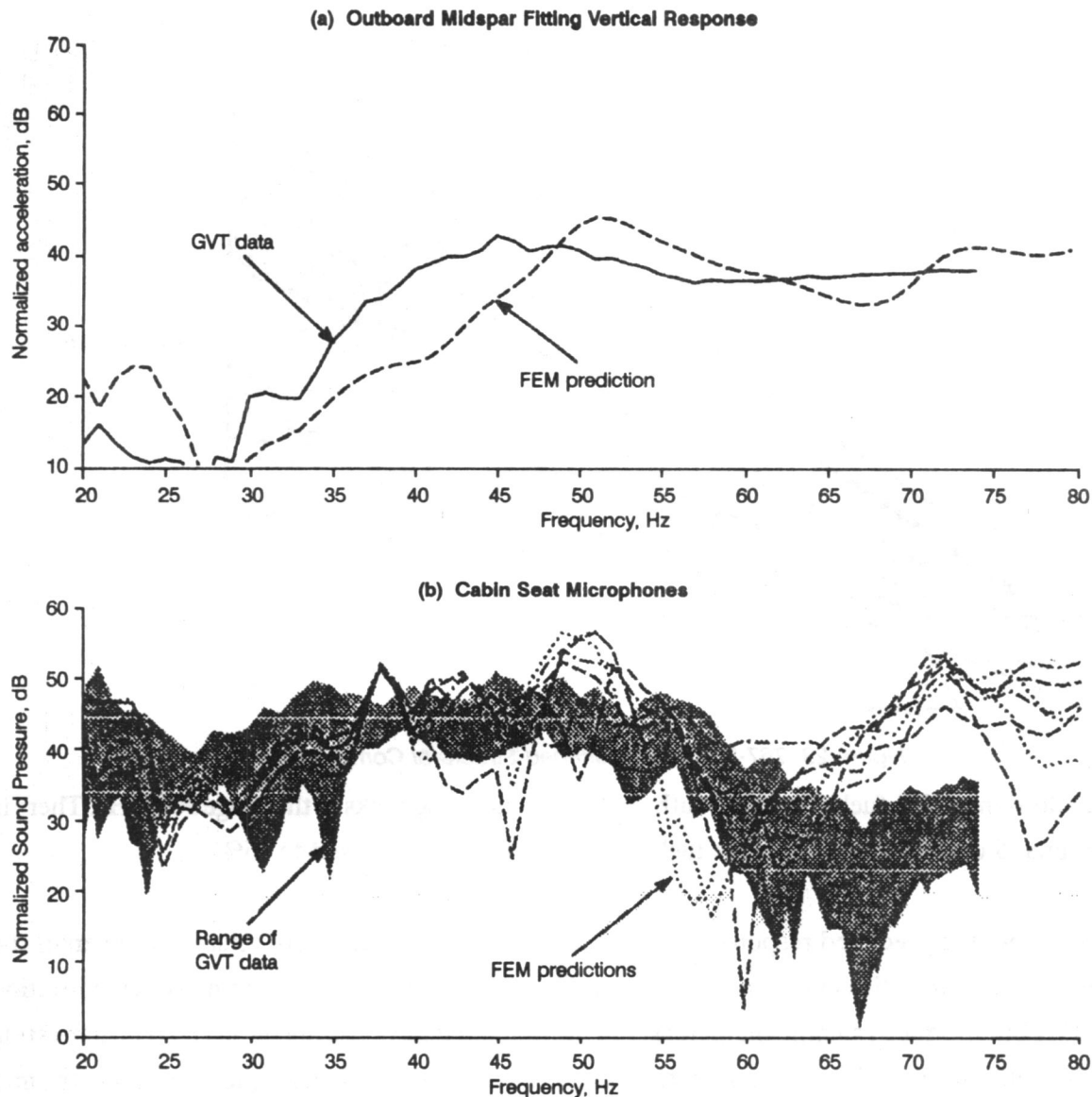


Figure 22. Finite Element Prediction Versus 767-300 Ground Vibration Test—Front Mount Lateral Stake

the outboard mid spar fitting on the wing. Predictions are made at the drive point, and average responses of the floor and fuselage acceleration, and cabin seat microphones.

Three different fuel levels were analyzed : 1) empty, 2) 40% fuel in the outboard wing tank, 40% fuel in the center wing tank, and 3) 75% fuel in the outboard wing tank, 40% fuel in the center wing tank. In all cases, fuel is modeled as mass only. Results show that the presence of fuel can have a significant impact on the cabin acoustic predictions and should be accounted for in a flight configuration. Figure 24 shows the predicted response for the three fuel levels. As one might expect, there are significant reductions in the response due to the addition of fuel for a vertical shake. These reductions are largely confined to the 30-60 Hz range. For the cabin acoustic response there are 5-7 dB reductions associated

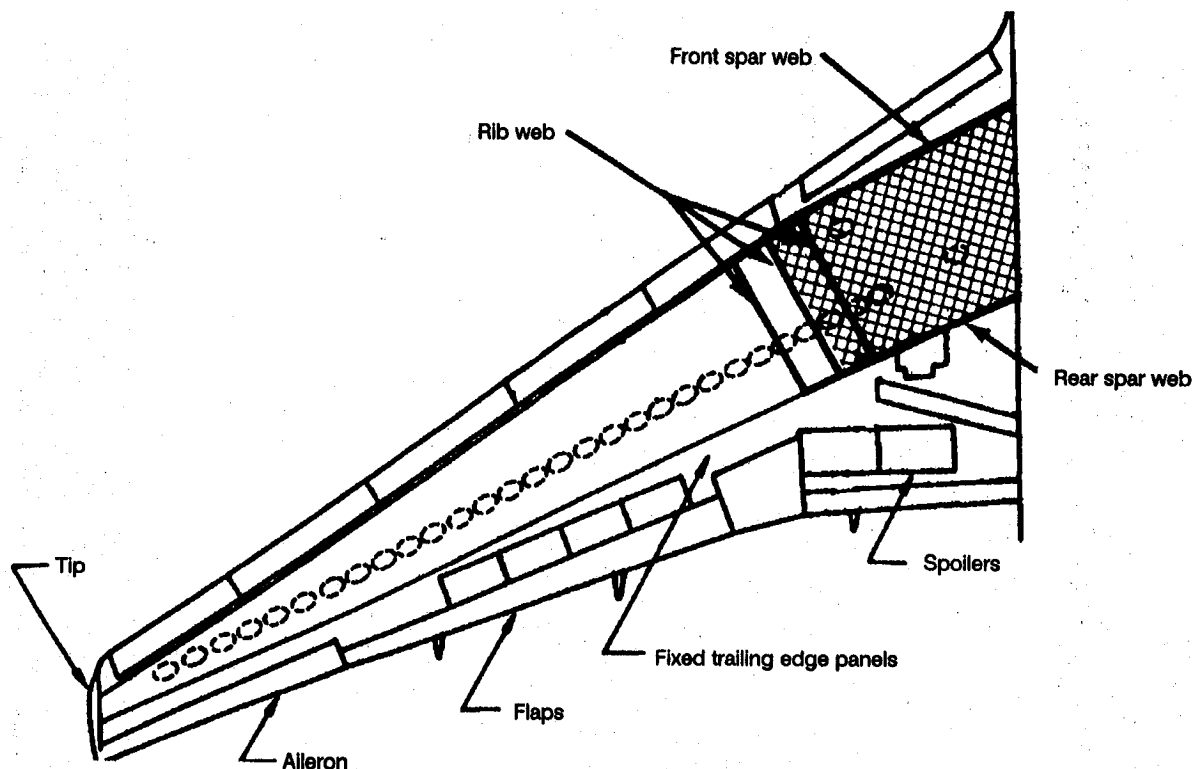


Figure 23. 767-300 EVRN Stiffened Structural Components

with the addition of 40% fuel in both the outboard and center wing tanks in the range 30-60 Hz. There is an additional 5 dB reduction when the fuel in the wing tank is increased to 75%.

Figure 25 shows the predicted response for a stiffer wing inboard of the strut attachments versus the baseline wing. Adding stiffness to the wing generally had no effect on the cabin noise and vibration under 50 Hz but produced significant increases in the predicted response above 50 Hz. It is interesting to note that although the stiffness modifications caused some fairly distinct frequency shifts in the mid spar fitting vertical response at 39 Hz and 57 Hz, similar distinct frequency shifts are not noted in the fuselage, floor, and cabin noise predictions. It was hoped that by increasing the wing stiffness, dominant structural modes could potentially be shifted out of a particular frequency range, and thus be beneficial to the cabin acoustic response. However, peaks in the cabin acoustic response appear to increase only in amplitude and are not generally shifted in frequency due to modifying the wing stiffness.

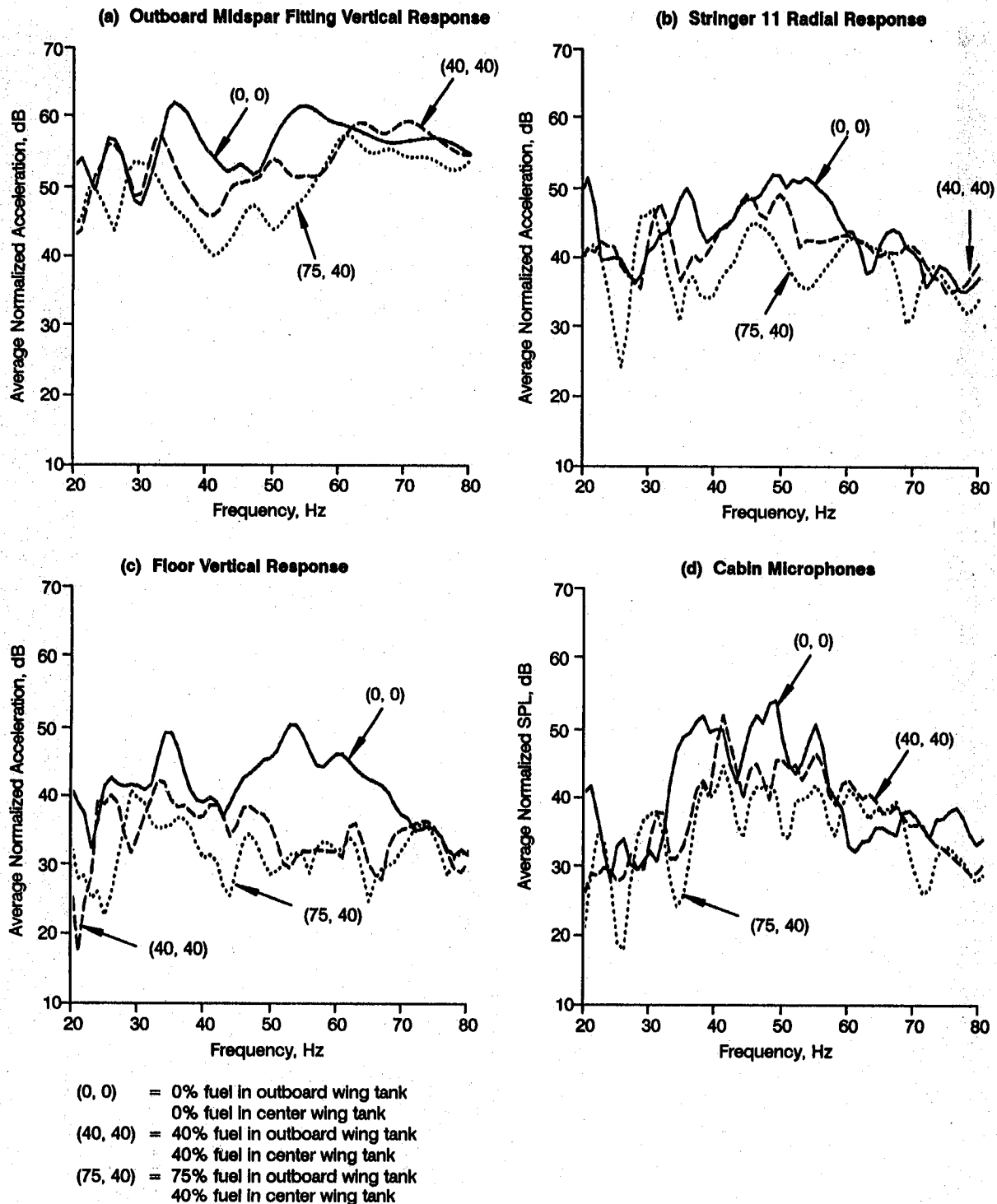


Figure 24. Effect of Fuel in the Outboard Wing and Center Wing Tanks for a Vertical Input to the Wing

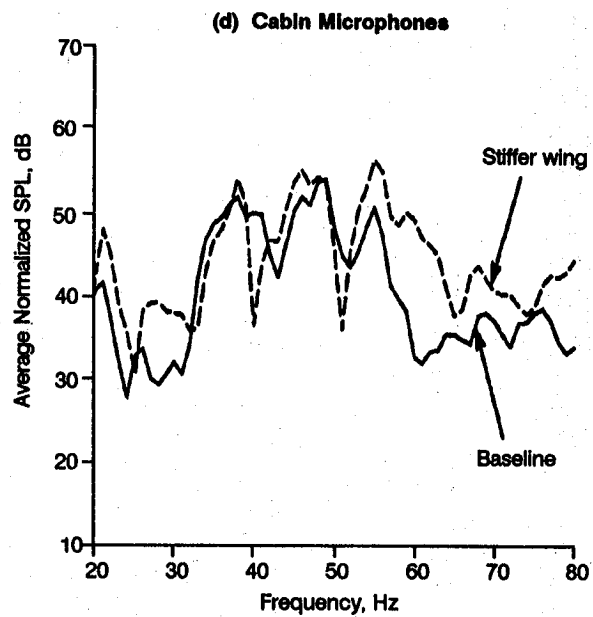
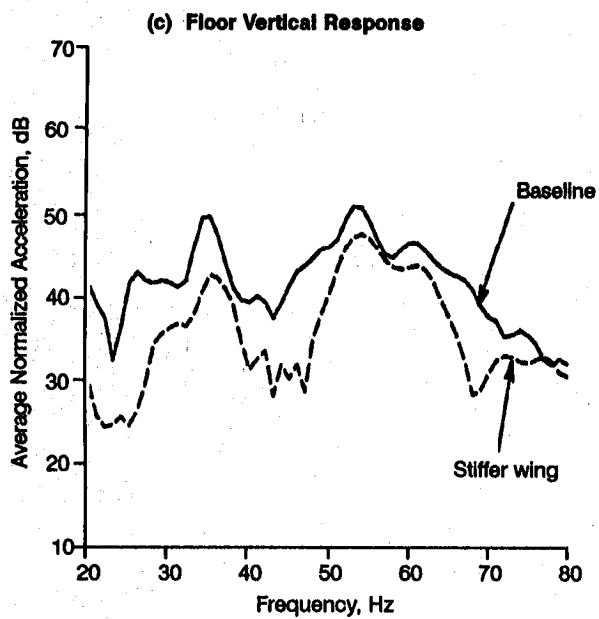
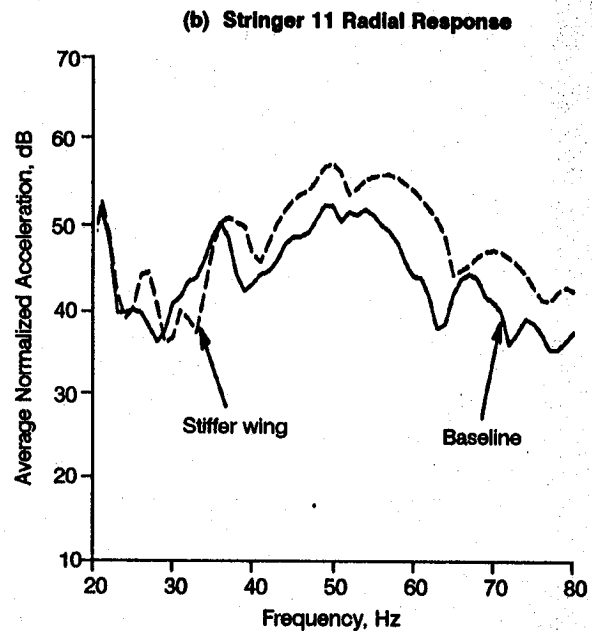
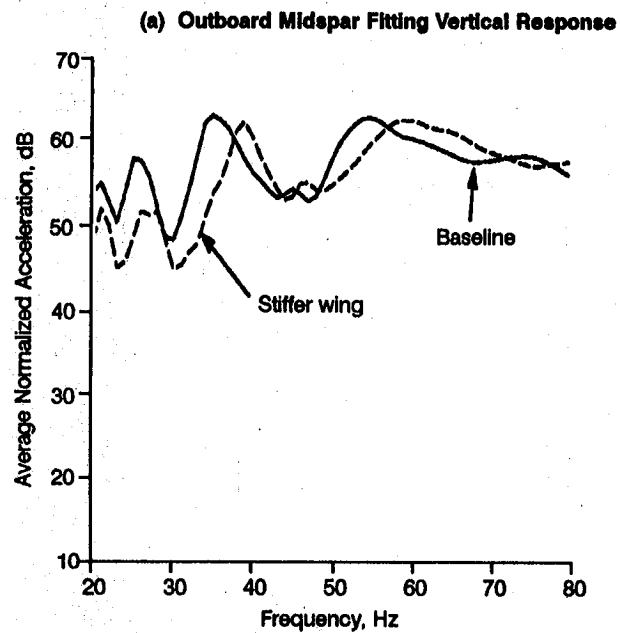


Figure 25. Effect of Stiffer Inboard Wing for a Vertical Input to the Wing

4.0 STATISTICAL ENERGY ANALYSIS

For the 727 Demonstrator airplane aft-mounted configuration a 26 element low-frequency (LF) model (fig. 26) was used for the shaft rotational frequency analysis up to 200 Hz and a 72 element mid-frequency (MF) model was used for the propeller blade-passage frequency and its harmonics up to 400 Hz. (More detail of these models can be found in ref.1.) The MF SEA model differed from the LF model in substructure element size, composition and handling of the trim panels. The substructure element boundaries were chosen to reflect finer variations in construction that were felt might affect response in this frequency range. Because on the actual airplane there was an acoustic barrier at station 890, this more detailed modeling was only done for the sections aft of this station for the aft-mounted configuration studies. For the airborne excitation studies on the wing-mounted configuration an expansion of the MF model was used. This model removed the barrier at station 890 and extended the detail forward to station 650 (fig. 27). For the wing-mounted configuration engine vibration studies a 41 element low frequency model of the 767-300 airplane was used (fig. 28). This model was handled the same as the 727 Demonstrator LF model except that more detail was put into the wing and wing-to-side-of-body junctions and less detail was put into the empennage section. Although the 767-300 airplane differs in size from the 727, they are so similar in basic design that energy transmission paths from the wing to the cabin will very likely be the same for both airplanes for wing excitation. Suppression concepts for structureborne noise based on the 767-300 model should carry over to the hypothetical 727 Demonstrator with wing mounted engines or any other wing mounted propeller aircraft.

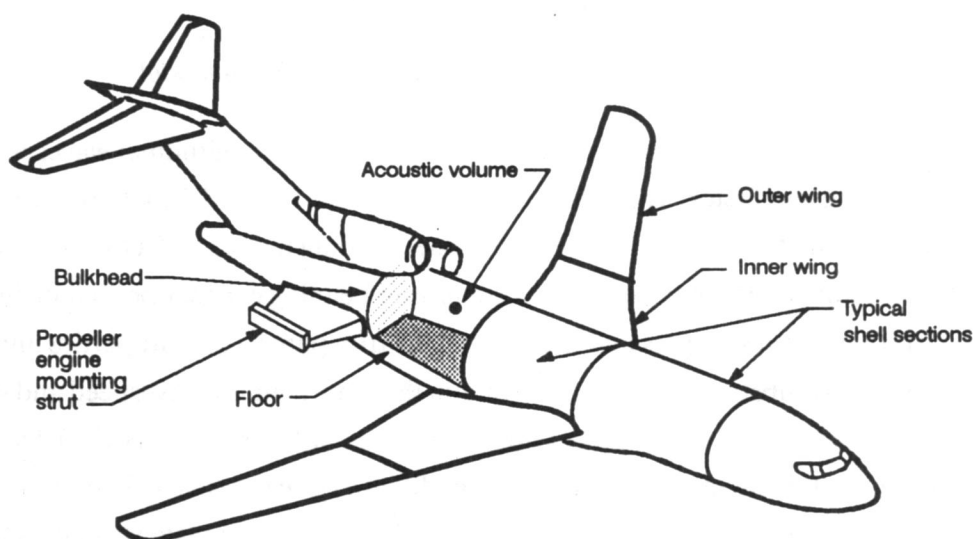


Figure 26. 26-Element, Low-Frequency SEA Model of 727 Demonstrator Airplane

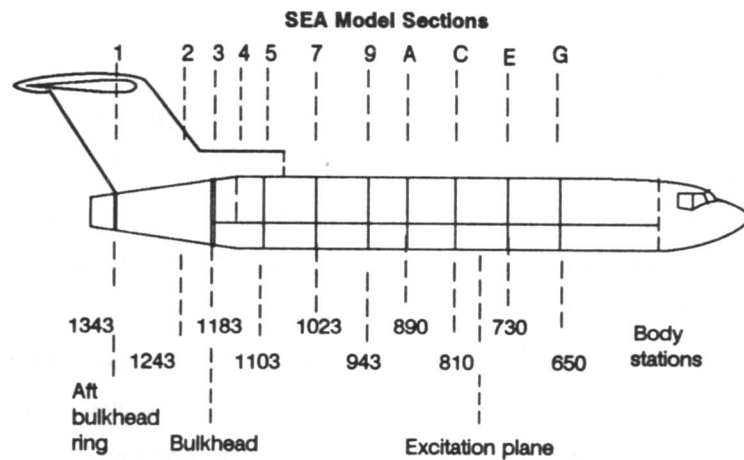


Figure 27. 727 Demonstrator SEA Mid-Frequency Model Subsystems

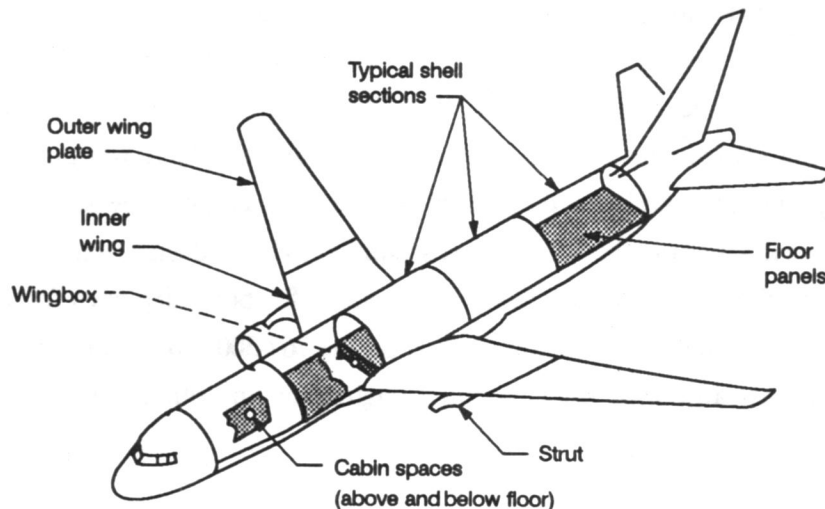


Figure 28. Schematic of 41-Element 767-300 SEA Model

The material properties required for the SEA model are density, longitudinal wavespeed, shear wavespeed and damping loss factor. The substructures used in the LF model contain composite bending and inplane modes. The MF model also uses skin panel bending modes. Effective material properties for the LF substructures were obtained from a composite bending calculation that includes the mass and stiffness of frames and stringers and the mass of the trim panels. The properties and thickness of the homogeneous SEA substructure were set to obtain the same bending wavespeed and surface density of the original structure. For the LF model shell subsystems an equivalent material density approach was used in which the thickness of the structure is modified to give the correct bending wavespeed and the density is modified to give the correct density per unit area. For the plate structures the equivalent wavespeed approach was used in which the thickness of the structure is modified to give the correct density per unit area and the longitudinal wavespeed is modified to give the correct bending

wavespeed. Use of the equivalent material density approach for shell substructures allowed the longitudinal wavespeed to remain unchanged so that the ring frequency of the substructure was unchanged.

4.1 AFT-MOUNTED CONFIGURATION

SEA predictions were made of aft-cabin sound pressure levels (SPLs) from a 1 lb force input to the engine mounts in the vertical and lateral (strut inplane) directions at both the front and rear mounts. Energy flow paths from the engine mounts to the cabin interior were identified. After upgrading the earlier SEA model with the addition of trim panels as separate subsystems, a parametric study was carried out to evaluate the effectiveness of structural changes and additions in reducing the vibratory energy reaching the cabin as sound. Modeling the trim panels as separate subsystems was helpful at frequencies above 100 Hz but their effectiveness was limited because the sidewalls were not the major contributor to the cabin SPL for structureborne noise. Adding a mass barrier in front of the rear pressure bulkhead reduced cabin noise by about 3 dB. Removing or isolating major transmission paths had marginal or even adverse effects on cabin SPL as the energy simply took a different path. The only concept tried that was significantly effective was that of a straight-through strut (left and right struts connected) which was isolated from its attachment to the empennage.

4.2 ADDITION OF TRIM PANELS

A study was performed to assess the effects of adding trim panel subsystems to the low-frequency 727 Demonstrator SEA model. By adding trim to the model, the accuracy of the predictions was significantly improved between 100 and 200 Hz .

The statistical energy analysis models developed earlier (ref. 1) to predict low and mid frequency noise of the 727 Demonstrator airplane included the effect of the trim panels by adding the trim panel mass density to the surface density of the sidewall and ceiling. This assumption was thought to be valid for the low frequencies below the double-wall resonance formed by the masses of the trim panels and sidewall and the stiffness of the air gap. Original comparisons of the SEA predictions with measured ground vibration test (GVT) data showed fairly good agreement below 100 Hz but at frequencies above 100 Hz the SEA predictions of the interior noise were higher than the data by as much as 15 dB.

The baseline SEA low frequency model used a single subsystem for the sidewall which included the mass of the sidewall, frames, trim and insulation. The effects of the interior trim and ceiling panels have been included by adding SEA bending subsystems for the trim and ceiling panels and acoustic subsystems for the cavity between the sidewall and the panels. The effect of adding the trim panels is

shown for the vertical drive condition in figure 29. These curves show an improvement in the noise prediction at frequencies between 100 and 200 Hz although the predictions continue to be above the data. Since most of the energy getting into the cabin for the vertical drive on the strut is radiated by the bulkhead, the trim panels are only reducing the energy from one of the minor flow paths.

4.3 PARAMETRIC STUDIES (AFT-MOUNTED ENGINE)

A parametric study was performed to evaluate the effects on cabin SPL of making selected changes to structural components in the aft section of the airplane. Figure 30 illustrates schematically the engine mounting strut and its attachment to the airplane for the aft-mounted 727 Demonstrator airplane configuration. The changes to the airplane structure were accomplished by varying either the characteristics of the baseline subsystems, by varying the junctions between subsystems or by adding subsystems.

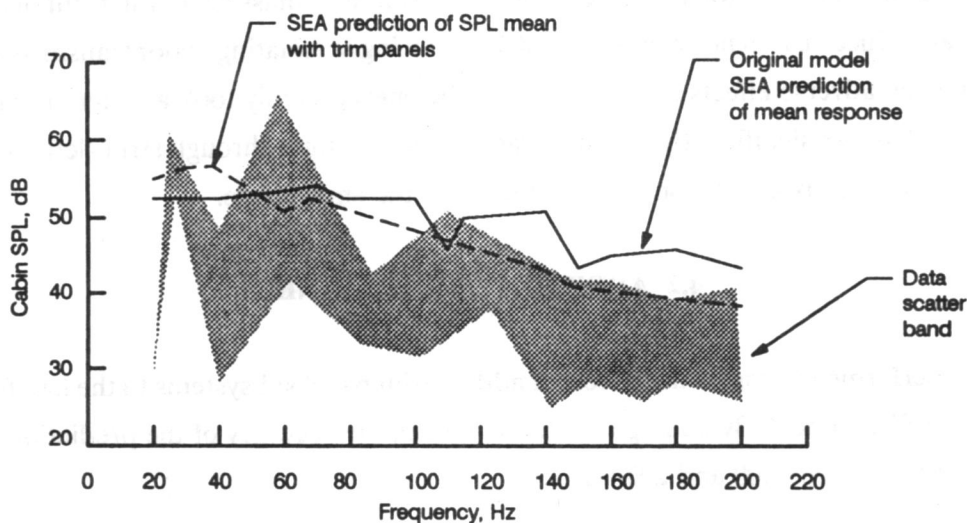


Figure 29. Effect of Trim Panels on Interior Noise of 727 Demonstrator for Vertical Strut Drive

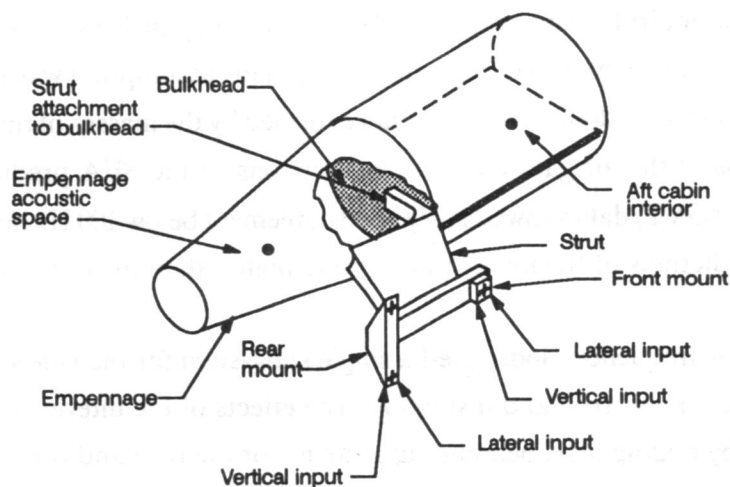


Figure 30. Schematic of 727 Demonstrator Baseline Engine Strut Attachment

Analysis of the baseline airplane showed that most of the energy reaching the interior acoustic space was being radiated from the rear pressure bulkhead. It was also noted that the cabin SPL was substantially higher for a vertical input force to the engine mounts than it was for a lateral force input. This was because of the strut attachment to the bulkhead which caused the lateral force to see the large impedance of the bulkhead. Although the bulkhead is the major source for both drive direction cases, the energy reaches the bulkhead via the strut attachment for the vertical drive and via the empennage for the lateral drive case. At 20 Hz there was also significant energy coming from the empennage acoustic space via mass law through the bulkhead.

4.3.1 HEAVY LIMP MASS BARRIER IN FRONT OF BULKHEAD

During the flight testing of the 727 Demonstrator airplane, one of the noise control measures tried was to place a heavy acoustic barrier in front of the rear pressure bulkhead. This was simulated in the model by adding a plate subsystem at a distance of four inches from the bulkhead. The plate was given the properties of rubber having a surface density of 2.5 lbs per sq. ft. The SEA predictions for the cabin SPL with the barrier in place are shown in figure 31. For the vertical drive, reductions of 2 dB are seen up to 40 Hz with increasing values above 40 Hz. Smaller values are seen for the lateral drive case. These reductions are consistent with those seen in flight. The lateral drive reductions are smaller because, for this case, there is a higher percentage contribution from the sidewall than in the vertical drive case and reducing the bulkhead contribution with the barrier thus removes a smaller amount of the total energy getting into the cabin.

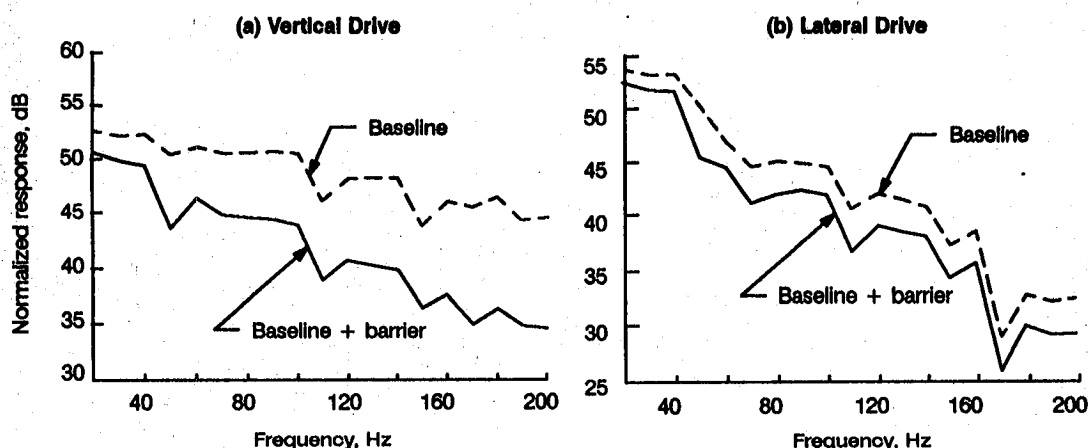


Figure 31. Effect on 727 Demonstrator Cabin SPL of Placing Heavy, Limp Mass Barrier in Front of Bulkhead

4.3.2 ENGINE STRUT DISCONNECTED FROM THE BULKHEAD

The effect on cabin SPL of removing the strut front spar connection to the bulkhead is shown in figure 32. For the vertical strut drive the decrease was very small and averaged about 1 dB. For the lateral drive there is an increase in SPL varying from about 2 dB to 10 dB as frequency increased from 20 to 200 Hz. The effect of disconnecting the front spar of the right engine strut from the pressure bulkhead was studied by altering two junctions. The junction between the strut bending subsystem, the empennage and the pressure bulkhead was changed by removing the pressure bulkhead. The bulkhead was still connected to the fuselage through a junction between the cabin sidewall, the empennage and the bulkhead. The other change was to completely remove the mass of the bulkhead from the junction involving the strut inplane subsystem and the empennage subsystem.

In the vertical drive case there is more energy going to the empennage from the strut when the spar is disconnected because of better impedance matching at that junction. There is thus more energy radiated into the empennage acoustic space, more energy going from empennage to bulkhead as well as more energy radiated from the sidewall to the cabin. These increases almost make up for the loss of energy getting to the interior via the bulkhead through the strut connection. The net result is a slight drop in cabin SPL.

The increase in cabin SPL for the lateral drive case was due to the removal of the pressure bulkhead mass impedance from the junction of the strut inplane subsystem and the empennage subsystem. Without the restraining effect of the bulkhead, the strut inplane motion was able to highly excite the empennage bending modes. In turn, the highly energized empennage transferred more energy to the

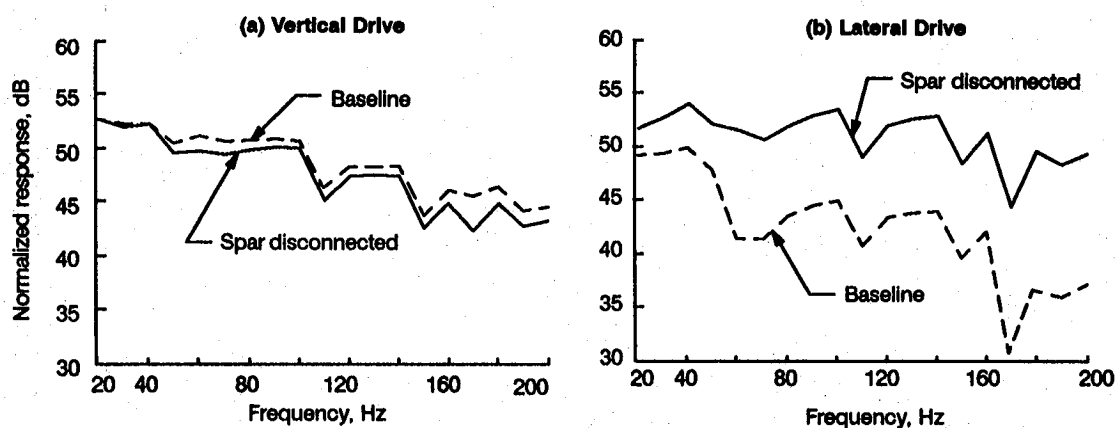


Figure 32. Comparison of SPLs for Baseline 727 Demonstrator Versus Disconnected Front Spar

bulkhead than it did with the spar attached. The result was more energy radiated to the cabin space from the bulkhead than for the baseline case.

4.3.3 STRAIGHT-THROUGH STRUT

Replacing the baseline strut with a straight-through strut (fig. 33) resulted in significant cabin SPL reductions for the vertical drive but almost no change in SPL for the lateral drive (fig. 34). For the vertical drive there is a decrease of approximately 1 dB at 20 Hz, increasing to 5 dB at 50 Hz and averaging about 5 dB out to 200 Hz. Recall that totally disconnecting the strut from the bulkhead resulted in a decrease of only 2 dB in cabin SPL. The greater reduction in SPL comes about for the following reasons. At all frequencies there is a decrease in the average energy level of the straight-through strut. This happens because of its greater area, ie., the strut now extends through to meet the left hand strut and has the same power input so that the energy density is lower. However, even though the energy level is

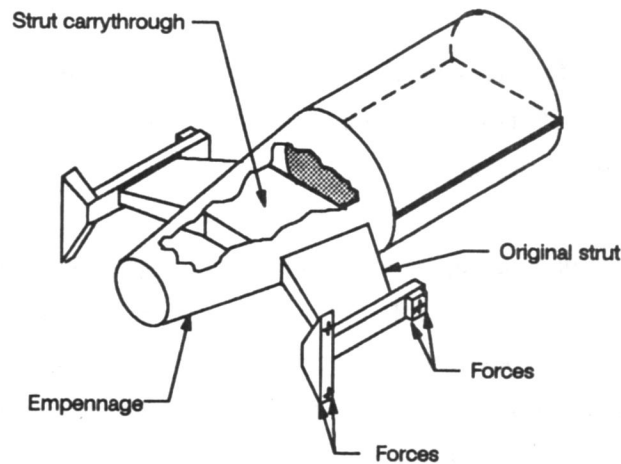


Figure 33. 727 Demonstrator Straight-Through Strut

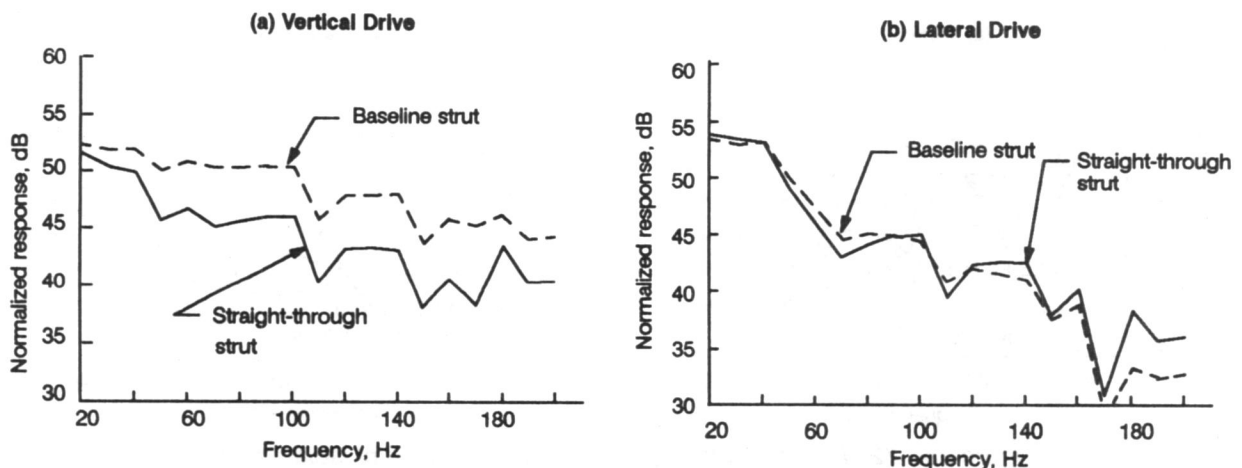


Figure 34. Comparison of Cabin SPL for 727 Demonstrator Baseline Strut and Straight-Through Strut

lower there is more energy getting into the empennage from the strut because there is now essentially one long strut which extends from one side of the empennage through to the other side and which is attached to the empennage at the left and right hand sides (two energy entry points). Some of this energy is radiated into the aft acoustic space and with the exception of that at 20 Hz very little of the energy in that space gets through the bulkhead into the cabin. The balance of the empennage energy flows to the bulkhead and to the cabin sidewall but in amounts that are small compared to the baseline.

For the lateral drive case the reason that we do not see any significant difference from the baseline is that, when we remove the attachment to the bulkhead and add a section joining left and right struts, we are simply replacing the bulkhead mass seen by the inplane modes at the strut-to-empennage junction with the mass of the left hand strut and mounting beam.

4.3.4 STRAIGHT-THROUGH STRUT ISOLATED FROM THE EMPENNAGE

The reductions in cabin SPL for the vertical and lateral drive cases for three different isolator spring constants are shown in figure 35. For both drive cases there are significant SPL reductions which get larger as the spring constant is reduced.

The effect of strut-to-empennage isolation was studied by inserting springs into the junction of the strut and empennage. This required two different models, one for bending (vertical input) and one for the inplanes (lateral input). Two types of springs were required because the the strut bending to empennage junction is a moment junction and the strut inplane to empennage junction is a force junction. The moment junction required a torsional spring, having units of N-m. The force junction required a longitudinal spring having units of N/m. The equivalent impedance of the isolated subsystem is given by

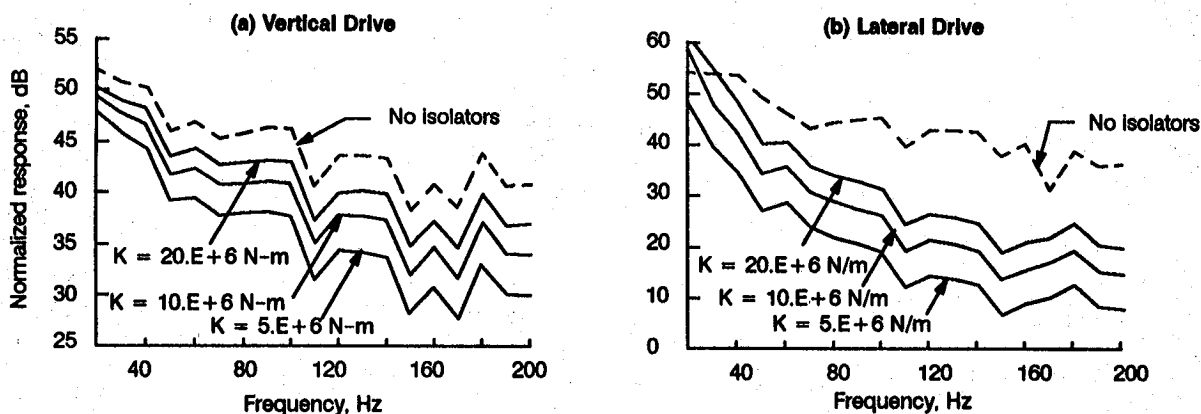


Figure 35. 727 Demonstrator Cabin SPL—Comparison of Isolated and Non-Isolated Straight-Through Strut

$$Z_{eq} = \frac{Z_k Z_s}{Z_k + Z_s}$$

where Z_k is the impedance of the spring and Z_s is the impedance of the isolated subsystem. When the impedance of the spring is much higher than the impedance of the isolated subsystem, the equivalent impedance approaches the impedance of the isolated subsystem. On the other hand, when the impedance of the spring is much lower than the impedance of the isolated subsystem, the equivalent impedance approaches that of the spring. This impedance is used to determine the transmission coefficient when the subsystem is isolated by a spring.

4.3.5 ADDITION OF FRAMES TO SUPPORT THE STRAIGHT-THROUGH STRUT

Additional frames would be required to support the strut to empennage connection when the strut is disconnected from the pressure bulkhead. Only the lateral strut drive was affected by this change. Figure 36 shows the reduction in aft cabin SPL for total additional frame masses of 200 kg and 400 kg. The maximum reduction was for the 400 kg mass and varied from about 2 dB at 20 Hz to about 5 dB at 200 Hz.

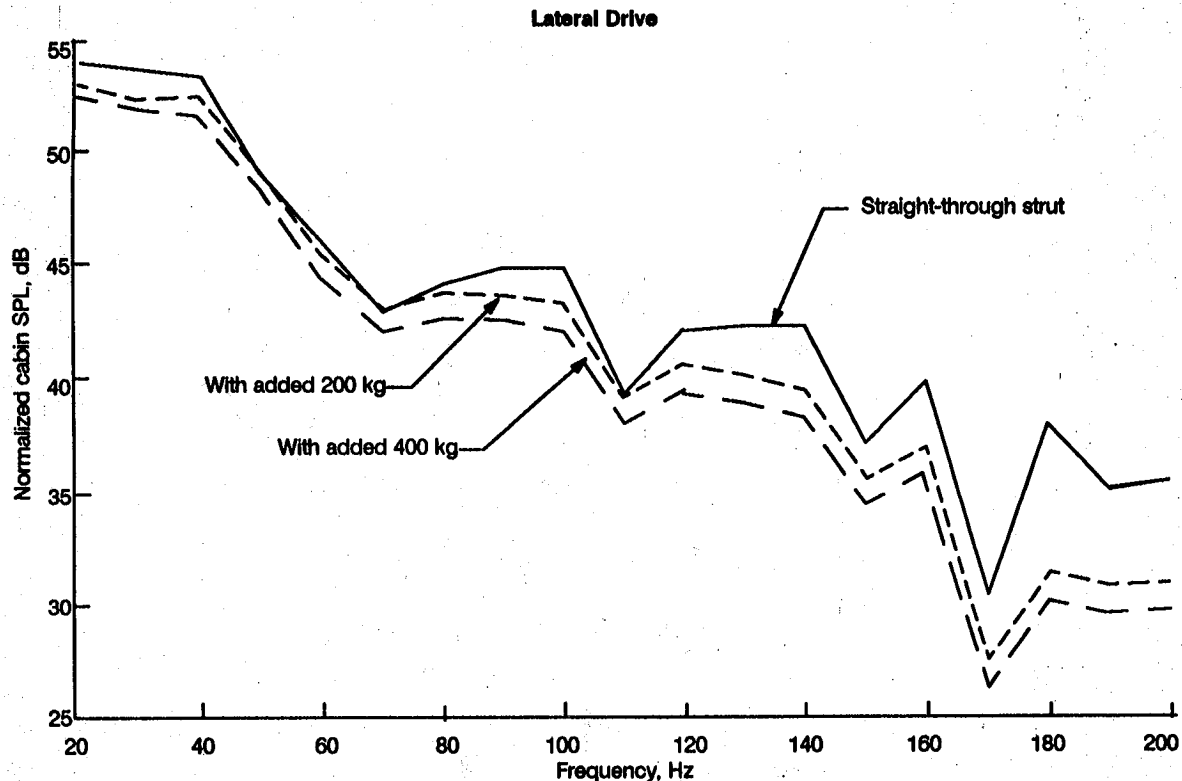


Figure 36. Effect on Cabin SPL of Adding Mass to Strut/Empennage Junction

The effect of the additional frames was simulated by adding a mass to the junction between the strut and the empennage. The added mass increased the total junction impedance which resulted in a reduction of the transmission coefficient thus lowering the energy flowing into the empennage and into the cabin.

4.3 WING-MOUNTED CONFIGURATION (AIRBORNE EXCITATION)

The SEA predicted in-flight cabin interior SPLs increase by as much as 36 dB in the one-third octave bands of the blade passage frequencies and their harmonics when the empennage-mounted engine is moved to a wing-mounted configuration. This difference is due primarily to differences in the drive point conductance of the empennage and the fuselage and to transmission path differences from the excitation point to the cabin interior. In particular, the pressure bulkhead and the lavatories cause a drop in modal power in the empennage-mounted transmission path; there is no similar drop in the wing-mounted transmission path.

A study of noise suppression concepts was conducted using the extended mid-frequency 727 Demonstrator SEA model. These concepts included modification of the fuselage wall construction, modification of the fuselage wall and cabin floor damping, modification of the trim panel configuration and mass, the installation of deep frames in the source impingement region and the installation of a lavatory in the source impingement region.

None of the noise suppression concepts alone provided more than 6 dB reduction in cabin SPL for the wing-mounted engine configuration. Some of the concepts may have an additive beneficial effect, however, it is unlikely that more than a 10 dB reduction could be obtained. Thus, the cabin SPL for the wing-mounted engine configuration would still exceed that for the empennage mounted engine configuration by 26 dB and by 13 dB in the 160 Hz and 315 Hz one-third octave bands respectively.

4.3.1 RESULTS FROM THE EXTENDED MID-FREQUENCY MODEL

For the hypothetical model of the 727 Demonstrator with wing mounted engines the propeller-induced noise was located in the vicinity of station 770. We have also assumed that the distance between the blade tips and the fuselage would be about the same as for the aft mounted configuration. With this assumption we can use the flight data that had previously been measured. The measured fuselage sound pressures were converted to point forces and applied to the predicted cabin force-to-SPL transfer functions from the SEA model. This report will focus on the flight levels of the blade passage

frequency and its second harmonic occurring in the 160 Hz and 315 Hz one-third octave bands, respectively.

For the aft-mounted configuration the transfer function was obtained by applying a 1 lb force to the empennage between the aft bulkhead ring and the rear pressure bulkhead. For the wing-mounted configuration the force was applied to the fuselage sidewall between sections C and E in figure 27. The transfer functions obtained are shown in figure 37. For the empennage-mounted engine the highest SPL is shown from the most aft cabin location. For the wing-mounted engine the highest SPL is shown from the cabin space between sections C and E which is in the propeller plane. The large increase in cabin SPL for the wing-mounted configuration is most likely due to two factors: 1) the substantial difference in the structure of the fuselage sidewall as compared with the empennage structure and 2) the presence of the pressure bulkhead and lavatories in the path from the empennage to the cabin. The structural differences become apparent by comparing the measured drive point conductance, taken as part of the 727 Demonstrator test. These were taken from the empennage and fuselage at points B and I

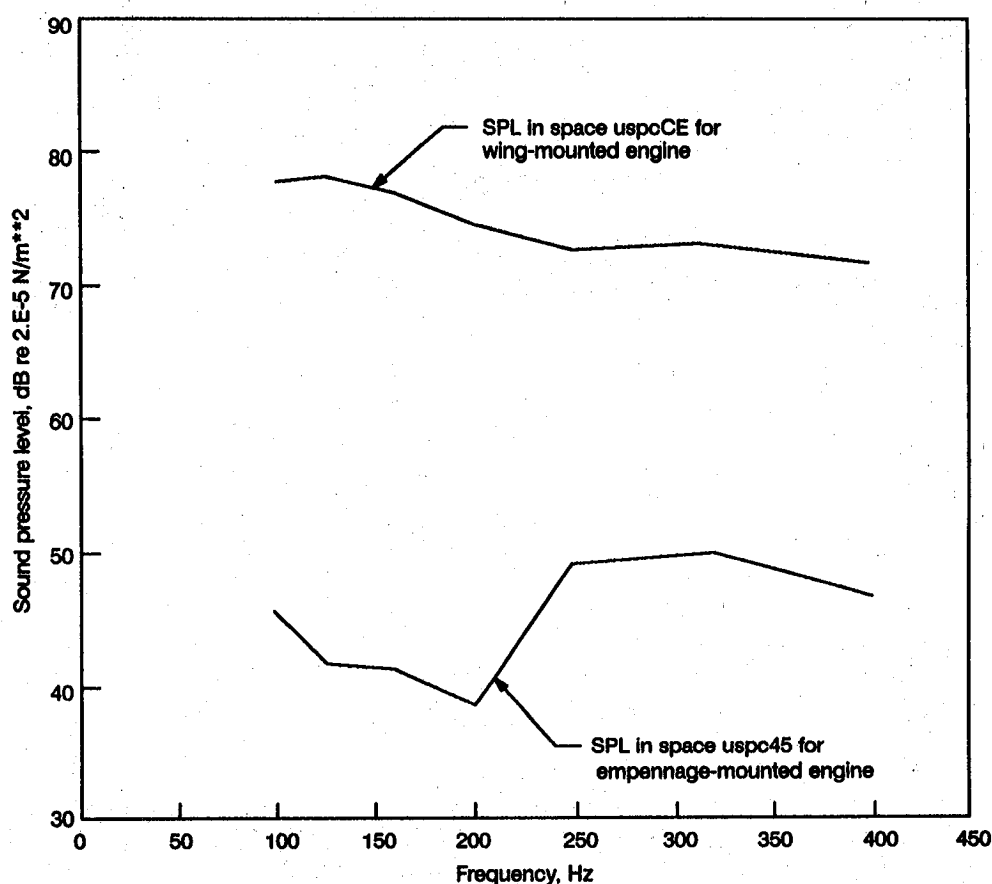


Figure 37. Comparison of the SPL to Force Transfer Functions for the Wing and Aft-Mounted Engines

respectively as shown in figure 38. The comparisons show a much higher level for the fuselage drive point conductance.

Using the measured pressure with the predicted transfer functions, the cabin flight SPLs were calculated. The resulting SPLs versus axial cabin location for the 160 Hz one-third octave band are shown in figure 39. The results show that the maximum level for the wing mounted engine in the propeller plane is about 30 dB higher than that for the aft-mounted engine.

4.4 NOISE SUPPRESSION CONCEPTS FOR THE WING-MOUNTED ENGINE

The noise suppression concepts for the study were chosen based on the following: ability to fit approximately within the existing aircraft geometry, realizability, weight increase and potential effectiveness. The four concepts analyzed were:

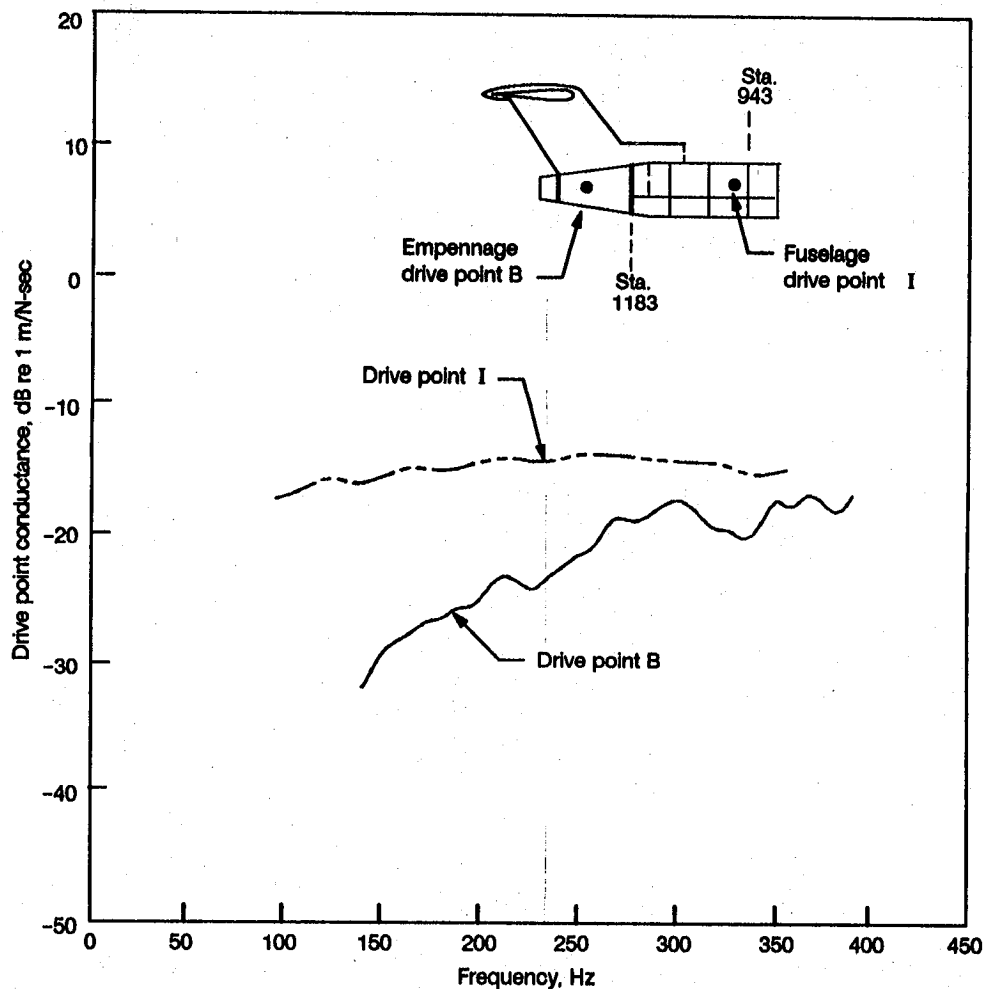


Figure 38. Measured Drive Point Conductances for 727 Demonstrator Airplane

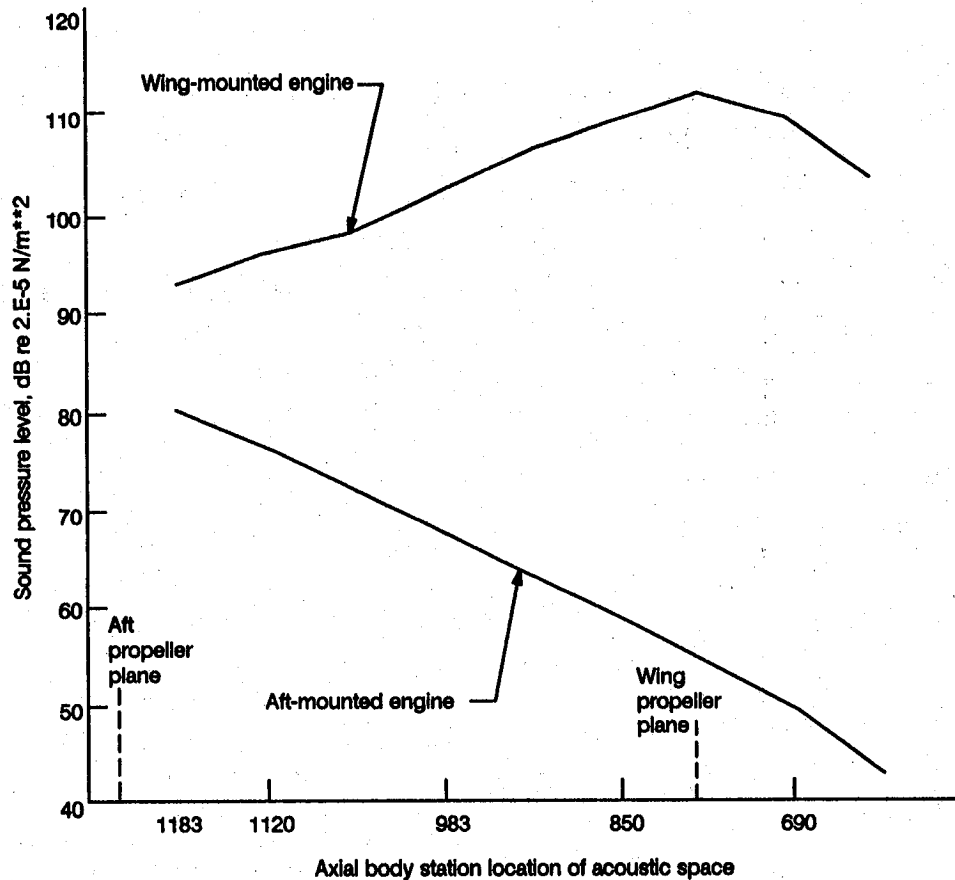


Figure 39. Predicted Cabin Sound Pressure Levels in Flight in the 160-Hz, One-Third Octave Band

1. Modification of the fuselage wall construction. The stiffness and mass of the fuselage wall control its input conductance. Thus the goal of modifying the fuselage wall construction is to lower its input conductance so that less power is input to the sidewall.
2. Increase of the fuselage wall and cabin floor damping. Applying damping to the fuselage walls and cabin floor will allow dissipation of some vibrational energy before it is radiated to the cabin interior.
3. Installation of a structural blocking impedance between the noise source and the receiver area and installation of an acoustic barrier between the noise source and the receiver area.

Installation of a blocking impedance between the source and receiver is a means of reducing the axial coupling along the fuselage. Structurally this is accomplished by adding a structural member such as a deep frame to the fuselage wall. Acoustically this is done by adding a barrier. For this study a lavatory was added as an acoustical barrier.

4.4.1 MODIFICATION OF THE FUSELAGE WALL

All fuselage modifications were made to the entire fuselage ring section under consideration. The first modification was to replace the roof and window wall constructions with that of the baggage compartment wall which is heavier and stiffer. The second wall modification was to replace the roof and window wall construction with an aluminum face-sheet honeycomb wall. For the third wall modification, a framed built-up all composite panel was designed to have the same stiffness as the baggage compartment wall but without the additional mass. The frame and stringer spacings were roughly the same as the conventional structure.

Figure 40, for the 160 Hz band, shows the results of the fuselage modifications made to the section around the propeller plane only (section CE). The SPLs predicted for the extended baggage wall case are about 1 dB below the baseline case. The honeycomb wall and built-up composite wall are about 6 dB below the baseline case with slightly better performance given by the honeycomb. The differences are due to changes in the input conductances of the different wall constructions. The extension of the

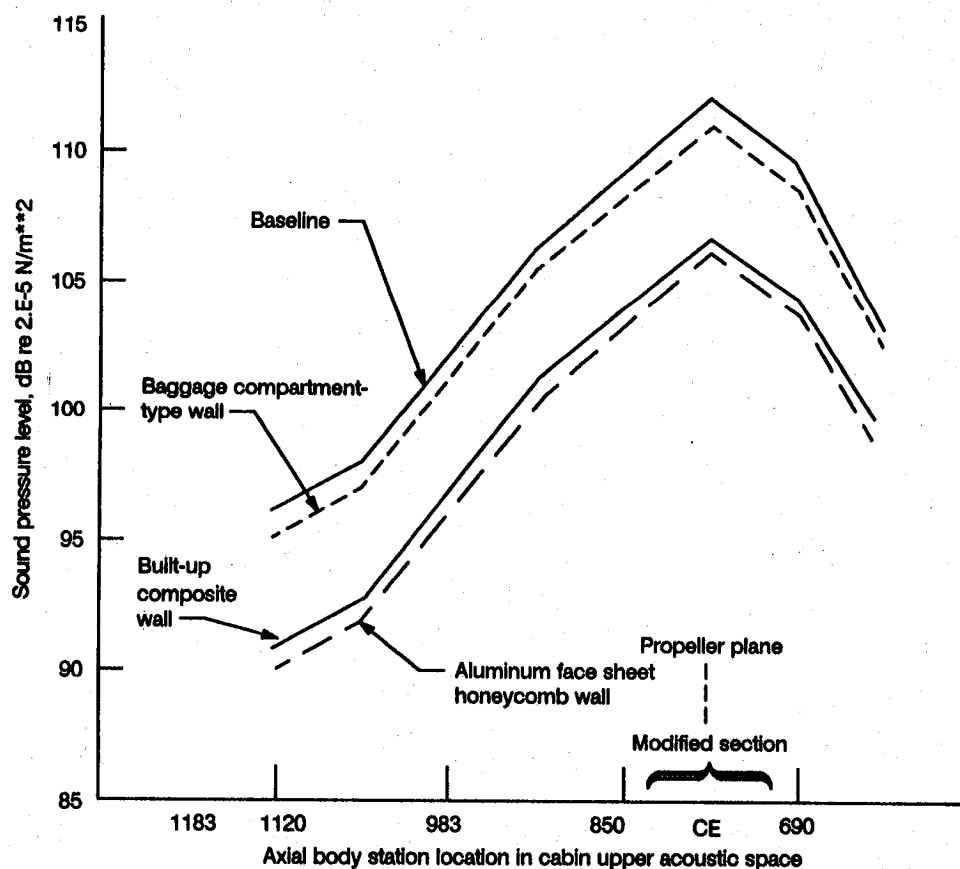


Figure 40. 160-Hz Cabin SPL for Section CE Fuselage Wall Construction Modifications

wall modifications to the sections on either side of section CE were only slightly more effective. Results for the 315 Hz band were similar.

4.4.2 DAMPING APPLICATION RESULTS

For the baseline 727 Demonstrator fuselage, the application of free-layer or constrained-layer damping over section CE had little effect on the cabin SPL because of the already high damping values of the baseline riveted construction. The application of a damping treatment that would provide damping significantly in excess of the riveted-construction damping would probably be difficult and add substantial weight. Similar applications of damping were made for the other three fuselage wall constructions. For the somewhat heavier baggage compartment wall type construction, damping also had a minimal effect again, because of the already high damping values assumed for the riveted construction. For the alternate fuselage wall constructions, the addition of damping resulted in cabin SPL reductions of 1 to 3 dB with, in general, more effectiveness at higher frequency. For the framed, built-up wall construction these effects are shown in figure 41 for the 160 Hz one-third octave band.

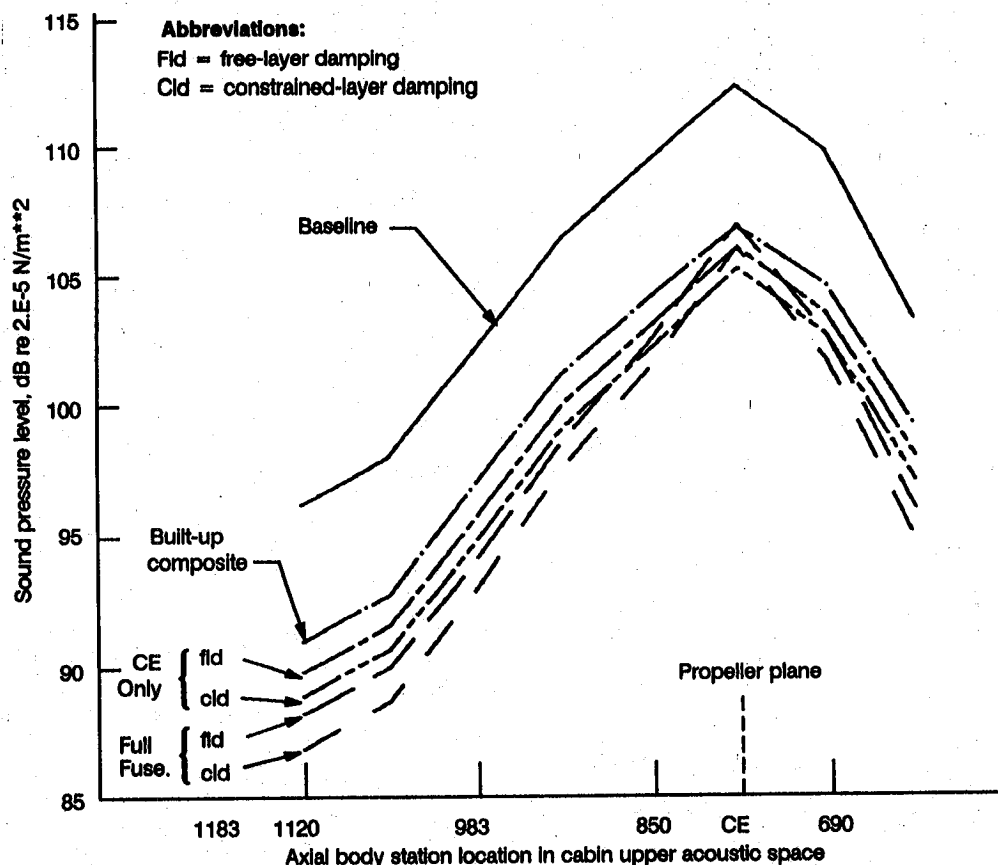


Figure 41. 160-Hz Cabin SPL for Various Damping Treatments Applied to the Cabin Floor and to Built-Up Composite Wall

4.4.3 RESULTS FOR ADDING DEEP FRAMES AND LAVATORIES

Adding the deep frames at stations 730 and 810, around the propeller plane, was expected to cause some blockage of energy travelling from section CE to fuselage sections on either side of section CE before radiating into the cabin. The addition of the frames had almost no effect on cabin SPL. The application of constrained layer damping to the fuselage wall in section CE increased the performance of the frames and a 1 to 2 dB reduction in cabin SPL was achieved as seen in figure 42 for the 315 Hz band. This reduction exceeds the reduction obtained by damping applied only to the baseline structure, i.e., no frames added.

An attempt was made to construct an acoustical barrier between the source and receiver by installing mid-fuselage lavatories in the SEA model section CE. The lavatories occupied the full axial length of section CE. A corridor passage was left open between stations 730 and 810 and extended from floor to ceiling. The effects of this barrier are also shown in figure 42. The cabin SPL is seen to be relatively unchanged outside the vicinity of the the lavatories (section CE/lav in the figure).

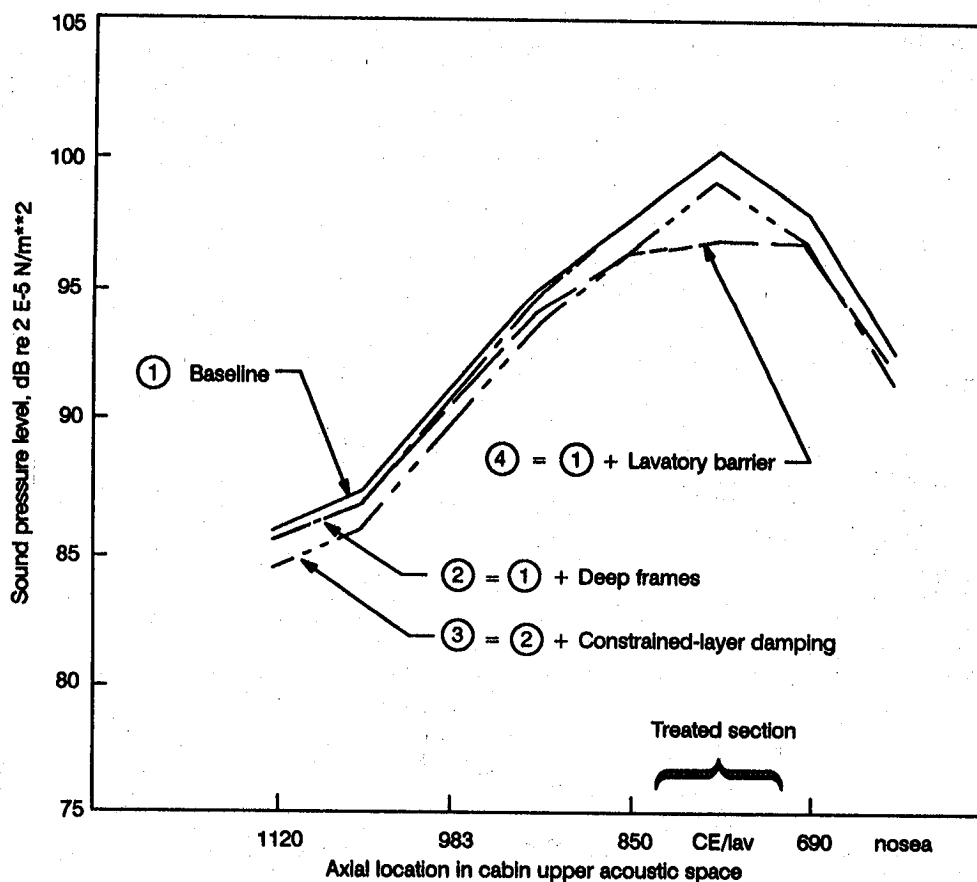


Figure 42. 315-Hz Cabin SPL for Addition of Deep Frames, Deep Frames Plus Damping, and Addition of Midfuselage Lavatories

4.4.4 ASSESSMENT OF THE IMPACT OF WING-MOUNTED VERSUS AFT-MOUNTED ENGINES FOR AIRBORNE EXCITATION

The maximum cabin SPLs for fuselage excitation were shown to be higher for the wing-mounted configuration by 36 dB at 160 Hz and by 23 dB at 315 Hz. This large difference is attributable to the difference between the wall constructions of the empennage and the fuselage. The empennage of the 727 Demonstrator airplane was reinforced to withstand the high fluctuating pressures caused by the propellers whereas the fuselage sidewall was not. In addition, the aft-mounted configuration had the pressure bulkhead and the aft lavatories located between the excitation region and the cabin interior. Assuming some additive effects of the suppression concepts tried, the total reduction that may be expected for the wing-mounted configuration is about 10 dB. After achieving this reduction, the maximum cabin SPL for the wing-mounted engine would still be in excess of that obtained with the aft-mounted engine by 26 dB at 160 Hz and by 13 dB at 315 Hz.

4.5 WING-MOUNTED CONFIGURATION (STRUCTUREBORNE EXCITATION)

To evaluate the effects of engine vibration on cabin noise for a wing-mounted configuration, an existing SEA model of the 767-300 airplane was used. The 767-300 was chosen because of the GVT data which existed against which to compare the model predictions.

A comparison of cabin SPLs due to structureborne noise from a 1 lb force input to the engine mounts showed that the wing mounted configuration was about 10 dB quieter than the aft mounted configuration. The suppression concept study using the SEA model showed that, inboard of the strut-to-wing interface, the only factor that influenced the cabin noise to any degree was the distribution of fuel in the tanks. We were able to show up to a 5 dB reduction in cabin noise with the fuel load equally divided between the center wing tank and outboard wing tanks compared to the usual procedure where the center tank is drained first.

4.5.1 VALIDATION OF 767-300 SEA MODEL

The 767-300 SEA model, for the GVT configuration, accurately predicted the cabin SPLs when test values of strut-to-wing acceleration were input to the SEA wing subsystem. These results indicated that the model is accurately accounting for the distribution of energy to the cabin.

The GVT on the 767-300 airplane consisted of attaching a shaker mechanism to one of the engine mounting points, inputting a one lb force, and measuring the response at the mounting point itself, at

all of the strut-to-wing attach points and in the cabin acoustic space. The shaker was then moved to other engine mounting points and the procedure repeated. This produced a set of sensitivity functions which described how critical points on the airplane respond to simulated engine unbalance forces. The experimental input and measurement points and the strut-to-wing attachment details are shown in figure 43.

The 767-300 SEA model was shown earlier in figure 28. The methods used to construct the model were the same as those used on the 727 Demonstrator model except that much more of the detailed properties were put into the wing, forward fuselage sections, and the connection between the wing and the fuselage. Figure 28 shows the presence of the engine mounting strut that was used in the GVT. The strut was not used for the final validation studies for reasons discussed in the next paragraph.

The engine mounting strut is a critical subsystem because this is where the force due to the engine unbalance is applied and from where power enters the model at the strut-to-wing attachments. The response of the strut to different force input locations and directions is extremely complex. The vertical forces and displacements at the mid-spar fitting, due to the input of a 1-lb force at various locations on the strut, can vary by as much as a factor of 50 (fig. 44). Because of this large variation in response we

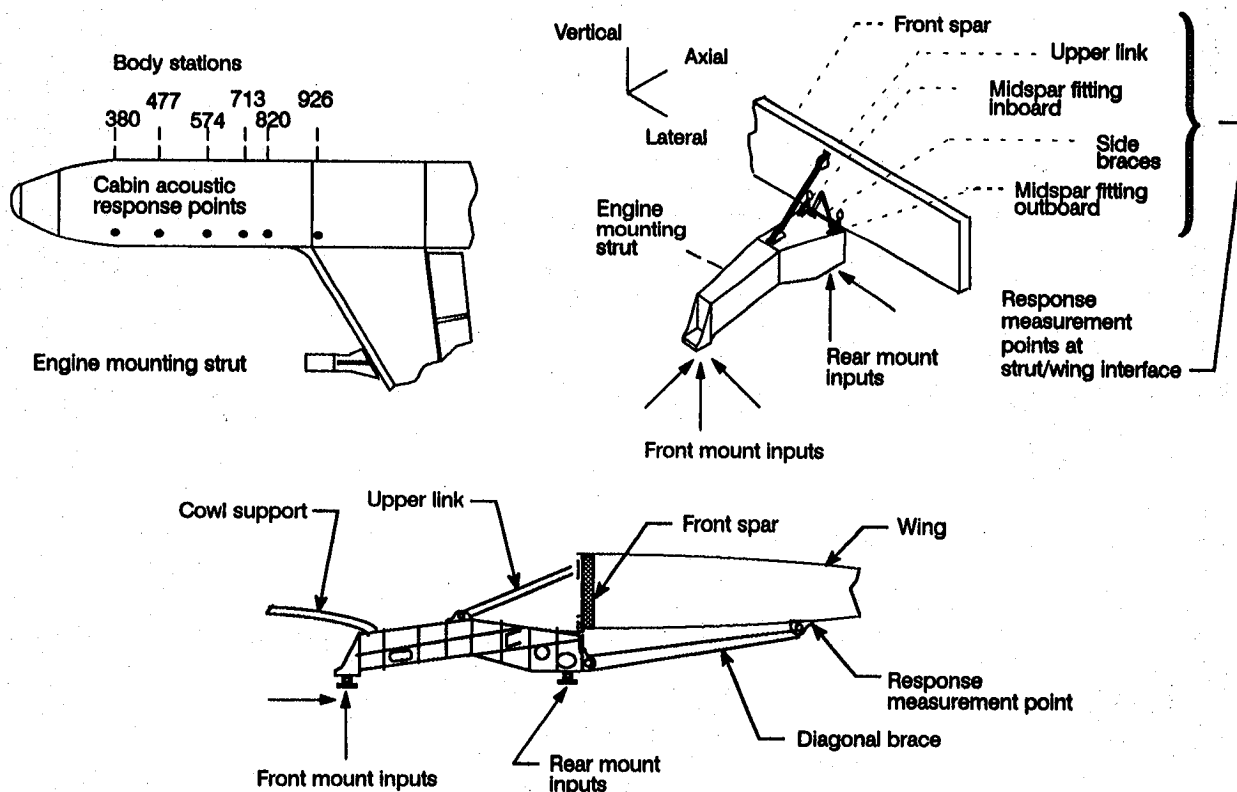


Figure 43. Input and Response Points for 767-300 Airplane Ground Vibration Test

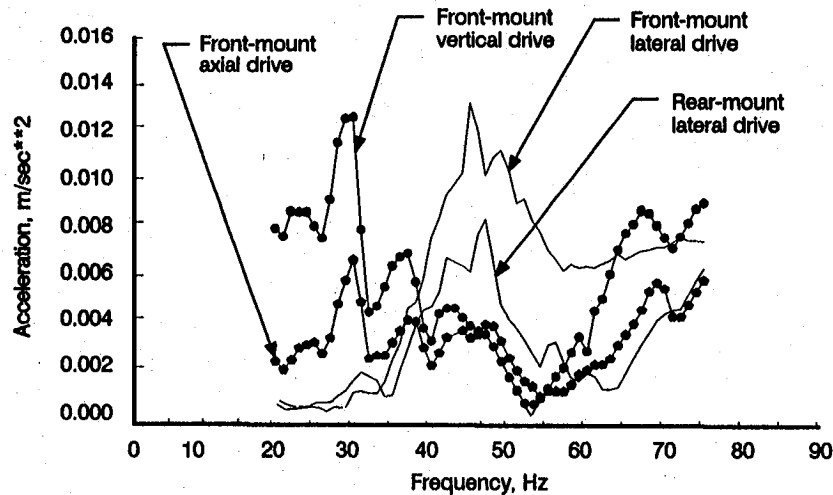


Figure 44. Response at Midspar Fitting Due to a 1-lb Force at the Engine Mounts

did not try to model the strut as a separate subsystem but instead, as a first effort, used the mass of the strut through which a one pound force was applied to the front spar of the wing. The results are shown in figure 45. The SEA predictions of the average cabin SPL are high by up to 20 dB at some frequencies for the two shake conditions presented. Since predicted SPLs were high we could not validate the model even in the average sense without artificially increasing the strut mass to lower the input power. To validate the rest of the model we decided to bypass the strut and use the measured accelerations at the strut-to-wing attach points from the GVT as inputs to the SEA wing subsystem. The magnitude average of only the vertical responses for each shake condition were input to the model.

The SEA predicted cabin SPLs, using the measured acceleration as input are shown compared with the measured SPL for two strut drive points in figure 46. The figure shows that the predicted cabin SPLs track the measured data extremely well in both magnitude and spectrum shape indicating that

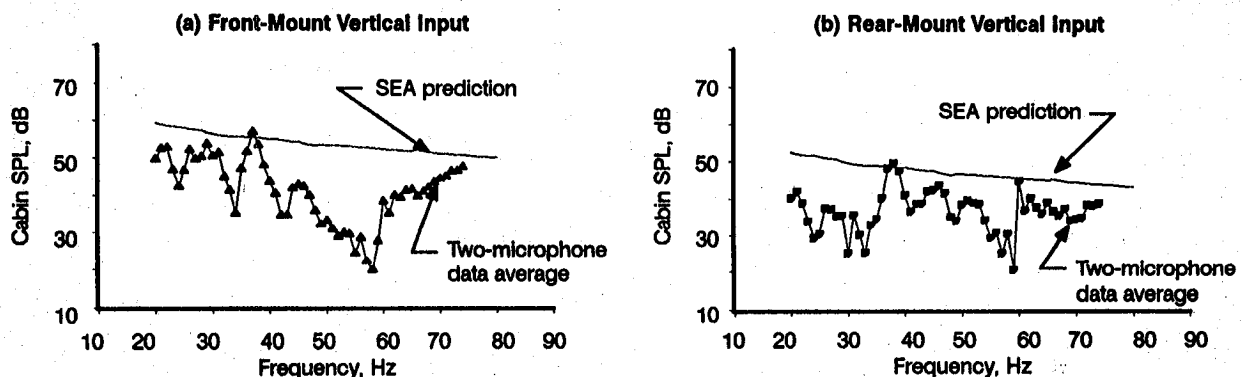


Figure 45. SEA Cabin Noise Prediction Using 1-lb Force Input Through Mass of Strut—Comparison With Data

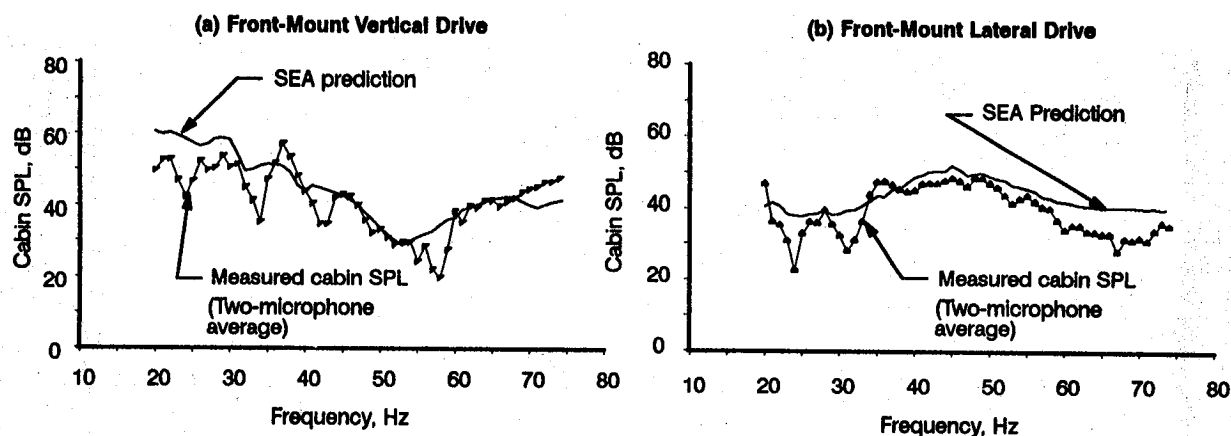


Figure 46. SEA Cabin SPL Prediction Using Measured Front Spar Acceleration as Input to Wing—Comparison With Data

the model is accurately modeling the flow of vibratory energy from the strut attachment point into the cabin.

4.6 NOISE AND VIBRATION REDUCTION CONCEPTS FOR WING-MOUNTED ENGINE

Vibratory energy originating at the engine can potentially be suppressed passively at the engine-to-strut mounting points, at the strut-to-wing attachment points or inboard of those points. Any suppression concept that addresses the engine mounting points or the strut-to-wing attachment points will be configuration specific, ie., will depend on the specific engine and strut combination. Since we could not model the strut properly in SEA, we decided to focus on the evaluation of suppression concepts applied to the structure inboard of the strut-to-wing attachment points. The concepts were each evaluated for the same 1-lb vertical force input to the edge of the wing subsystem.

4.6.1 THE EFFECTS OF FUEL MASS LOADING ON AIRPLANE RESPONSE

Having fully loaded fuel tanks gives as much as 10 dB reduction in the cabin SPL over the case with dry tanks. The amount of SPL reduction depends on the amount of fuel present and how it is distributed between the center wing tank and the outboard wing tanks.

The GVT was run with no fuel in the airplane. In flight there is always fuel in the tanks so credit cannot be taken for a reduction of the cabin noise level over the dry tank case. However, the distribution of fuel between the tanks can be controlled, and this, rather than the presence of fuel, is what becomes the passive concept evaluated to control the cabin SPL due to engine vibration.

In the following, a configuration having both wing tanks and center wing tank full at takeoff is assumed. As fuel is burned, the distribution between the tanks can be controlled in a way which minimizes the cabin SPL due to engine vibration. For any given total amount of fuel, the worst noise condition results from having maximum fuel in the wings and the minimum amount of fuel in the center wing tank. The lowest noise condition results from having maximum fuel in the center wing tank and minimum fuel in the wing tanks.

The normal way of burning the fuel for the assumed mission configuration is to draw from the outboard wing tanks during takeoff and climb to cruise altitude. Once cruise altitude is reached the fuel is drawn solely from the center wing tank until it is empty and then fuel is drawn from the outboard wing tanks until final destination. However, as pointed out above, this fuel distribution allows the most noise to get through to the cabin.

A reasonable compromise might be to draw equally from both outboard wing and center wing tanks for most of the flight and then, for safety reasons, drain the center wing tank before final approach. For all cases studied, having equal fuel in both the outboard wing and center wing tanks gives almost as much cabin noise benefit as having maximum fuel in the center wing tank. Also, there is only a slight increase in wing acceleration for the equally divided case. This alternate fuel management concept should be acceptable but would require scrutiny and acceptance by other disciplines such as stress, flutter and aero before implementation.

In the following paragraphs, and on the figures, the amount of fuel in the tanks will be designated as a percentage of the tank maximum (40,000 lb for each tank). For example, a fuel loading represented as (30% OW/40%CW) means that there is 12,000 lb in each of the outboard wing tanks and 16,000 lb in the center wing tank.

Figure 47 shows the cabin SPL for the baseline (dry tanks) and for several variations of the distribution of 78,000 lbs of fuel between the center and outboard wing tanks. One can clearly see the decrease in cabin SPL progressing from having all of the fuel in the outboard wing tank to having most of the fuel in the center wing tank. The trend is clear that having all of the fuel in the outboard wing tanks is the worst noise case and that having most of the fuel in the center wing tank is the best noise case. These results from the SEA model are fairly constant with frequency.

The relative contributions of the different vibratory energy paths from the strut-to-wing input location to the cabin acoustic space change with the fuel distribution. The differences between the 60%OW/0%CW case and the 20%OW/80%CW case where the total fuel loading is 48,000 lb are illus-

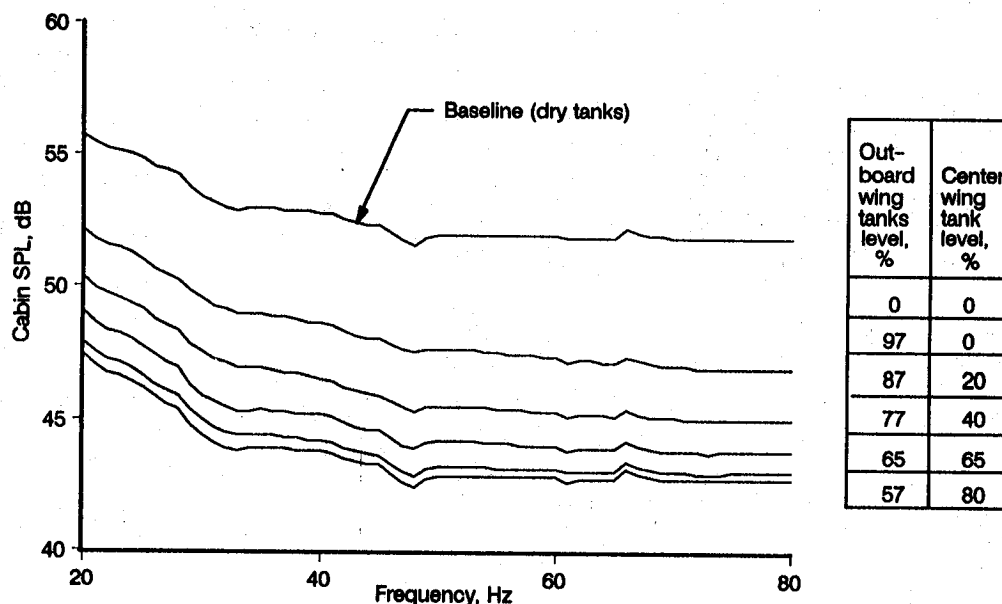


Figure 47. Effect of Fuel Distribution on Cabin Sound Pressure Levels—SEA Prediction, 78,000 lb Total Fuel

trated. Figure 48a shows for the 60%OW/0%CW case that at 20 Hz the fuselage sidewall is the dominant contributor to the cabin SPL. Between 30 and 80 Hz the floor above the wingbox becomes increasingly dominant as frequency increases. Figure 48b shows that for the 20%OW/80%CW case the dominant contributor at all frequencies is the fuselage.

The key items to note are how the power flowing to the fuselage and wingbox are altered when we go from the 60%OW/0%CW case to the 20%OW/80%CW case. These indicate why the power getting to the cabin is reduced. Figure 49 (absolute power flow to the fuselage) shows that at 20 Hz the primary contributor is the wing bending motion for the 60%OW/0%CW case. In the 20%OW/80%CW case there is almost no contribution from the wing bending. The wing, at the junction of the wing, wingbox and fuselage cannot move because of the impedance of the now more massive wingbox. At 80 Hz the impedance going from the wing bending to the fuselage is higher than at 20 Hz (smaller transmission co-efficient) for both of the cases and no bending energy gets through. Also, at 80 Hz, the wing inplane motion energizes the fuselage for the 60%OW/0%CW case and the wingbox inplane motion does the same for the 20%OW/80%CW case where the wingbox is heavier. In figure 48 it was seen that the wingbox (floor) contribution to cabin SPL decreased markedly for the 20%OW/80%CW case. Figure 50 shows that in both cases the wingbox gets energy from the wing bending motion and that this energy is much less for the 20%OW/80%CW case, again, because of the higher impedance seen by the wing when the wingbox is more heavily loaded with fuel. However, there is also more energy lost from the wingbox in the 60% OW/0%CW case with the net result being equal total energy of the wingbox at 20 Hz for the two cases.

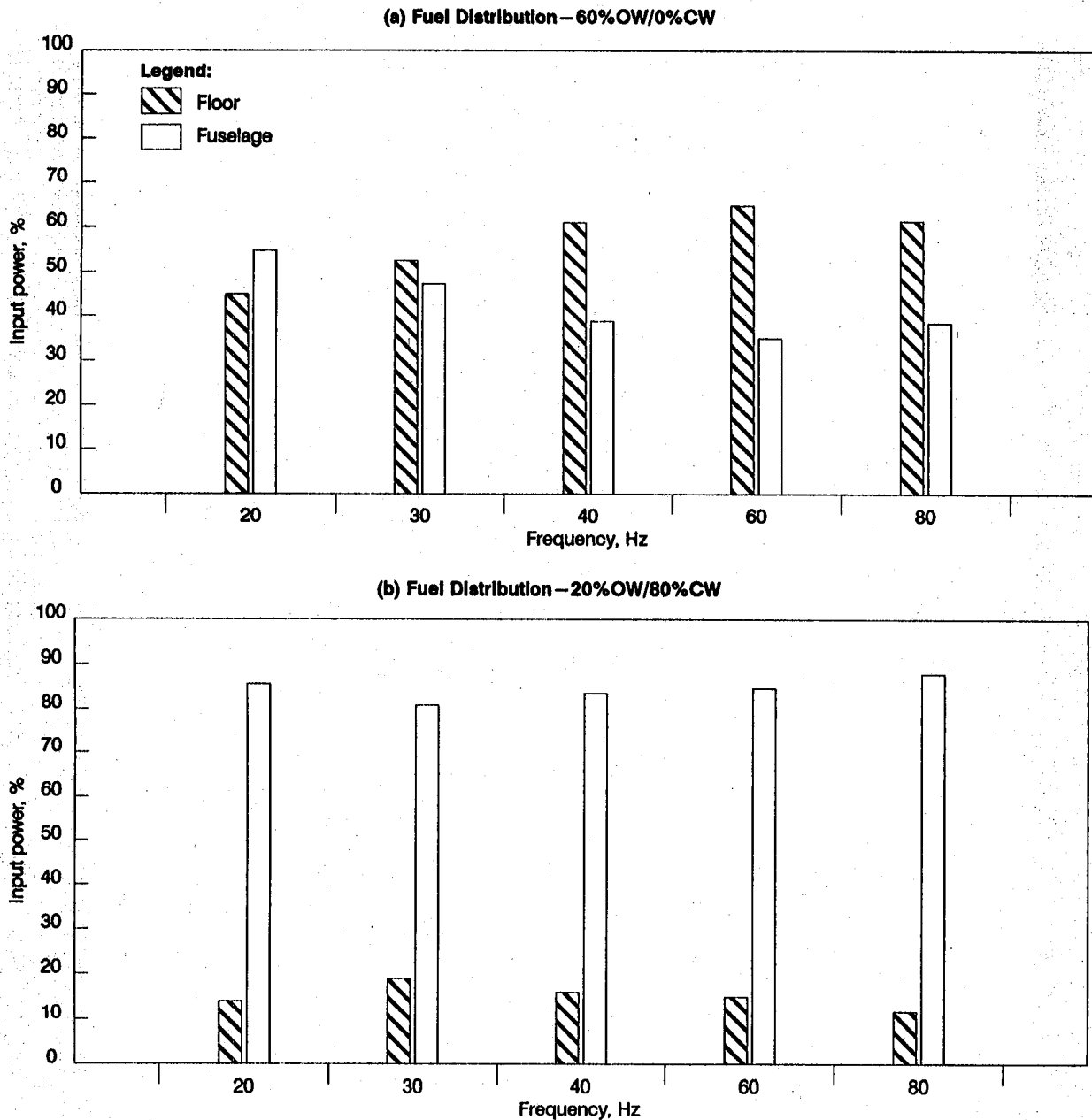


Figure 48. Percentage of Input Power to Cabin Acoustic Space for Fuel Loadings of 60%OW/0%CW and 20%OW/80%CW—48,000 lb Total Fuel

Figure 51 shows the customary and the proposed order in which the fuel tanks are drained. Figure 52 shows the predicted increase in wing energy that would occur when all tanks are drained equally. The increase is predicted to be about 1 dB, or a factor of 3 in wing displacement. Figure 53 shows the potential reduction in cabin SPL at the shaft rotational frequency as a function of fuel burn when the fuel burn pattern is modified. Up to 5 dB reduction is predicted. This might seem contradictory at first, in light of the higher wing energy, but closer inspection of the power flows shows that more energy from the wing bending is getting into the wing inplane modes for the equal fuel-split case. The wing inplane

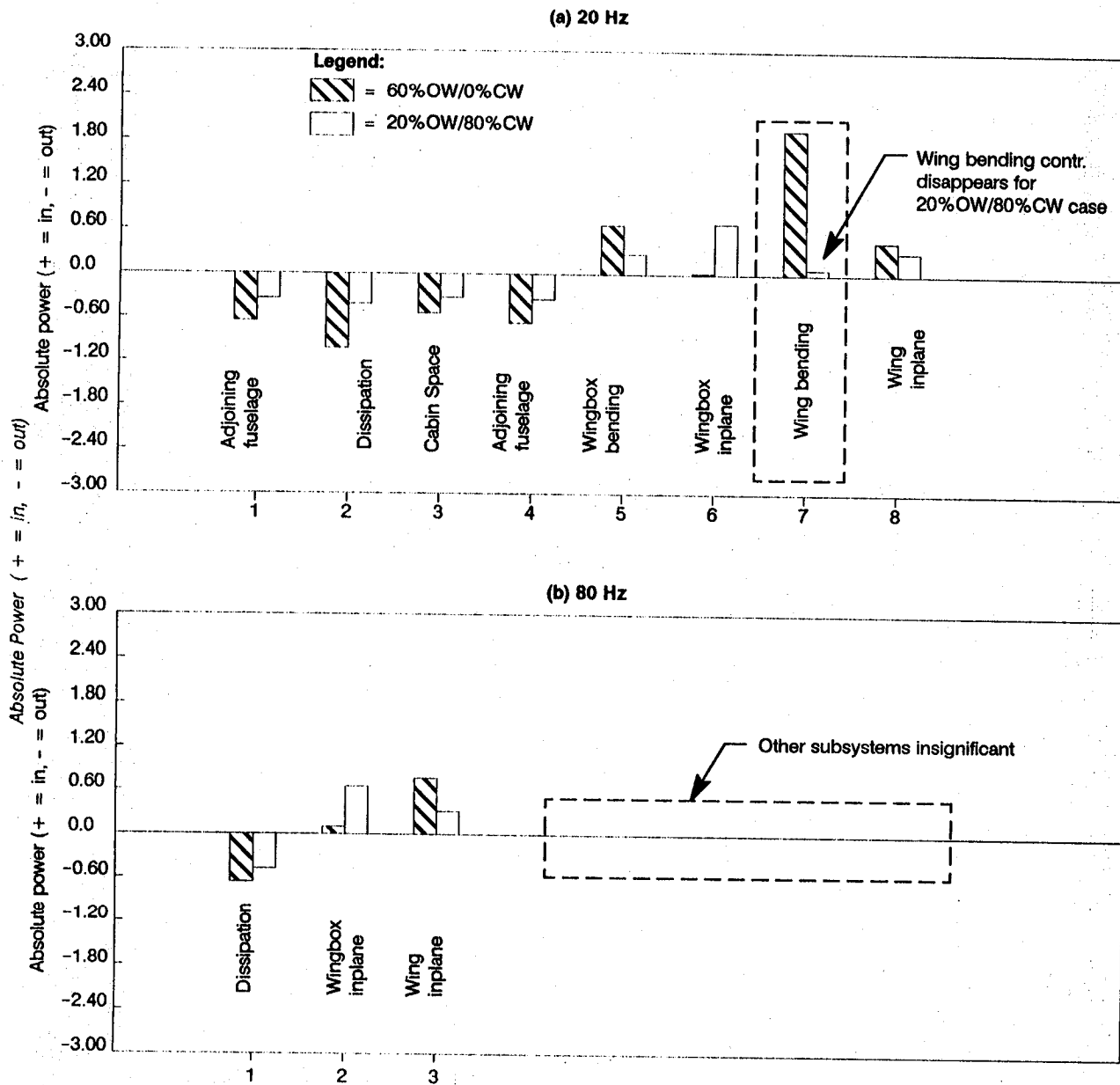


Figure 49. Absolute Power Flow to Overwing Fuselage for Fuel Loadings of 60%OW/0%CW and 20%OW/80%CW – 48,000 lb Total Fuel

modes then drive the wingbox inplane modes which, in turn, drive the inplane modes of the wing on the opposite side of the airplane. The right wing inplane modes transfer energy to the right wing bending modes which then dissipate more energy.

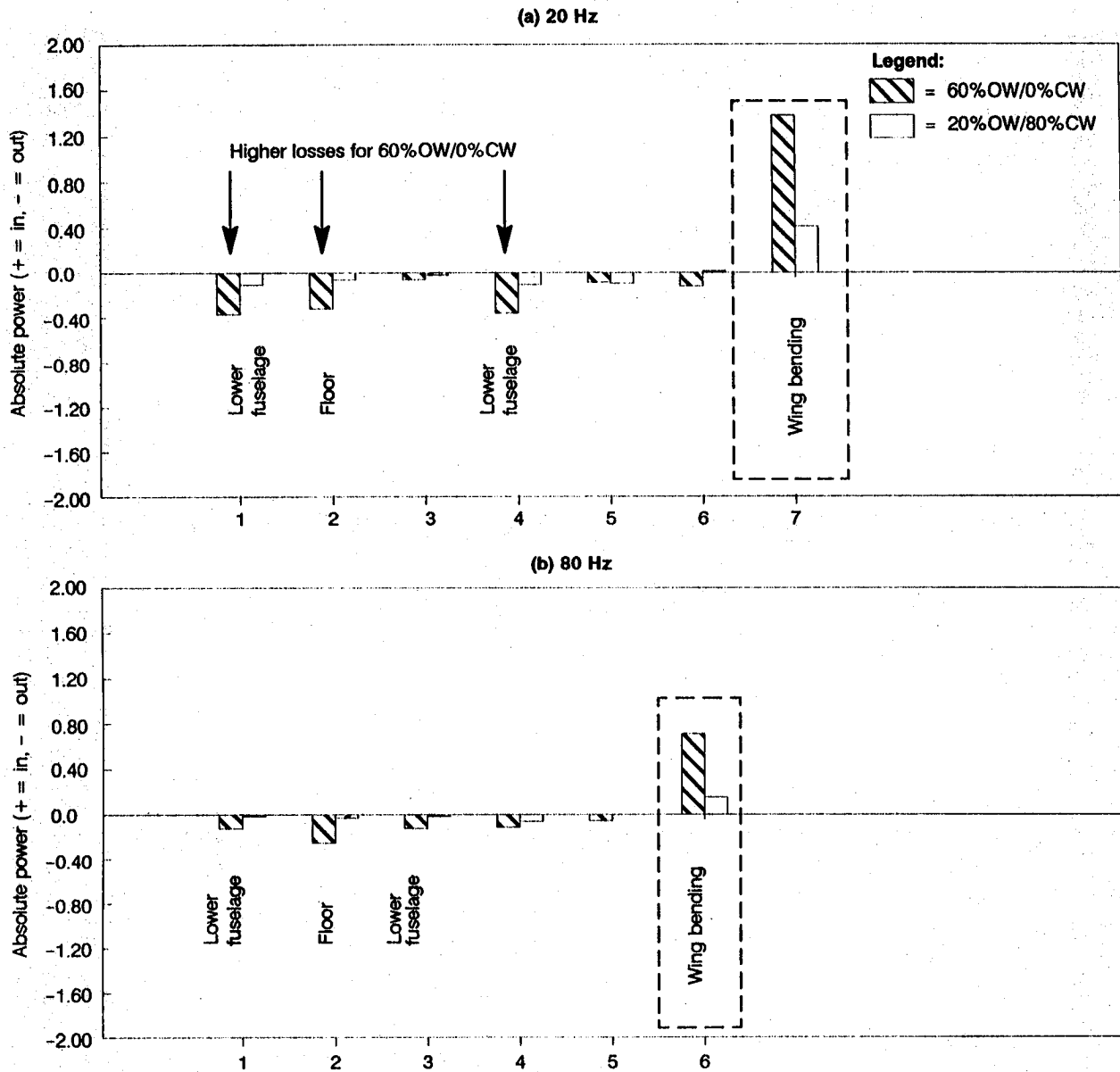


Figure 50. Absolute Power Flow to Wingbox for Fuel Loadings of 60%OW/0%CW and 20%OW/80%CW—48,000 lb Total Fuel

4.6.2 THE EFFECT OF A STIFFER WING ON REDUCTION OF CABIN NOISE

Stiffening of the inner wing subsystem, to which the strut attaches, resulted in less than a one-half dB increase in the cabin SPL. Still higher stiffness, even if practical, would lead to even greater increases in cabin SPL because of better coupling.

Because of the added stiffness, the power getting into the wing, for the same force input, decreased slightly because of the higher wing impedance. At the same time the greater stiffness of the wing re-

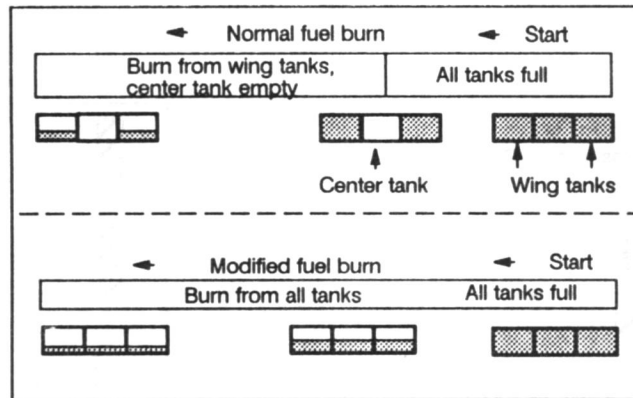


Figure 51. Normal and Modified Fuel Burn Methods

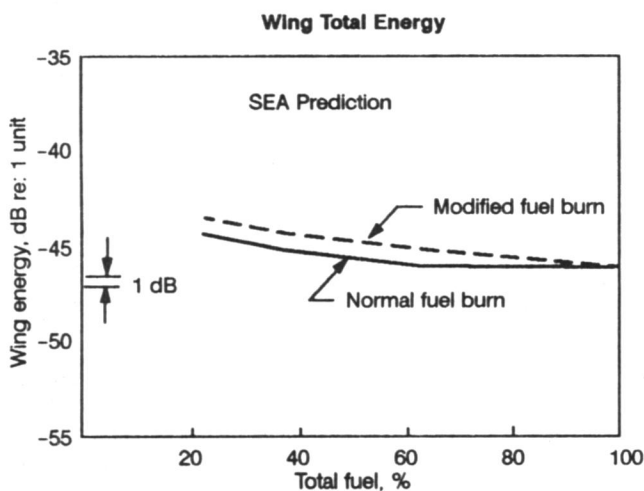


Figure 52. Fuel Loading Effect on Wing Energy – Shaft Rotational Frequency – SEA Prediction

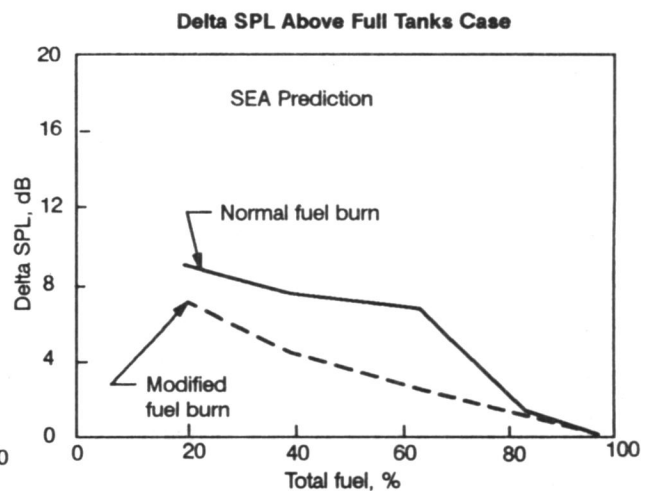


Figure 53. Fuel Loading Effect on Cabin Noise at Shaft Rotational Frequency – SEA Prediction

sulted in better coupling between the wing and the wingbox and slightly more power getting from the wing to the wingbox. Increasing wing stiffness as a means of reducing cabin SPL is obviously not a useful concept.

4.6.3 THE EFFECT OF INCREASED FUSELAGE MASS ON REDUCTION OF CABIN NOISE

Increasing the mid-fuselage sidewall mass by a factor of two resulted in approximately one dB increase in the cabin SPL.

Since the fuselage was the prime contributor to the cabin noise, for the case with fuel in the tanks, it was a likely candidate for treatment. Damping is not effective at the frequencies under consideration so increasing the mass was considered as a potential reduction method. To test this idea the density of the

sidewall above the wingbox was increased by a factor of two. Figure 54a shows the increase in cabin SPL and in the fuselage energy. A look at power flows showed increased contribution to the cabin noise from the sidewall and also increased contribution to the fuselage energy. The reason for this became clear after looking at the expression for the energy transmission coefficients for the four involved subsystems feeding energy to the fuselage subsystem. This expression is:

$$\tau = \frac{(4 R_1 R_2)}{|Z_1 + Z_2|^2}$$

Where R_1 and R_2 are the real part of the subsystem impedances and Z_1 and Z_2 are the complex impedances (subscript 2 being the fuselage). Increasing the impedance of subsystem 2 results in an increase in the transmission coefficient τ from subsystem 1 to the fuselage. As reflected in figure 54b, because of this increase in τ , the energy flowing from the wing bending and inplane subsystems and the wingbox bending and inplane subsystems to the fuselage are all increased. The more active fuselage then radiates more energy into the cabin.

4.6.4 REDIRECTION OF ENERGY AS A MEANS OF REDUCING CABIN NOISE

Redirection of energy to the lower fuselage sidewall proved to be ineffective in reducing cabin noise. The concept was valid but the amount of energy that could be removed was small.

A seemingly logical suppression concept was to try to reroute energy from areas that were radiating into the cabin to other areas that would not contribute to the cabin SPL. The intent was to try to get energy from the fuselage and wingbox into the lower fuselage sidewall. The wingbox bending subsystem attaches directly to the lower fuselage both fore and aft of the wingbox. From previous analysis it was known that the wingbox was not contributing much to the cabin space and that the energy that the fuselage was radiating to the interior was coming from the wing. The expectation was that changes could be made such that more energy would flow from the wingbox to the lower fuselage and that this would cause more energy to flow from the wing to the wingbox and less to the upper fuselage resulting in less upper fuselage radiation to the cabin.

Improved coupling between the wingbox and lower fuselage was accomplished by increasing the impedance (increasing the mass) of the lower fuselage. There was no change in cabin SPL although, as shown in figure 55, there was a small increase (1 dB) in the total energy of the lower fuselage.

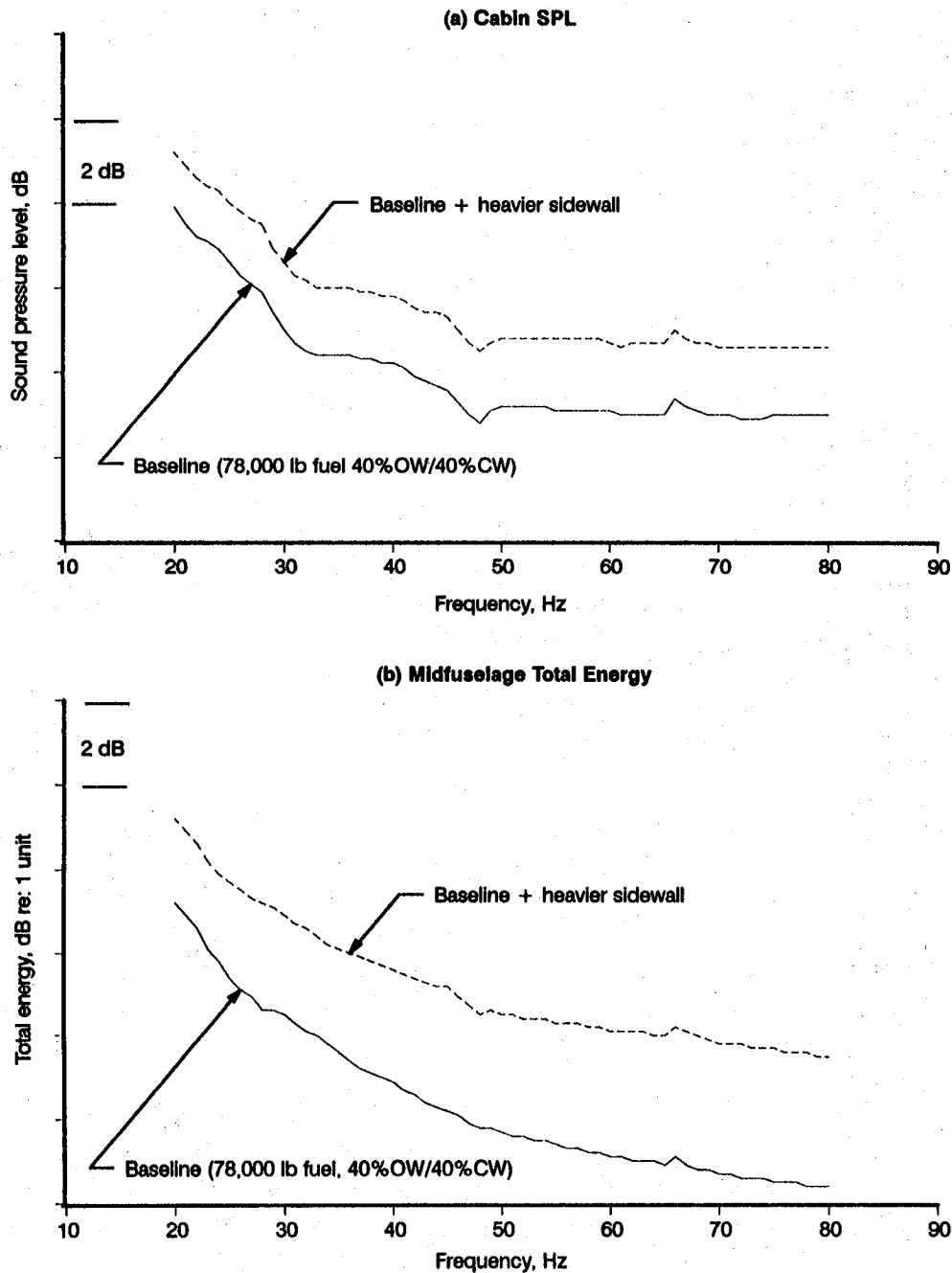


Figure 54. Effects of Doubling Midfuselage Mass

On an absolute power basis the variations in power flows of the subsystems are discernible, although small, and are shown in figures 56 and 57. Figure 56a shows that with the higher impedance lower fuselage there is slightly less energy getting to the cabin space from both the floor and the upper fuselage. However, the reduction amounts to less than 1 dB and is accompanied by smaller losses from the cabin space to the adjoining acoustic spaces. The result is no change in the cabin SPL. Figure 56b shows a very slight increase in the energy going from the wing to the wingbox. Figures 57a and 57b show

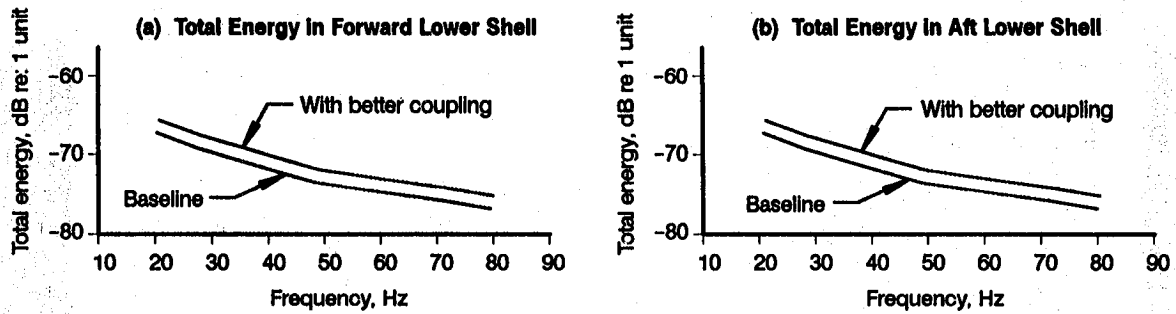


Figure 55. Rerouting of Energy to Lower Fuselage

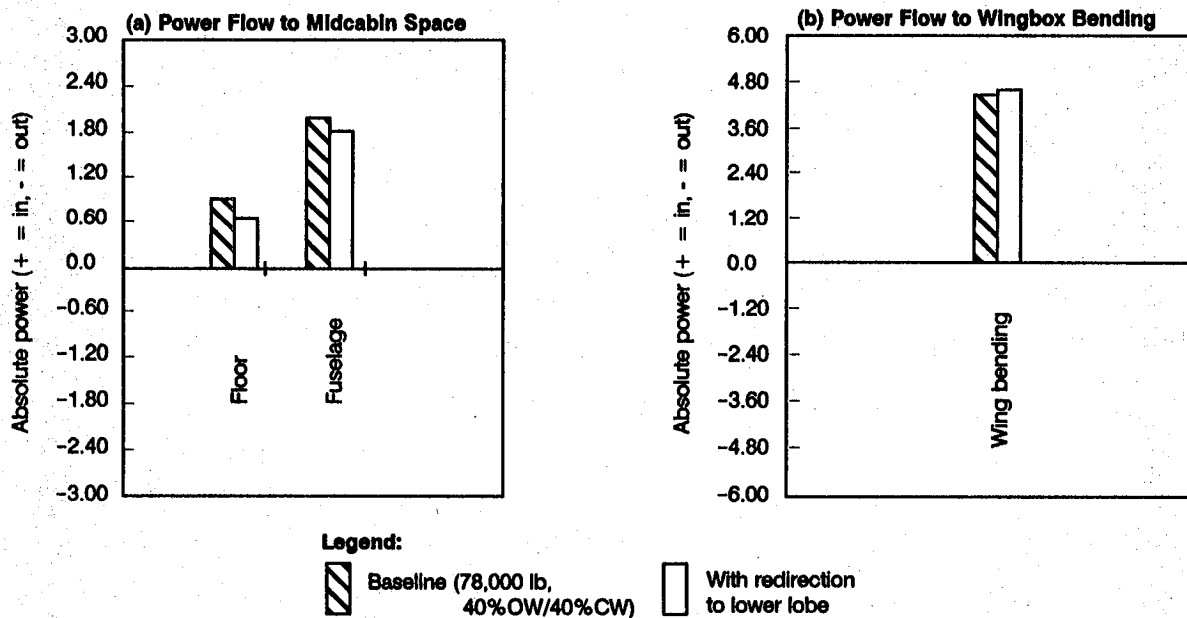


Figure 56. Effect of Redirection of Energy on System Power Flows at 20 Hz

what happens to the energy going to the upper and lower fuselage subsystems. In figure 57a less energy is getting from the wingbox bending to the upper fuselage as planned. However, there is also less energy flowing from the upper fuselage to the fore and aft adjoining fuselage sections because of the lower total energy now in the subsystem. This results in the net energy in the upper fuselage being almost unchanged. As seen earlier, in figure 56a, the decrease in energy going from the upper fuselage to the cabin space is too small to be of value. In figure 57b we can observe that there is more energy getting into the lower fuselage when we improve the coupling and that it is coming from the wingbox as planned.

The redirection of energy concept worked as expected but the amount of energy that could be diverted to the lower fuselage was too small to make the concept useful.

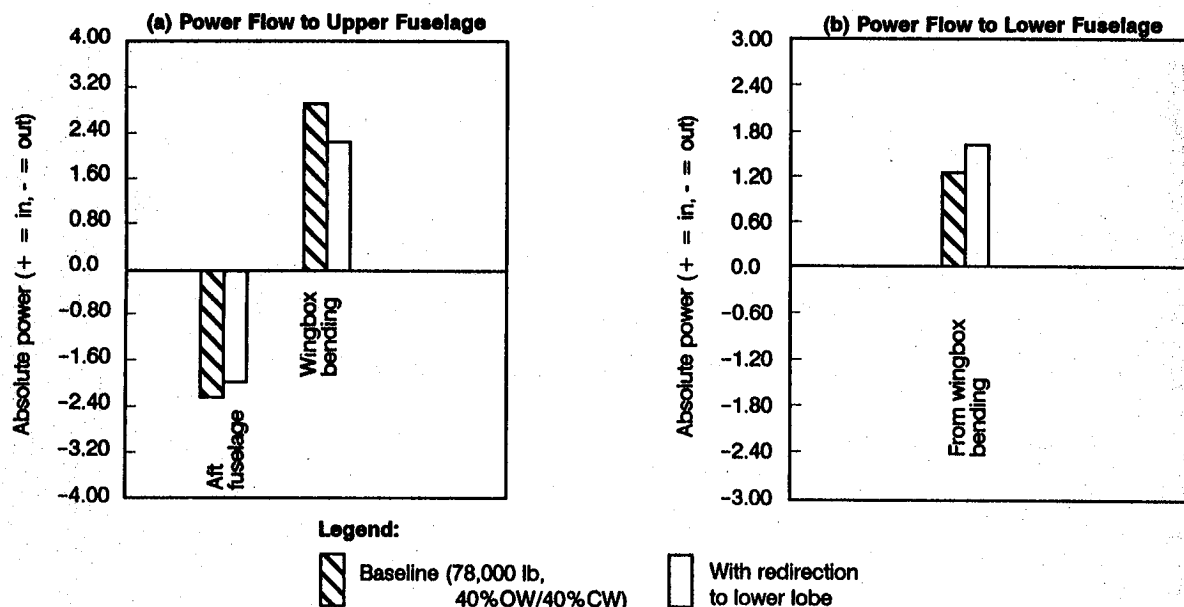


Figure 57. Effect of Energy Redirection on System Power Flows at 20 Hz

4.7 COMPARISON OF WING-MOUNTED VS. AFT-MOUNTED CONFIGURATIONS FOR STRUCTURE-BORNE NOISE

As described in a previous section, the predicted cabin SPLs for the 767-300 were higher than the measured values due to our inability (in SEA) to model the complex strut motion. The resulting predicted curve due to a 1 lb input force to the wing through the mass of the strut was adjusted downward to follow a mean line through the data. This adjusted curve, compared in figure 58 to an earlier predicted curve for the 727 Demonstrator, show that the 767-300 cabin levels were from 10 to 12 dB lower. The indications are that, for structureborne noise due to engine vibration, a wing mounted configuration is more desirable.

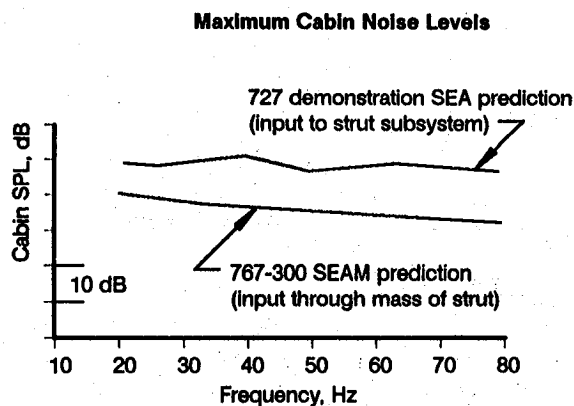


Figure 58. Comparison of Aft-Mounted Versus Wing-Mounted Engine Configuration for Structureborne Noise

5.0 PAIN ANALYSIS

5.1 FY 1989 PAIN MODEL UPGRADES

In 1989, PAIN work focused on completing two model upgrades recommended as a result of 1988 feasibility studies (ref. 1). These model upgrades were 1) modification of the PAIN method for predictions of cabin sound level axial gradients, and 2) extension of PAINUDF to include radiation from and transmission through the aft pressure bulkhead in calculation of cabin average sound level. PAINUDF was the designation given to the PAIN method for the case of propeller excitation to the empennage.

5.1.1 PREDICTIONS OF CABIN SOUND LEVEL GRADIENTS

The PAIN method was modified to calculate an axial variation of the average mean square pressure in cabin cross-section, both for reflecting and absorbing bulkheads, for airplanes with propeller excitation of the fuselage. The mathematical details of this work, performed under NASA Contract NAS1-18027, have been previously documented in reference 2. The volume average interior level computed from the cross-section averages agrees well with the volume average level computed directly from PAIN. Since there were no known published tests of sufficient detail, PAIN gradient predictions were not compared directly to test data.

Figure 59 shows cabin noise gradient predictions for a typical small body turboprop airplane. Interior predictions were made with and without absorptive terminating partitions at two different propeller speeds. At the blade passage frequency of the higher propeller rpm (70 Hz), the model predicts a rather strong gradient in the cabin. The fuselage in this case is a very stiff structure. At the excitation frequency of 70 Hz, only one transmitting structural mode is predicted to be mass controlled, one is essentially resonance controlled, and all of the other transmitting modes are stiffness controlled. Calculations indicate that acoustic modes having non-uniform pressure in cross-section with resonance frequencies slightly above the excitation frequency are the dominant responding modes for the sidewall motion induced by the propeller field at 70 Hz and that these highest modal responses are to a antisymmetric structural mode that is resonant at 74.9 Hz. The first predicted non-uniform pressure cross section acoustic mode cannot propagate axially below 81.0 Hz. The second occurring cannot propagate below 96.6 Hz, nor can the third below 142.3 Hz. The dominant responding acoustic modes are therefore non-propagating, composed of cross section modes inhibited to axial propagation at 70 Hz. Thus the response is fundamentally independent of axial propagation features. The dominance of non-propagating waves in the cabin appears to be the reason that the axial variation of the interior response is predicted to be similar in character to the predicted dominant sidewall motion, and the reason that the levels near the bulkheads are predicted to be higher when the bulkheads are slightly absorptive.

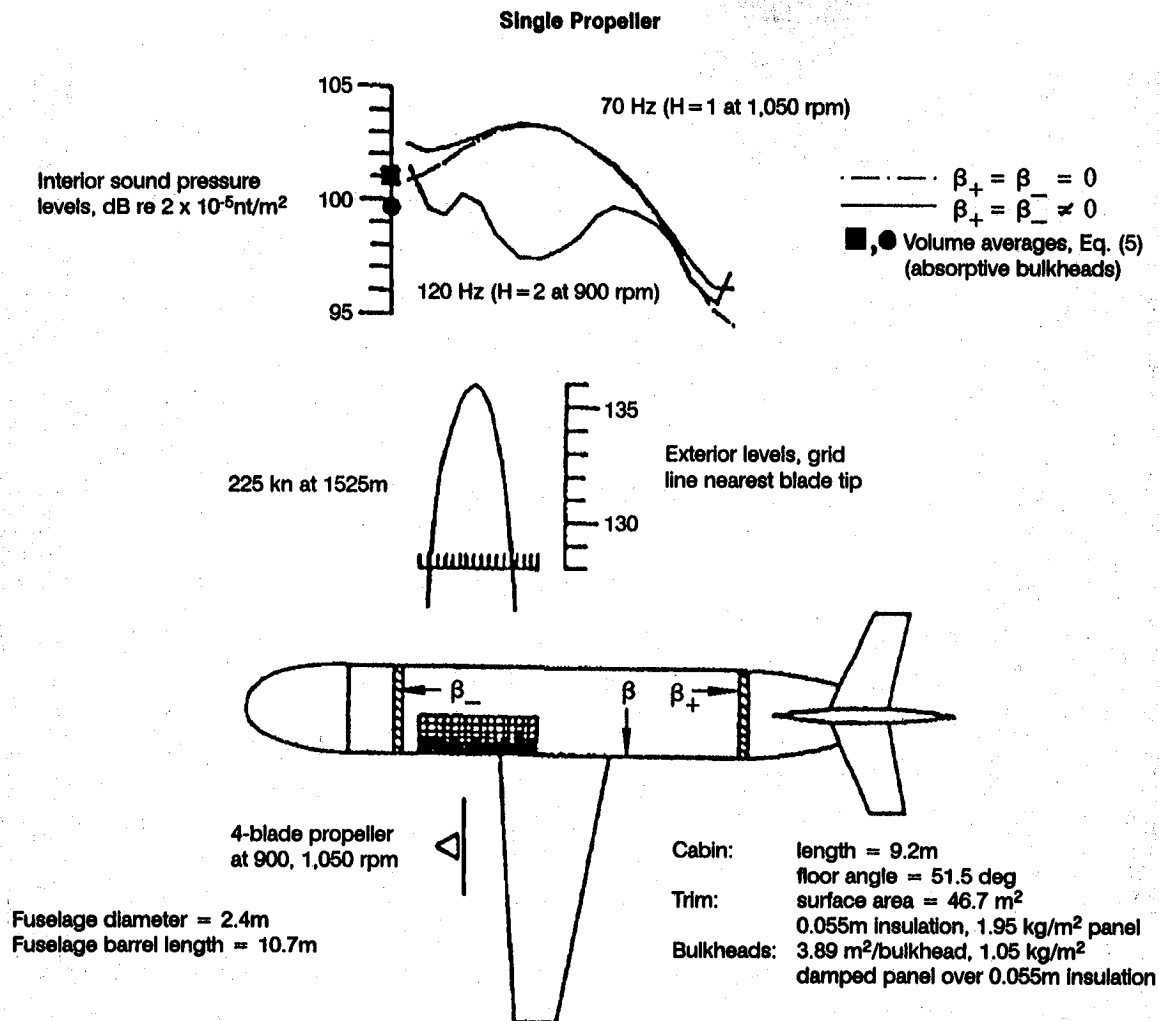


Figure 59. Predictions for a Small-Body Turboprop Commuter Airplane

At the lower propeller rpm, the small body airplane can have a second harmonic at 120 Hz. The predicted response at 120 Hz to the same amplitude field is also shown in figure 59. Here the acoustic response is more complicated. The model predicts that the most significant transmission is by resonance and mass controlled structural modes (having between two and five axial half-waves) which are transmitting to resonant acoustic modes composed of cross section modes of non-uniform pressure with axial propagation occurring.

Figure 60 shows cabin noise gradient predictions for a narrow body airplane (727) with a wing-mounted propeller. The interest, in 1989, was to look at the levels and gradient if an intense external field, such as might occur from a propeller, is present. Exterior data are not of the best quality, but are felt to be reasonably ample for the present purpose of examining the resulting interior field. The PAIN model predicts 95 structural modes below 169 Hz. Predictions are that at 169 Hz, resonant structural modes having axial wavenumbers characterized by 6 to 11 half-waves will dominate the transmis-

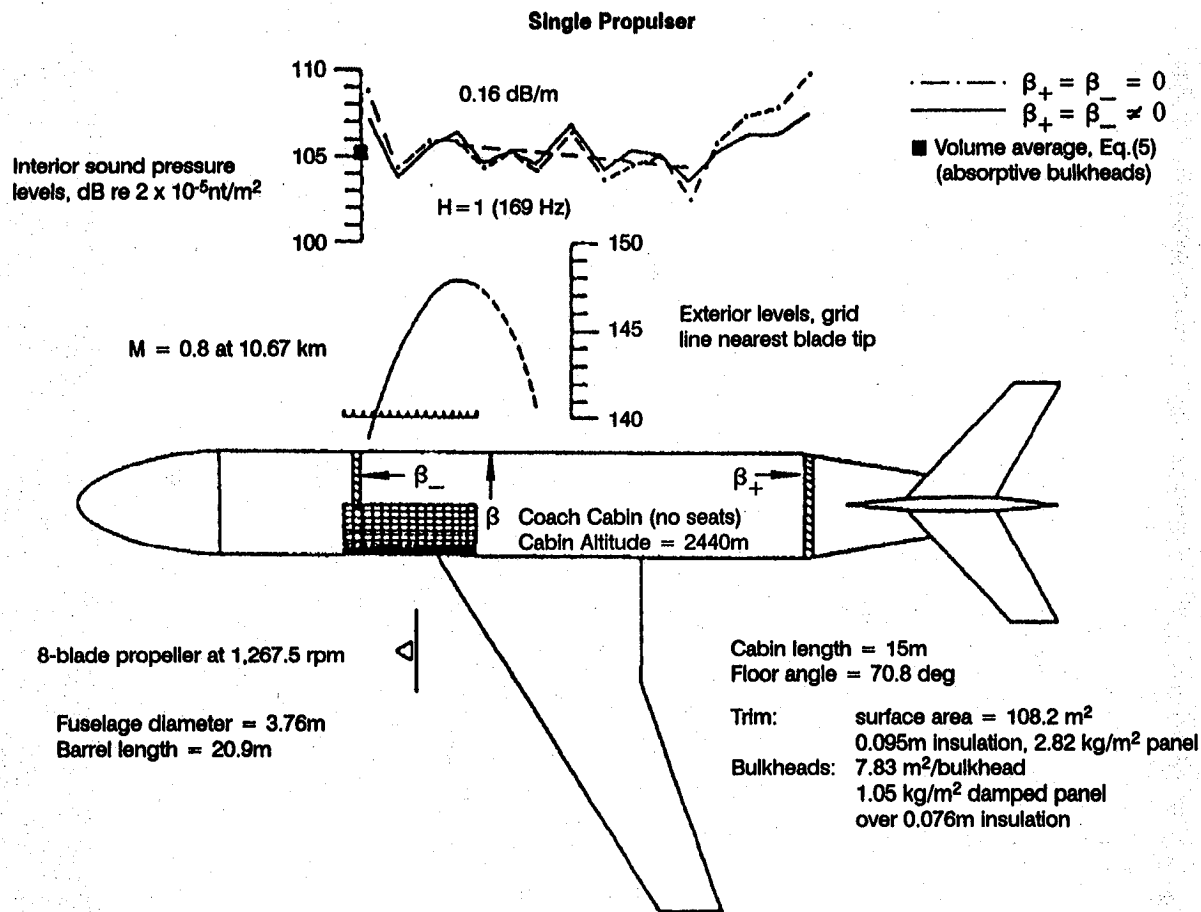


Figure 60. Predictions for a Narrow-Body Airplane With Wing-Mounted Propulser

sion to resonant acoustic modes. The dominant resonant acoustic modes replicate cross section modes having axial propagation capability. The predictions show a rather slow decrease in the average cross section levels as one moves aft of the propeller plane and then an increase in the levels near the aft pressure bulkhead. Thus, significant power appears to flow toward the rear of the cabin with the aft bulkhead reflecting the waves. Although similar gradient predictions were made in 1990, only the space average sound levels are given in this report because of relatively flat cabin gradient predictions.

5.1.2 PRESSURE BULKHEAD TRANSMISSION AND RADIATION

For propeller excitation of the empennage, PAINUDF was extended to include radiation from and transmission through the aft pressure bulkhead in calculation of cabin average sound level. In addition, PAINUDF was extended to predict a space average acceleration level of the empennage structure. A description of the upgraded PAINUDF follows.

The aft-mounted propeller version of the Propeller Aircraft Interior Noise (PAIN) Model is a generic model designed for prediction of cabin propeller tones in propfan airplanes having aft-mounted propellers (fig. 61). The system model consists of five basic elements indexed as follows:

1. Empennage frustum.
2. Fuselage sidewall (with installed trim) and cabin floor.
3. Cabin volume (with installed trim).
4. Bulkhead structure (with or without lavatory wall).
5. Empennage cavity.

The empennage model is a ring-and-stringer stiffened truncated conical shell coupled to the primary fuselage structure through a generic pressure bulkhead. It is assumed that the aft end on the frustum empennage is terminated by a rear bulkhead. Empennage vibrations induced by the propeller pressure field are transmitted to the fuselage shell and the bulkhead via the common juncture.

The PAINUDF fuselage structural model (sidewall and floor) is the same as the PAIN model fuselage (refs. 3, 4).

The PAINUDF cabin volume extends aft to the pressure bulkhead. Radiation and transmission through the aft bulkhead are acoustic sources for the cabin volume in addition to the sidewall and floor radiation. The sidewall analytical model accounts for the reduction of radiation into the cabin volume by the installed trim, the damping induced by the trim on the sidewall modes, and the increase in the cabin volume bounding surface sound absorption capacity (ref. 3, 4). The sidewall can be modeled with up to five layers.

The aft pressure bulkhead is generic. It is modeled as a flat continuous surface closing the cabin volume, having approximately uniform distribution of stiffeners yielding some reasonable average composite bending rigidities for the bulkhead in the vertical and horizontal directions. The composite rigidity in cross section perpendicular to the vertical direction is assumed to exceed that in section perpendicular to the horizontal direction. Because pressure bulkheads can be very complicated structures, with door frames, non-uniform placement of stiffeners, and possibly curvature, PAINUDF does not attempt modal calculations. The requirement for an estimate of modal density is satisfied by assuming the subpanels lying between major stiffeners do not break up, in a modal sense, at the excitation frequencies. A wall may be located forward of the aft pressure bulkhead to simulate lavatory installation. In addition, the wall is isolated from fuselage sidewall and floor vibrations.

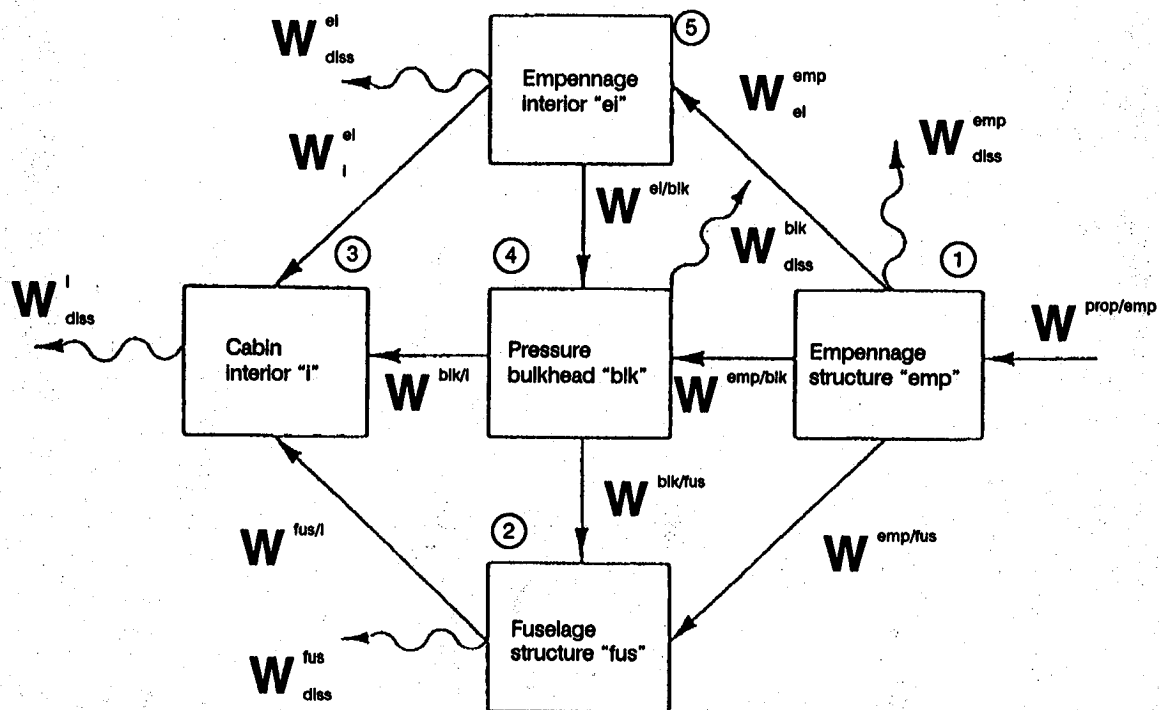
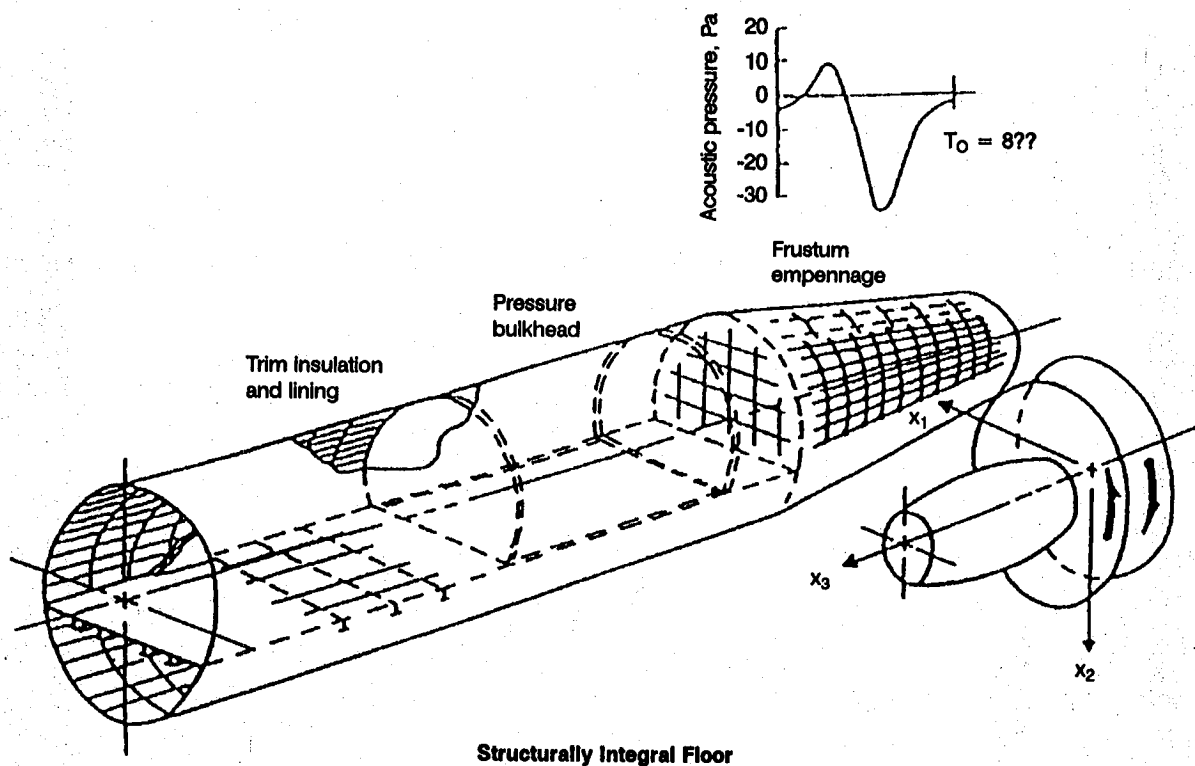


Figure 61. Propeller Aircraft Interior Noise Model and Power Flow Diagram – Empennage-Mounted Propeller

The empennage cavity is a bare walled closed volume equal to the interior volume of the frustum. Sound energy in the cavity originating from the empennage or the bulkhead can propagate through the bulkhead to the cabin volume.

Propeller signatures used are blocked pressure amplitude and phase data on a grid lying on the surface of the frustum. The physical nature of the propeller signature field (both amplitude and phase characteristics) is very important in the prediction for stiff structures having low modal densities such as the empennage. Therefore, realistic propeller signature data which includes effects caused by non-uniform inflow into the rotor disk, refraction by turbulent boundary layer and reflection from the structure surface should be specified.

PAINUDF predictions for space average cabin sound level should be considered as a potential upper bound provided that the propeller data are realistic and that subpanels of the empennage shell will not break up, in a modal sense, at the excitation frequency. Space average sound levels of aft-mounted propeller airplanes in flight should lie below predictions since engine pylon and vertical stabilizer stiffening and inertial effects on the empennage structure are not included in the PAINUDF model.

5.2 FY 1990 PREDICTIONS FOR WING-MOUNTED AND AFT-MOUNTED PROPELLER AIRPLANES

In 1990, PAIN predictions were made of cabin propeller tone sound levels in a 727 airplane with advanced high speed turboprop engines. Two different configurations were investigated, one with wing-mounted engines and one with aft-mounted engines. Parametric variations were made to the baseline airplane to determine the effects on predicted interior noise levels caused by changes in fuselage stiffness, mass, and damping, and by changes in the configuration and weight of the cabin trim installation. Predictions were made for the tonal levels occurring at the blade passage frequency (169 Hz) and at the frequency of the second harmonic (338 Hz) of the propeller field. Predictions were made with the latest, undocumented version of the PAIN computer program, PAIN90. PAIN90 combines into one program the up to date versions of the PAIN method for wing-mounted propellers and the previously designated PAINUDF for aft-mounted propellers.

5.2.1 727 PAIN MODEL

The baseline fuselage cylindrical structural model of the 727 airplane is assumed to extend between station 300 and station 1183 (fig. 62). The baseline cabin consists of a first class section and a coach section separated by a galley. The model consists basically of four acoustical partitions located within the fuselage segment. The first class cabin is assumed to be closed by a forward partition at station 360

and a second partition representing the forward end of the galley at station 635.4. The galley extends from station 635.4 to station 675.4. The aft end of the galley is assumed to be the forward partition of the coach section which extends from station 675.4 to the aft pressure bulkhead at station 1146 where the aft partition of the coach section is assumed to be located, corresponding to the lavatory wall. The pressure bulkhead is located at station 1183.

The baseline empennage is modeled as a frustum having structural and dimensional properties that are similar to those of the 727 Demonstrator airplane empennage. Properties of the frames were selected to simulate the bending stiffness of the frames on the demonstrator, which were basically deep shear webs with heavy caps. Generally, it can be stated that the modal density of the frustum empennage is sufficiently reduced, so that at blade passage frequency the frustum response vibration level is on the verge of being stiffness controlled. Thus, the baseline empennage is modeled as a very stiff structure. The generic bulkhead model is based on the average properties of the 727 pressure bulkhead.

Predictions are made, in every case, for a trimmed cabin with seating structure dead weight on the floor structure. Passenger load is not considered, being assumed dynamically isolated. Also the cabins are assumed to be empty acoustically. Neither passengers or seats are present to absorb and reflect/scatter sound in the cabin. All sound absorption occurs on the treated cabin sidewall and ceiling.

The propeller plane for the configuration involving wing-mounted engines is located at station 640. The propeller is located at 90° relative to the bottom center line (fig. 63). The propeller plane for the aft-mounted configuration is 3.3m aft of the pressure bulkhead at station 1183. The rotor is located at 105° relative to the bottom center line of the frustum, in the same position as on the demonstrator airplane (fig. 63).

Representative propeller tone excitation pressure field data are developed for two harmonics. These correspond to the blade passage frequency at 169 Hz and the second harmonic at 338 Hz of the aft-mounted forward rotor of the 727/GE36 propeller. Predictions for the aft-mounted propeller are made using the forward rotor measured amplitude data and the harmonic phase data that were computed with the NASA Langley Aircraft Noise Prediction Program (ANOPP). The selected exterior data represent a flight cruise condition.

Propeller tone data for the case where the rotor is located on the wing are developed using the assumption that the forward rotor is simply shifted forward to the wing and that the blade tip clearance remains the same. Propeller amplitude and phase data are derived for the propeller signature grid on the cylindrical fuselage by manipulation of the data for the empennage frustum. Ideally the phase data

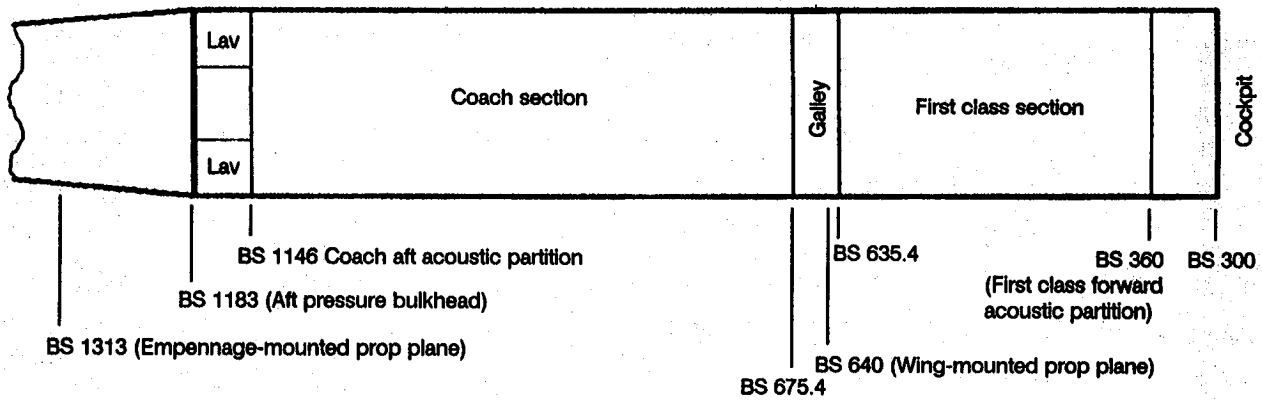


Figure 62. 727 Baseline Airplane Model

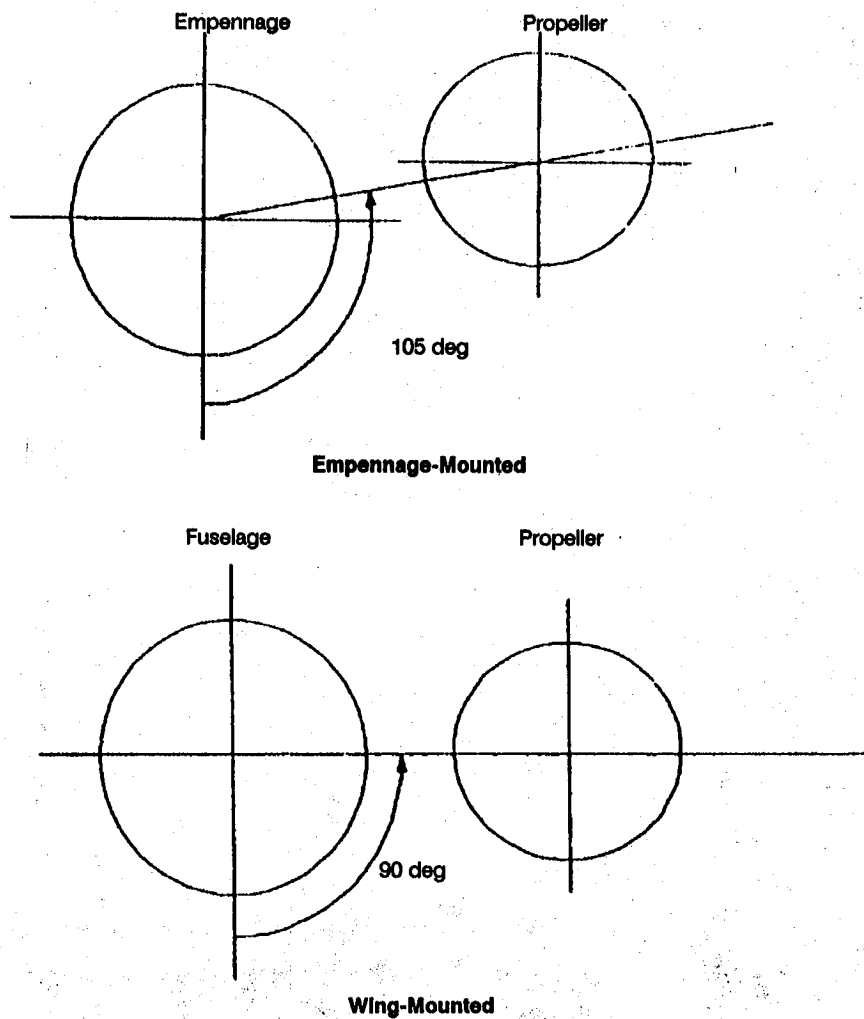


Figure 63. Propeller Locations Relative to Bottom Centerline

should be recomputed with the ANOPP program using the new grid coordinate positions but this was not practical within the constraints of the present program. Thus both amplitude and phase data are a simulation of what can be expected if: a) measurements were made of the exterior sound levels with wing-mounted engines, and b) ANOPP predictions were made of the phase data. Note in the present case that, theoretically, the inflow to the propeller disk is uniform for a wing-mounted configuration. Thus the ANOPP phase data that were computed for the forward rotor with uniform inflow can actually be expected to be more applicable to the wing-mounted configuration than the empennage configuration where the pylon causes a non-uniform inflow into the rotor disk. However, some adjustments have to be made in the empennage phase data for use on the cylindrical fuselage to account for the difference in the diameters of the empennage and fuselage in the region where propeller acoustic field phase varies slowest.

There remains considerable uncertainty about the adequacy of the ANOPP computed phase data for the aft-mounted propeller (ref. 1). In the interest of avoiding a problem area that cannot be resolved until better propeller predictions are available (the case of non-uniform inflow into the rotor disk) it is assumed that the ANOPP data are at least a first approximation to the propeller phase field. The dummy phase field used in previous studies (ref. 1) has been discarded. Nevertheless, it is necessary to remember that the existence of a pressure field with relatively slower phase variation over a significant area of the propfan grid, as typified by the dummy phase field, remains a possibility until the effects of non-uniform inflow into the rotor disk and boundary layer refraction have been shown not to reduce the rapidity of the phase variation. A slower varying phase field could yield a 10 dB increase in predicted interior levels for aft-mounted propellers. In an attempt to overcome this problem in the present study, a calibration run was made to compare predictions with the 727 Demonstrator airplane measurement data. Interior levels predicted for frustum aft-mounted rotor with ANOPP phase data are adjusted according to the experimental findings. Results of the calibration run are discussed below.

5.2.2 BASELINE PREDICTIONS

For wing-mounted propellers, the average level predicted in the first class cabin is 109.0 dB at 169 Hz and 88.9 dB at 338 Hz. In the coach cabin, the predicted average levels are 110.7 dB at 169 Hz and 88.7 dB at 338 Hz.

For aft-mounted propellers, the average level predicted in the coach cabin, with lavatories, is 92.8 dB at 169 Hz and 77.1 dB at 338 Hz. With the lavatories removed, the predicted levels are 95.4 dB and 79.7 dB, respectively. The aft-mounted levels have been adjusted by a calibration run to account for the uncertainty in the phase field.

Table 1 gives the results from a calibration run where predictions were made for the aft-mounted configuration in the baseline airplane with the baseline empennage, but with the demonstrator cabin forward of the lavatories. In the demonstrator airplane, the cabin was configured with an acoustic barrier approximately 7.62 m forward of the pressure bulkhead. Predicted levels can be compared to the demonstrator measurements, also given in table 1. Considering $H = 1$, the demonstrator cabin prediction is 85.2 dB versus the measured 92.7 dB, an underprediction of about 7.5 dB. The empennage cavity level for $H = 1$ is underpredicted by approximately 6.6 dB. Thus, there is about a 7 dB underprediction when using the ANOPP phase data. For $H = 2$, one must use the empennage cavity difference of table 1. The predicted level is 96.3 dB and the measured is 93.4 dB or an overprediction of 2.9 dB. The values of the previous paragraph have been obtained by adding 7 dB to the raw prediction for $H = 1$ and subtracting 3 dB for $H = 2$.

Table 1. 727 Demonstrator Cabin Predictions for Aft-Mounted Propeller

Normalized space average sound pressure levels, dB		
	H = 1 at 169 Hz	H = 2 at 338 Hz
PAIN predictions		
• Cabin	85.23	79.67
• Empennage cavity	98.91	96.30
Measured data		
• Cabin	92.70	Not available
• Empennage cavity	105.50	93.40

For this study, all aft-mounted configuration predictions of interior levels, both baseline and parametric variations, have been adjusted by the calibration run.

5.2.3 PERFORMANCE OF THE BASELINE TRIM SYSTEM

Cabin trim has three fundamental acoustical functions: 1) it increases the transmission loss of the sidewall system, 2) it increases the sound absorption capacity of the sidewall surface, and 3) it adds damping to the structure. All three of these effects are included in the PAIN90 model (ref. 2).

The trim transmission coefficient defines the mean square driving velocity of the trim panel as a percentage of the mean square sidewall velocity. Power flow to the cabin from the sidewall is reduced according to that ratio thus defining an increase in the sidewall transmission loss.

The acoustic loss factor in the cabin is a direct reflection of the trim system's absorption capacity. Thus the cabin loss factor defines an increase in the absorption coefficient.

The structural damping level of the structural modes is determined by the so-called "adjutant" structural loss factor. The factor includes the inherent structural damping, the radiation losses to the exterior of the fuselage, and the effect of the trim, which is by far the greater effect when insulation is included in the trim system.

Table 2 gives the computed values of these parameters for the one-third octave bands from 50 Hz to 400 Hz. The computer program uses the values in the 160 Hz band for the blade passage frequency at 169 Hz and in the 315 Hz band for the second harmonic at 338 Hz. There are some important things to note about these parameters. When the trim transmission coefficient is near zero or negative, resonance of the simple trim model on the structure is implied. The adjutant structural loss factor and the acoustic loss factor will be high. As the trim becomes more effective as a transmission loss device, the adjutant loss factor will drop.

Table 2. Sidewall Trim Performance Parameters for the Baseline Cabin (Three-Layer Trim)

One-third octave band center frequency, Hz	Transmission coefficient, dB	Cabin space acoustic loss factor	Adjutant structural loss factor
50	-1.29	0.072	0.279
63	-0.66	0.085	0.143
80	1.06	0.084	0.424
100	3.67	0.059	0.318
125	6.97	0.041	0.155
160	10.47	0.025	0.109
200	12.81	0.017	0.095
250	14.37	0.011	0.063
315	15.39	0.007	0.049
400	21.17	0.004	0.045

5.2.4 CONTRIBUTION OF THE FLOOR FOR WING-MOUNTED CONFIGURATION

The PAIN90 model does not separate out the contributions of the sidewall and floor to the interior levels. However, a slight modification to FORTRAN code allows that contribution to be estimated. This was done for the baseline first class cabin in the following manner. The trim was assumed to be laid over the floor to achieve the velocity reduction of the trim system. At 169 Hz, this reduction is about 10.5 dB, and at 338 Hz the reduction is about 15.4 dB. The results show that the cabin floor is a major contributor. At 169 Hz, the volume average level of 106.7 dB is approximately 2.3 dB lower than the 109.0 dB that is predicted with full floor contribution. In effect, a 10 dB reduction in the floor contribution is predicted to reduce the cabin level by 2 dB. At 338 Hz, a 15 dB reduction in the floor contribution is predicted to reduce the level in the cabin from 88.9 dB down to 81.5 dB. Thus as the trim on the sidewall becomes more effective, the floor contribution will rise until it dominates. This effect must be kept in mind as the trim system is revised.

5.2.5 CONTRIBUTION OF THE PRESSURE BULKHEAD FOR AFT-MOUNTED CONFIGURATION

The PAIN90 program separates out the contributions of the bulkhead and fuselage sidewall to the cabin levels for aft-mounted propellers. At 169 Hz and 338 Hz, the predicted levels in the coach cabin would be only 91.87 dB and 70.75 dB respectively if the bulkhead radiation could be totally neglected. These levels are approximately 3.5 dB lower at $H = 1$ and 7 dB lower at $H = 2$ than the baseline with the lavatories removed. Obviously an untreated bulkhead is the major contributor.

5.2.6 CABIN TRIM VARIATIONS

Table 3 contains basic information about the three different trim configurations that were used in this study. Two variations of the baseline trim are indicated.

The fundamental differences between the four-layer trim and the baseline trim are the inclusion of an internal septum and the absence of an air gap. The finishing trim panel weighs the same as the baseline trim panel. A slight increase of 0.9 kg/m^2 in the average surface mass density is indicated. Total sidewall depth remains at 0.096 m.

The five-layer trim is designed to increase the overall weight of the baseline sidewall trim by about 7 kg/m^2 . It features an air gap, an internal septum of twice the weight of that in the four-layer trim, and a very heavy trim panel.

Table 4 gives the sidewall performance parameters for the four- and five-layer trims. The data may be compared to the results for the baseline trim in table 2. The four-layer trim has about the same transmission loss at the baseline at 169 Hz, with about a 4 dB improvement at 338 Hz. The acoustic loss factors are about the same as the baseline trim. Some improvement in the effective sidewall damping occurs.

The five-layer trim achieves a significantly higher transmission loss, but at the expense of a greatly decreased cabin loss factor. This is due to the reflectivity of the heavy trim panel. Thus absorption by passengers and seating are more critical in the case of a heavy trim panel. The effective structural damping is closer to the baseline case than that of the four-layer trim, presumably because the air gap is present as in the baseline. Thus there is some slight benefit from having the insulation lay directly against the skin.

Table 3. Cabin Trim Variations

Baseline Three-Layer Trim			
Layer No.	Description of layer	Depth, m	Mass/area, kg/m ²
1	Airgap	0.032	Negligible
2	Insulation	0.064	0.61
3	Trim panel	—	2.82
Totals		0.096	3.43
Four-Layer Trim With Internal Septum of 0.61 kg/m ²			
Layer No.	Description of layer	Depth, m	Mass/area, kg/m ²
1	Insulation (PF-105)	0.032	0.30
2	Septum	—	0.61
3	Insulation (PF-105)	0.064	0.61
4	Trim panel	—	2.82
Totals		0.096	4.34
Five-Layer Trim With Internal Septum of 1.22 kg/m ²			
Layer No.	Description of layer	Depth, m	Mass/area, kg/m ²
1	Airgap	0.032	Negligible
1	Insulation (PF-105)	0.032	0.30
2	Septum	—	1.22
3	Insulation (PF-105)	0.064	0.61
4	Trim panel	—	8.41
Totals		0.128	10.54

Table 4. Comparison of Sidewall Performance Parameters (Four- and Five-Layer Trims)

Four-Layer Trim With Internal Septum			
One-third octave band center frequency, Hz	Transmission coefficient, dB	Cabin space acoustic loss factor	Adjutant structural loss factor
50	-1.37	0.077	0.330
63	-0.78	0.114	0.166
80	0.67	0.084	0.520
100	2.83	0.055	0.414
125	5.89	0.040	0.214
160	9.21	0.024	0.165
200	11.56	0.015	0.163
250	14.62	0.011	0.138
315	19.26	0.007	0.105
400	25.43	0.004	0.061
Five-Layer Trim With Internal Septum			
One-third octave band center frequency, Hz	Transmission coefficient, dB	Cabin space acoustic loss factor	Adjutant structural loss factor
50	6.01	0.064	0.345
63	9.02	0.057	0.136
80	12.19	0.029	0.343
100	15.13	0.016	0.246
125	18.21	0.011	0.130
160	21.89	0.007	0.117
200	26.24	0.004	0.121
250	32.33	0.003	0.080
315	37.94	0.002	0.049
400	41.99	0.001	0.028

Predictions of the interior levels when the four and five layer trims are used in the wing-mounted configuration are given in table 5. Observe that the $H = 1$ results are down only slightly as compared to the case of the baseline trim. The $H = 2$ levels are down for the four-layer trim but are up for the five-layer trim. At first, these results may seem anomalous, especially for the five-layer trim with a much higher transmission loss. But there is a simple explanation. The floor has become the major contributor to the cabin levels. Also, in the case of the five-layer trim, there is much less absorption in the space.

Also given in table 5 are the results for the first class cabin if the velocity reduction achieved on the sidewall with the five-layer trim is also achieved for the floor. These results show that in order for there to be a significant decrease in cabin levels in the wing-mounted configuration, the floor must be well isolated with an unknown, but significant associated additional weight penalty.

Table 5. Predictions for the Baseline Fuselage With Four- and Five-Layer Trims for Wing-Mounted Propellers

Normalized space average sound pressure levels, dB				
Configuration	H = 1 at 169 Hz		H = 2 at 338 Hz	
	First class	Coach	First class	Coach
Baseline (three-layer trim)	106.02	107.67	85.92	85.76
Four-layer trim	105.46	107.25	82.94	82.55
Five-layer trim	104.91	107.65	87.58	86.36
Five-layer trim with isolated floor	95.49	—	58.14	—

Table 6 gives the results for the case of the aft-mounted configuration with the two trim variations in the coach cabin. Again, the sound levels are higher for the five layer trim. Now, however, the reason is because of the dominance of the bulkhead into a less absorptive space. Unless the bulkhead radiation is suppressed, the sidewall contribution is negligible. The floor may not be negligible. In PAIN90, the floor is assumed to be isolated to the same degree that the sidewall is isolated, for empennage excitation. Obviously, for the aft-mounted propeller configuration, noise reduction should focus first on the bulkhead.

Table 6. Predictions for the Baseline Empennage/Fuselage/Bulkhead With Four- and Five-Layer Trims for Aft-Mounted Propellers

Normalized space average sound pressure levels in coach section, dB		
Configuration	H = 1 at 169 Hz	H = 2 at 338 Hz
Baseline (three-layer trim)	92.76	77.10
Four-layer trim	92.71	74.32
Five-layer trim	97.51	79.40

5.2.7 FUSELAGE VARIATIONS

Three variations of the baseline fuselage were made. The simplest of the variations was the doubling of the number of stringers. This change causes an increase in the axial bending rigidity of the sidewall and an increase in the average sidewall surface mass density. The second variation significantly increases stiffness without changing the sidewall mass by assuming thicker composite stiffeners replace the aluminum frames and stringers. The third and final fuselage variation simulates the addition of sufficient constrained layer damping materials to the sidewall of the baseline configuration to achieve a significant increase in the structural damping present in the fuselage. Previously, an increase of 7.0 kg/m^2 in the trim system using the heavy five-layer trim has been shown to reduce levels about 10 dB at $H = 1$ and 27 dB at $H = 2$ in the first class cabin if the floor contribution is suppressed (table 5). It is of interest to determine how much reduction can be achieved with the same 7.0 kg/m^2 in the form of constrained layer damping material on skin, frames, and stringers. The estimated loss factors of the untrimmed baseline fuselage with and without constrained layer damping material are given in table 7.

Table 7. Estimated Loss Factor of the Untrimmed Baseline Fuselage Structure With and Without Constrained Layer Damping Material Totalling 7.0 kg/m^2

One-third octave band center frequency, Hz	Loss factor with constrained layer damping	Loss factor without constrained layer damping
50	0.0873	0.040
63	0.0790	0.032
80	0.0723	0.025
100	0.0673	0.020
125	0.0633	0.016
160	0.0598	0.013
200	0.0573	0.010
250	0.0553	0.008
315	0.0536	0.0064
400	0.0523	0.0050
500	0.0513	0.0040

Table 8 presents the computed interior levels for the wing-mounted configuration in the first class and coach sections for the three fuselage variations. In each case, the baseline trim is used.

For the case with double the number of stringers, there is about one dB decrease in the cabin interior sound levels. For the case of the composite stiffeners, a one to two dB increase in interior levels should be expected if the axial and circumferential stiffnesses are increased in accordance with the present variations and if the baseline sidewall surface mass is not increased.

There is a 2 to 2.5 dB reduction from the baseline levels at $H = 1$ and about 10 dB reduction at $H = 2$ for the case with constrained layer damping. The prediction is limited by the fact that the baseline trim already significantly dampens the structural modes (table 2). If the results for the constrained layer

Table 8. Predictions for Fuselage Variations for Wing-Mounted Propellers

Normalized space average sound pressure levels, dB				
Configuration	H = 1 at 169 Hz		H = 2 at 338 Hz	
	First class	Coach	First class	Coach
Baseline	106.02	107.67	85.92	85.76
2X stringers	105.12	106.92	85.19	84.42
Composite stiffeners	108.00	109.12	83.82	82.17
2X sidewall mass (constrained layer damping)	103.67	105.86	75.30	74.32

damping case are compared to those of the non-isolated floor case in table 5, it can be observed that the effectiveness of the additional 7.0 kg/m^2 in the trim is about the same as if on the sidewall for $H = 1$. For $H = 2$, adding weight in the damping material is more efficient. However, remember that the floor contribution is not suppressed. If the results for the first class cabin for the case of constrained layer damping is compared to the results for which the floor is isolated, it is found that the 7.0 kg/m^2 is much more effective in the trim system. However, the weight penalty of an isolated floor has not been estimated. In a design process, there is an optimum configuration that would possibly include some increase in the trim weight, some increase in the sidewall weight via constrained layer damping material, and some increase in the weight of the floor structure to isolate the exposed floor surface.

Table 9 gives the predictions for the coach cabin levels for the aft-mounted configuration when the three fuselage variations are made. Only a slight improvement is shown, again because the bulkhead is the major contributor. Recall that earlier it was pointed out that the cabin floor is assumed to be isolated to the same degree as the sidewall by the trim when the PAIN90 program is run for the aft-mounted configuration. If the bulkhead radiation could be suppressed sufficiently, the floor could become a significant contributor to the overall levels, especially with a heavy sidewall trim in the coach section.

Table 9. Predictions for Fuselage Variations for Aft-Mounted Propellers

Normalized space average sound pressure levels in coach section, dB		
Configuration	H = 1 at 169 Hz	H = 2 at 338 Hz
Baseline	92.76	77.10
2X stringers	92.26	77.20
Composite stiffeners	91.24	77.53
2X sidewall mass (constrained layer damping)	90.19	73.59

5.2.8 VARIATION OF THE PRESSURE BULKHEAD

Predictions were made for the case of aft-mounted rotors in which the bulkhead was assumed to be damped with constrained layer damping totaling 7.0 kg/m^2 , the same as used in the sidewall studies.

Table 10 gives predicted results for the sound levels in the coach cabin with the damped bulkhead, and with the baseline trim, baseline empennage, and baseline fuselage. Also given is the predictions for the case of a damped bulkhead having the same damping level as the previous case but without the weight penalty. A 2.5 to 3 dB reduction might be expected to occur for a heavily damped bulkhead, about 2 dB of which would be due to the damping material, with the remainder caused by the addition of the mass.

Table 10. Predictions for Bulkhead Variations for Aft-Mounted Propellers

Normalized space average sound pressure levels in coach section, dB		
Configuration	H = 1 at 169 Hz	H = 2 at 338 Hz
Baseline	92.76	77.10
Damped bulkhead	89.73	76.06
Damped bulkhead with no weight penalty	90.72	76.63

5.2.9 NONCONVENTIONAL SIDEWALL TREATMENTS

The final variations of the 727 airplane involve the replacement of the baseline trim with a multi-layer treatment consisting of a layer of insulation against the skin, an air gap, and Helmholtz resonators attached to the backside of the trim panel and tuned to the blade passage frequency. The absolute maximum allowed trim depth would be about 0.152m. The use of a resonator panel over the bulkhead might also be useful where space limitations are not as severe as on the sidewall.

The following design was found to be a feasible sidewall configuration, to fit in a six inch space:

1. Trim panel: 0.80mm thick damped aluminum panel with a surface mass density of 2.82 kg/m².
2. Helmholtz resonators: aluminum hemispheres, each weighing approximately 0.144 kg, having a volume of $8.96 \times 10^{-4} \text{ m}^3$ or 54.68 in³, having a radius of approximately 0.0753m-mounted to the backside of the trim panel with a density of 36 resonators per square meter for a total surface mass of approximately 5.18 kg/m², with resonator nozzles having a length of approximately 0.0325m and a throat radius of approximately 0.0118m.
3. Insulation: 0.0432m of PF-105 Fiberglass, against the skin of the airplane, with surface mass of 0.41 kg/m².

The total resonator-trim (R/T) panel assembly surface mass density would be 8.41 kg/m², a value that is identical to the surface mass of the heavy trim panel of the five-layer trim, but less than the 10.54 kg/m² of the five-layer trim assembly (see table 3).

Table 11 gives what are believed to be conservative estimates of the values of the trim coefficient at the blade passage frequency and the second harmonic. The absorption of an R/T assembly trim panel will be low, as was the five-layer trim. Based simply on the prediction of the transmission coefficient at 160 Hz, it is estimated that the blade passage frequency can be reduced in the first class and coach cabin, for wing-mounted propellers, by as much as 8.5 dB beyond that which can be achieved with the five-layer trim. With an isolated floor, this yields a level for one propeller of 90.5 dB for the first harmonic. The second harmonic level would be about 13 dB higher with the R/T assembly than with the five-layer trim, or about 74 dB for one propeller. This would be done with slightly less weight. However, if engine tones were significant, the R/T assembly, unless designed properly, could pass a tone relatively easily to the cabin because of the dip in the transmission coefficient that will occur above the blade passage frequency.

5.2.10 RESONATOR APPLICATION TO THE PRESSURE BULKHEAD

Assuming that an R/T assembly similar to that of the nonconventional sidewall treatment above is applied to the pressure bulkhead, and that the treatment is supported solely by the pressure bulkhead without any structural ties to the fuselage forward of the bulkhead and sealed at the juncture to an isolated sidewall trim panel, the radiation should be reduced approximately by the velocity reduction given in table 11. Sound transmission through the bulkhead coming from the empennage cavity should be down about 16 dB at the blade passage frequency, but virtually none at 338, versus the baseline bulkhead. The reduction in the tonal levels in the coach section should be significant.

Table 11. Estimated Performance of a Resonator Trim Panel Assembly Versus the Baseline and Five-Layer Trims

Velocity reduction (trim coefficient), dB			
Frequency, Hz	Baseline (3-layer)	5-layer	R/T panel assembly
50	-1.29	6.01	-12.12
63	-0.66	9.02	-1.83
80	1.06	12.89	5.24
100	3.67	15.13	10.52
125	6.97	18.21	15.87
160	10.47	21.89	30.31
200	12.81	26.24	9.88
250	14.37	32.33	19.17
315	15.39	37.94	23.04
400	21.17	41.99	26.37

6.0 CONCLUSIONS AND RECOMMENDATIONS

Three analysis tools were used to predict low frequency cabin noise and vibration, and evaluate potential suppression concepts, associated with both aft-mounted and wing-mounted advanced propeller-powered airplanes. Finite element analysis and statistical energy analysis were used to assess the structureborne aspects of the problem, and statistical energy analysis and the PAIN method were used to assess airborne aspects of the problem. The techniques, either individually or in combination, show good potential for being able to assess low frequency airplane interior noise and vibration problems.

The application of each prediction tool to their specific problems was validated within the scope of the contract. However, due to the limited nature of the available data, more data are still required for detailed validation of any of the models. Particularly, no data currently exists to validate model predictions for the case of airborne excitation from a wing-mounted propeller. Additional data for the wing-mounted structureborne noise problem would also be useful.

Although each analysis technique was applied independently for this study, a combination of SEA and finite element techniques may offer an attractive alternative for assessing the structureborne noise. For structureborne excitation, the SEA approach was limited by the difficulty in modeling the response at the strut-to-wing attachments when forces were applied to the engine mounts on the 767-300 strut. However, when the measured GVT responses at the strut-to-wing attachments were used as input into an SEA model of the wing, fuselage, and acoustic space, reasonably good predictions were obtained of the cabin sound pressure levels. It was concluded that SEA could be used with reasonable accuracy if the responses at the strut-to-wing attachments could be predicted by some other method, such as the finite element method. Although the finite element method (FEM) is fully capable of making a structure-acoustic prediction, the size of the model can become unwieldy. It is currently assumed that the size of the finite element model required for accurate predictions at the strut-to-wing attachments will be significantly smaller than the existing model used for a purely finite element structure-acoustic analysis. Thus, a hybrid approach that combines finite element analysis and statistical energy analysis is an attractive alternative. Assumptions regarding the required FEM model size should be verified. If large portions of the fuselage model are required, a FEM-SEA hybrid approach becomes less attractive.

Other conclusions based on the application of each of the three analysis techniques are discussed below.

6.1 FINITE ELEMENT ANALYSIS

In FY 1989, the 727 Demonstrator airplane finite element model was upgraded for predictions up to 100 Hz. Predictions were compared with GVT data and parametric studies were performed to identify transmission paths and evaluate suppression concepts.

Modeling requirements for the interior cabin trim were investigated using simplified 727 airplane fuselage models. Results showed that a lumped mass representation of the interior trim is a reasonable approximation up to 100 Hz. In addition, the cabin acoustic response is fairly insensitive to modifications of the sidewall parameters (panel stiffness, isolator stiffness, airgap thickness, and panel density). As a result, trim was represented as lumped mass only in the full airplane model. Modeling the trim as only lumped mass saved several thousand degrees of freedom from being added to an already large model. Conclusions regarding the modeling of the 727 Demonstrator airplane interior trim were applied to the construction of the 767-300 airplane finite element model.

The cabin acoustic space model was modified to reflect the surface geometry of the interior trim rather than the primary structure. Results show that below the first cross cabin resonance the model is fairly insensitive to the geometric changes incorporated. Above the first cross-cabin resonance the geometric changes have significant impact on the predicted acoustic response.

Overall, the 727 Demonstrator airplane finite element model shows good correlation with GVT data under 60 Hz. Above 60 Hz, the model tends to overpredict the fuselage and floor response. This in turn leads to an overprediction of the cabin acoustic response in the same frequency range. Differences between prediction and data are believed to be primarily related to modeling discrepancies of a complex aft end, modified to accept the demonstrator strut. The model predicts that the fuselage shell and floor, and not the bulkhead, are controlling the cabin acoustic response. For the suppression concepts investigated, no one concept leads to a general reduction of cabin noise for all frequencies and shake directions. The biggest benefit to noise appears to be the result of shifting dominant structural modes out of the frequency range of interest.

In FY 1990, a 767-300 structure-acoustic finite element model was compared to ground vibration test data (20-75 Hz). The model was then used to investigate the sensitivity of cabin noise and vibration to various parametric changes.

The 767-300 airplane finite element model generally shows good correlation with GVT data. However, for the front mount vertical shake condition the model fails to predict a sharp drop in the mid spar

fitting vertical response between 50-55 Hz. This in turn leads to an overprediction in the cabin acoustic response by as much as 20 dB. These differences are primarily believed to be the result of modeling deficiencies in the strut and/or strut-to-wing connections. Further data and analyses are required to determine the modeling requirements of the strut and/or strut-to-wing connections for accurate predictions at the mid spar fitting.

For the rear mount vertical and front mount lateral shake conditions, the model overpredicts the fuselage and cabin acoustic response around 50 Hz by 7-10 dB. Although the suspected modeling deficiencies in the strut and/or strut-to-wing connections may be contributing to this overprediction, a potential modeling deficiency in the wing-fuselage portion of the model exists. It is very difficult to separate the effects of the strut from the rest of the model in determining the source of the deficiency. As such, it is recommended that the wing-fuselage model be validated independent of the strut. This would require additional ground vibration testing with the strut removed, and shaker inputs going directly into the wing at the strut attach points.

Results from sensitivity studies show that the presence of fuel can have a significant impact on the cabin acoustic predictions and should be accounted for in a flight configuration. Adding stiffness to the wing generally had no effect on the cabin noise and vibration under 50 Hz but produced significant increases above 50 Hz. The number of parametric studies was somewhat limited by budget constraints. More sensitivity studies would be beneficial in understanding modeling requirements and load paths, as well as identifying potential suppression concepts.

As was noted for the 727 Demonstrator airplane finite element model (ref. 1), the large size of the 767-300 airplane model made model preparation, checkout and turnaround of predicted results time consuming and expensive. Reducing the existing model, while maintaining accuracy in the structure-acoustic response predictions, could possibly be accomplished by replacing additional forward and aft fuselage detailed models and the outboard wing detailed model with simpler beam representations.

6.2 STATISTICAL ENERGY ANALYSIS

Noise and vibration studies were conducted using SEA models of both an aft-mounted and a wing-mounted propeller configuration. The aft-mounted configuration model was the 727 Demonstrator airplane which had the right turbofan engine and strut replaced by the GE36 advanced propeller engine and a much heavier, stiffer strut. Airborne excitation from the propeller field impinged mainly on the empennage. Structureborne noise due to engine unbalance travelled from the engine mounts through the strut to the rear pressure bulkhead and to the empennage and sidewall on its way to the

cabin interior. Earlier work had validated that this model accurately predicted the power flow through the structure to the cabin. The present work showed that the addition of trim panels as separate subsystems improved the predictions above 100 Hz. Parametric studies aimed at reducing the cabin noise met with mixed results. It was found that even when major energy flow paths were disconnected that the cabin sound pressure levels (SPL) were either only marginally reduced or, in some cases, even increased. The vibratory energy very easily found a new path to travel to the cabin. Interrupting the flow paths did not prove to be a viable method of reducing cabin noise for this configuration. The addition of a heavy, limp wall in front of the rear pressure bulkhead reduced the cabin SPL by about 6 dB at the shaft rotational frequency and about 8 dB at the second harmonic but only at the expense of several hundred pounds of added mass. The most effective and promising concept tried was that of extending the engine struts inward through the empennage until they met at the center, in effect, generating a single straight-through strut. When the strut was isolated at both left and right side empennage attachment points, reductions of 10 dB at the shaft rotational frequency were obtained for both vertical and lateral drive conditions.

The wing-mounted configuration studies used two models. For airborne excitation an extended version of the 727 Demonstrator model was used which used the same pressure excitation as the aft-mounted configuration. For the structureborne noise studies an SEA model of the 767-300 airplane was developed because there was existing ground vibration test data against which to validate the model. Suppression concepts based on the 767-300 model should carry over to the hypothetical 727 wing-mounted configuration or any other wing-mounted propeller aircraft.

For airborne excitation, the predicted cabin interior SPL increased by as much as 36 dB over the aft-mounted configuration due to a higher fuselage conductance and transmission path differences. Several airborne noise suppression concepts were tried which modified the construction of the sidewall, added acoustical barriers or added damping. No single concept provided more than 6 dB reduction in cabin SPL and, additively, might achieve a maximum of 10 dB. These suppressed levels would still exceed the maximum aft-mounted configuration levels by 26 dB in the third octave band containing the blade passage frequency.

The SEA model predicts the structureborne interior noise to be very insensitive to structural changes inboard of the strut. The only factor found to affect the cabin noise to any degree was fuel loading. A fuel management procedure was worked out which indicated that up to a 5 dB reduction in cabin noise at the shaft rotational frequency could be realized.

6.3 PAIN ANALYSIS

The PAIN method was modified to calculate an axial variation of the average mean square pressure in cabin cross-section for airplanes with propeller excitation of the fuselage. For propeller excitation of the empennage, PAIN was extended to include radiation and transmission through the aft pressure bulkhead in calculation of cabin average sound level. PAIN90 combines into one program the up to date versions of the PAIN method for wing-mounted propellers and the previously designated PAI-NUDF for aft-mounted propellers.

PAIN predictions were made of cabin propeller tone sound levels in a 727 airplane with advanced high speed propellers. Two different configurations were investigated, one with wing-mounted engines and one with aft-mounted engines. Parametric variations were made to the baseline airplane to determine the effects on predicted interior noise levels caused by changes in fuselage stiffness, mass, and damping, and by changes in the configuration and weight of the cabin trim installation. Predictions were made for the tonal levels occurring at the blade passage frequency (169 Hz) and at the frequency of the second harmonic (338 Hz) of the propeller field.

The predicted baseline interior noise level for the wing-mounted configuration is approximately 109.0 dB at 169 Hz and 88.9 dB at 338 Hz. The cabin floor is a major contributor to cabin noise for the wing-mounted configuration. In order for there to be a significant decrease in cabin levels, the floor must be well isolated. With a heavy five layer trim and a well isolated floor, the predicted cabin levels are 98.5 dB at 169 Hz and 61.1 dB at 338 Hz. A trim panel incorporating Helmholtz resonators has the potential to lower the cabin levels at the blade passage frequency an additional 8 dB. Changes to the primary structure had little effect on the predicted levels. Future research for interior noise suppression of wing-mounted propeller airplanes should concentrate on developing high performance trims and practical floor isolation techniques.

The predicted baseline interior noise levels for the aft-mounted configuration is approximately 92.8 dB at 169 Hz and 77.1 dB at 338 Hz. The aft pressure bulkhead is the major radiator for the aft-mounted configuration. Unless the bulkhead radiation is suppressed, the sidewall contribution is negligible. The prediction for the cabin level in which the bulkhead is heavily damped with constrained layer damping is 89.7 dB at 169 Hz and 76.1 dB at 338 Hz. Predictions for the aft-mounted configuration have been adjusted by a calibration run to account for uncertainties in the predicted propeller phase field.

7.0 REFERENCES

1. A.E. Landmann, H.F. Tillema, and S.E. Marshall, "Evaluation of Analysis Techniques for Low Frequency Interior Noise and Vibration of Commercial Aircraft," NASA CR-181851 (1989).
2. L.D. Pope, "On the Prediction of Propeller Tone Sound Levels and Gradients in an Airplane Cabin," *J. Acoust. Soc. Am.*, 88 (6), 2755-2765 (1990).
3. L.D. Pope, E.G. Wilby, and J.F. Wilby, "Propeller Aircraft Interior Noise Model," NASA CR-3813 (1984).
4. L.D. Pope, E.G. Wilby, and J.F. Wilby, "Propeller Aircraft Interior Noise Model, Part I: Analytical Model," *J. Sound and Vib.*, 118(3), 449-467(1987).

REPORT DOCUMENTATION PAGE			Form Approved OMB No. 0704-0188	
Public reporting burden for this collection of information is estimated to average 1 hour per response, including the time for reviewing instructions, searching existing data sources, gathering and maintaining the data needed, and completing and reviewing the collection of information. Send comments regarding this burden estimate or any other aspect of this collection of information, including suggestions for reducing this burden, to Washington Headquarters Services, Directorate for Information Operations and Reports, 1215 Jefferson Davis Highway, Suite 1204, Arlington, VA 22202-4302, and to the Office of Management and Budget, Paperwork Reduction Project (0704-0188), Washington, DC 20503.				
1. AGENCY USE ONLY (Leave blank)	2. REPORT DATE January 1992	3. REPORT TYPE AND DATES COVERED Contractor Report		
4. TITLE AND SUBTITLE Application of Analysis Techniques for Low Frequency Interior Noise and Vibration of Commercial Aircraft		5. FUNDING NUMBERS C NAS1-18027 WU 535-03-11-04		
6. AUTHOR(S) A. E. Landmann, H. F. Tillema, and G. R. MacGregor				
7. PERFORMING ORGANIZATION NAME(S) AND ADDRESS(ES) The Boeing Company P. O. Box 3707 Seattle, WA 98124		8. PERFORMING ORGANIZATION REPORT NUMBER D6-55817		
9. SPONSORING/MONITORING AGENCY NAME(S) AND ADDRESS(ES) National Aeronautics and Space Administration Langley Research Center Hampton, VA 23665-5225		10. SPONSORING/MONITORING AGENCY REPORT NUMBER NASA CR-189555		
11. SUPPLEMENTARY NOTES Langley Technical Monitor: Kevin P. Shepherd				
12a. DISTRIBUTION/AVAILABILITY STATEMENT Unclassified-Unlimited Subject Category - 08			12b. DISTRIBUTION CODE	
13. ABSTRACT (Maximum 200 words) Finite Element analysis (FEA), statistical energy analysis (SEA), and a power flow method (computer program PAIN) were used to assess low frequency interior noise associated with advanced propeller installations. FEA and SEA models were used to predict cabin noise and vibration and evaluate suppression concepts for structure-borne noise associated with the shaft rotational frequency and harmonics (< 100 Hz). SEA and PAIN models were used to predict cabin noise and vibration and evaluate suppression concepts for airborne noise associated with engine radiated propeller tones. Both aft-mounted and wing-mounted propeller configurations were evaluated. Ground vibration test data from a 727 airplane modified to accept a propeller engine were used to compare with predictions for the aft-mounted propeller. Similar data from the 767 airplane was used for the wing-mounted model comparisons.				
14. SUBJECT TERMS Acoustics, Advanced Turbo Prop Aircraft, Aircraft Noise, Aircraft Cabin Noise			15. NUMBER OF PAGES 92	
			16. PRICE CODE	
17. SECURITY CLASSIFI- CATION OF REPORT Unclassified	18. SECURITY CLASSIFICA- TION OF THIS PAGE Unclassified	19. SECURITY CLASSIFI- CATION OF ABSTRACT	20. LIMITATION OF ABSTRACT	

